

CONVERGENCE, DESIGN AND TRAINING OF CONTINUOUS-TIME DROPOUT AS A RANDOM BATCH METHOD

ANTONIO ÁLVAREZ-LÓPEZ AND MARTÍN HERNÁNDEZ

ABSTRACT. We study dropout regularization in continuous-time models through the lens of random-batch methods—a family of stochastic sampling schemes originally devised to reduce the computational cost of interacting particle systems. We construct an unbiased, well-posed estimator that mimics dropout by sampling neuron batches over time intervals of length h . Trajectory-wise convergence is established with linear rate in h for the expected uniform error. At the distribution level, we establish stability for the associated continuity equation, with total-variation error of order \sqrt{h} under mild moment assumptions. During training with fixed batch sampling across epochs, a Pontryagin-based adjoint analysis bounds deviations in the optimal cost and control, as well as in gradient-descent iterates. On the design side, we compare convergence rates for canonical batch sampling schemes, recover standard Bernoulli dropout as a special case, and derive a cost–accuracy trade-off yielding a closed-form optimal h . We then specialize to a single-layer neural ODE and validate the theory on classification and flow matching, observing the predicted rates, regularization effects, and favorable runtime and memory profiles.

CONTENTS

1. Introduction	1
2. Formulation	3
3. Main results	5
4. Design	10
5. Example: neural ODEs	13
6. Numerics	14
7. Conclusions and discussion	20
8. Proofs	22
Acknowledgments	35
References	35

1. INTRODUCTION

Deep neural networks have achieved (and redefined) state-of-the-art performance across a wide range of applications [58, 10]. However, their large scale often results in significant computational costs [12, 4].

Pruning techniques eliminate redundant parameters that contribute minimally to the loss, thereby reducing memory usage and computational load. Conceptually similar, *dropout* was proposed as a training regularizer that temporarily masks random neurons during each forward pass, without permanently removing any weights [59, 67, 69]. While pruning targets model compression, dropout aims to prevent overfitting during training [47]. In recent years, however, the scheme has also been applied to testing under the name of Monte-Carlo dropout, where multiple forward passes are averaged to quantify model uncertainty, mirroring Bayesian inference [20, 66].

Both pruning and dropout have been successfully applied to various discrete-time architectures such as feed-forward [2], convolutional [43, 61, 13], and recurrent neural networks [68]. More recently, deep learning models based on continuous-time dynamical systems driven by a learnable vector field have emerged. These models offer new opportunities and challenges, as they can be computationally demanding, and naive adaptations of discrete pruning or dropout techniques might compromise the theoretical guarantees of ODE solvers.

Departamento de Matemáticas, Universidad Autónoma de Madrid, 28049 Madrid, Spain. antonio.alvarezl@uam.es.

Chair for Dynamics, Control, Machine Learning, and Numerics, Department of Mathematics, Friedrich-Alexander-Universität Erlangen-Nürnberg, 91058 Erlangen, Germany. antonio.alvarezl@uam.es, martin.hernandez@fau.de.

An example is neural ordinary differential equations (*neural ODEs*), which interpret depth in residual networks as an integration interval rather than discrete layers [7, 15, 25]. Models that inject noise into these dynamics have been proposed as neural stochastic differential equations (*neural SDEs*). Specifically, when this noise is multiplicative and follows a Bernoulli distribution, the scheme can be viewed as an implementation of continuous-time dropout [47]. Rigorous theoretical analysis is still needed, however, to understand the best design for this approach and its impact on (i) trajectory approximation error and (ii) training loss and optimization dynamics [8, 54].

In this work, we study *continuous-time dropout* through the lens of random batch methods, providing a stochastic framework that applies beyond neural ODEs and yields explicit error and design guarantees.

1.1. Contributions. Random batch methods (RBMs), originally developed to speed up N -body simulations by evaluating interactions only within small batches, are adapted here to continuous-time learning by treating neurons/units as particles sampled during integration. Our main contributions include:

- (1) **Dropout-RBM formulation and convergence.** We construct the estimator by using a time grid of step h and sampling at each subinterval a neuron batch according to prescribed probabilities; Horvitz–Thompson–type weights then make the estimator unbiased [33]. Under Lipschitz assumptions ensuring well-posedness, we show that the expected squared error between full and random trajectories scales linearly with h .
- (2) **Measure–transport stability.** We study the effect of dropout on the continuity equation that describes transport of a probability measure by the flow. Under mild conditions, we prove that the expected pointwise squared error scales linearly with h , while in Wasserstein and total variation it scales as \sqrt{h} —ensuring stable density estimation [55, 57].
- (3) **Training.** We frame supervised learning as an optimal control problem (see [44, 16]) and analyze dropout via Pontryagin’s Maximum Principle. We derive the adjoint system and use it to characterize optimal controls, and bound adjoint trajectories, optimal costs/controls, and establish stability of gradient–descent iterates. Unlike conventional dropout, we keep the sampling schedule fixed across epochs, directly connecting the setting to structured pruning.
- (4) **Design.** We quantify how design levers—trajectory variance, sampling imbalance, and minimal inclusion probability—control the constants in our bounds. We analyze canonical pruning schemes (leave–one neuron, pick–one neuron, balanced subsets, all possible subsets), derive wide–width asymptotics, and show that standard Bernoulli dropout is a special case of our model with explicit variance and sampling factors. We then establish a cost–accuracy trade–off and give a closed–form expression for the cost–minimizing h , together with RBM vs. full–model cost comparisons.
- (5) **Validation.** We specialize our general results to a single–layer neural ODE as a canonical example, and perform numerical experiments on classification and measure transport (flow matching) for both time–independent and time–dependent parameters. The tests confirm the predicted convergence rates and demonstrate substantial reductions in memory usage and runtime, with regularization effects and, in some regimes, improved test accuracy compared to the full model.

1.2. Related Work. We briefly review related developments.

Pruning. First approaches, in the late 1980s and early 1990s, removed weights with minimal loss increase but required costly Hessian inversions [41, 29]. Simpler magnitude/structured pruning later achieved higher sparsity with minor accuracy impact. Methods are often classified as (i) *static* pruning (during/after training for memory and speed) [28, 27, 30]; and (ii) *dynamic* sparsity (prune/reactivate during inference) [24, 51]. The Lottery Ticket Hypothesis formalizes the existence of accurate, highly sparse subnetworks (*winning tickets*) inside a dense neural network [19]. For continuous-depth models, [46] showed empirically that pruning neural ODEs often improves their generalization power in normalizing flows by reducing mode collapse and smoothing the loss landscape, achieving sparsity of up to 98% without compromising accuracy. Building upon this, [50] proposed SpODE for continuously transitioning from dense to sparse neural ODEs while preserving accuracy. We refer to [8] for a broad overview.

Dropout. Dropout can be viewed as approximate Bayesian inference and a strong regularizer against overfitting [21, 39], with variants for CNNs [53] and convergence analyses in specific settings (e.g. two-layer nets [49]). For residual architectures, noise-injected formulations are interpreted as weak approximations to SDEs [60], seeking connections with optimal control and backward Kolmogorov equations. Monte–Carlo dropout at test time matches our approach of averaging random forward passes [66]. Neural SDEs [47] improve robustness/generalization of neural ODEs. Related lines include Neural

Jump SDEs (model temporal point processes as continuous dynamics with discrete stochastic jumps, see [35]) and STEER’s regularization technique which randomly samples the terminal integration time [23]. More recently, [42] simulates continuous-time dropout via an alternating renewal process that randomly activates neurons, but without quantitative error analysis. Our work fills this gap with explicit rates and extensions via RBMs.

Splitting. Splitting schemes decompose dynamics into simpler sub-operators (Lie–Trotter/Strang style) solved separately and sequentially over small timesteps. This strategy—inspired in the principle of divide-and-conquer—exploits structure and leverages the lower cost of solving individual subproblems, often via specialized methods or analytical solutions [63, 48, 40]. Random batch methods (RBMs) stochastically select sub-operators each step. They have been effective in interacting particle systems [37, 38], finite-dimensional optimal control [65], including model predictive control [64], and extended to PDEs [36, 5, 56, 17, 14, 32, 31]. To our knowledge, methods based on RBMs have not been developed for continuous-time deep learning models or general nonlinear controlled ODEs; this work makes that connection via a principled dropout formulation with convergence and design guarantees.

1.3. Roadmap. The paper is organized as follows. In Section 2 we introduce the continuous-time dropout scheme via RBMs, present the standing assumptions used throughout the paper, and establish well-posedness and unbiasedness. Section 3 presents our main results: (i) forward-dynamics convergence (Section 3.1); (ii) population-level convergence for the continuity equation (Section 3.2); and (iii) training as optimal control based on the PMP, including adjoint systems and bounds (Section 3.3). In Section 4 we analyze design: Section 4.1 compares canonical sampling schemes and identifies standard Bernoulli dropout as a particular RBM; Section 4.2 derives a cost-accuracy trade-off and an explicit cost-minimizing dropout switching step. In Section 5 we specialize and interpret the results for a single-layer neural ODE as a model example. Section 6 reports experiments that confirm the predicted rates and show runtime/memory/regularization gains (with fixed schedules acting as a structured-pruning surrogate). Section 7 summarizes findings, discusses extensions, and lists open problems. All proofs are deferred to Section 8.

1.4. Notation. We denote $[n] = \{1, \dots, n\}$. Scalars use plain font, vectors are bold, and matrices are uppercase. For $x, y \in \mathbb{R}$, set $x \wedge y = \min\{x, y\}$ and $x \vee y = \max\{x, y\}$. The Euclidean inner product of \mathbf{x} and \mathbf{y} is $\langle \mathbf{x}, \mathbf{y} \rangle$ and the norm is $\|\cdot\|$. On matrices we use the operator norm $\|\cdot\| \equiv \|\cdot\|_{\text{op}}$. We use subscripts to indicate time and write $f_t(\cdot) = f(t, \cdot)$. For $1 \leq p \leq \infty$, we denote by L^p the usual Lebesgue space, and $\mathcal{AC}([0, T]; \mathbb{R}^d)$ is the space of absolutely continuous curves on $[0, T]$ —equivalently, $W^{1,1}(0, T; \mathbb{R}^d) \cap \mathcal{C}^0([0, T]; \mathbb{R}^d)$. The closed ball in \mathbb{R}^d with radius $R > 0$ and centered at the origin is B_R .

We write $\mathbf{f} \in \mathcal{C}^{0,1}$ if \mathbf{f} is (globally) Lipschitz with Lipschitz constant $\lambda_{\mathbf{f}}$, write $\mathbf{f} \in \mathcal{C}^{1,1}$ if $\mathbf{f} \in \mathcal{C}^1$ and $\nabla \mathbf{f}$ is Lipschitz, and write $\mathbf{f} \in \mathcal{C}_{\text{loc}}^{1,1}$ if both $\mathbf{f} \in \mathcal{C}^1$ and $\nabla \mathbf{f}$ is locally Lipschitz. For a function $\mathbf{f}(\mathbf{x}, \theta)$ of two variables, write $\lambda_{\mathbf{f}, \mathbf{x}}$ for the Lipschitz constant in \mathbf{x} (uniformly in θ), and $\lambda_{\mathbf{f}, \theta}$ for the Lipschitz constant in θ (uniformly in \mathbf{x}). If that uniformity only holds over a subset, we indicate it by adding a third subscript. For example, $\lambda_{\mathbf{f}, \mathbf{x}, A}$ means the Lipschitz bound of \mathbf{f} in \mathbf{x} holds for all $\theta \in A$.

2. FORMULATION

2.1. Continuous-time model. Let $d \geq 1$ and $T > 0$. Consider a controlled differential equation

$$\begin{cases} \dot{\mathbf{x}}_t &= \mathbf{F}(\mathbf{x}_t, \vartheta_t), & t \in [0, T], \\ \mathbf{x}_0 &\in \mathbb{R}^d, \end{cases} \quad (\text{FM})$$

where the control is $\vartheta \in L^\infty(0, T; \Theta)$ with $\Theta \subseteq \mathbb{R}^m$, and for some $p \geq 1$

$$\mathbf{F}(\mathbf{x}, \theta) = \sum_{i \in [p]} \mathbf{f}_i(\mathbf{x}, \theta_i), \quad \theta = (\theta_i)_{i \in [p]} \in \prod_{i \in [p]} \Theta_i =: \Theta, \quad \|\theta\|^2 := \sum_{i \in [p]} \|\theta_i\|^2. \quad (2.1)$$

Assume each Θ_i is closed and convex, and hence Θ is as well.

Motivated by neural ODEs, where \mathbf{F} is realized as a neural network and p denotes its (constant) width, we will refer to each $\mathbf{f}_i : \mathbb{R}^d \times \Theta_i \rightarrow \mathbb{R}^d$ as a “neuron”. Indeed, as a running example, consider \mathbf{F} as a single-layer neural network with time-dependent parameters:

$$\begin{cases} \dot{\mathbf{x}}_t &= \sum_{i \in [p]} \mathbf{w}_{i,t} \sigma(\langle \mathbf{a}_{i,t}, \mathbf{x}_t \rangle + b_{i,t}), & t \in [0, T], \\ \mathbf{x}_0 &\in \mathbb{R}^d. \end{cases} \quad (\text{NODE})$$

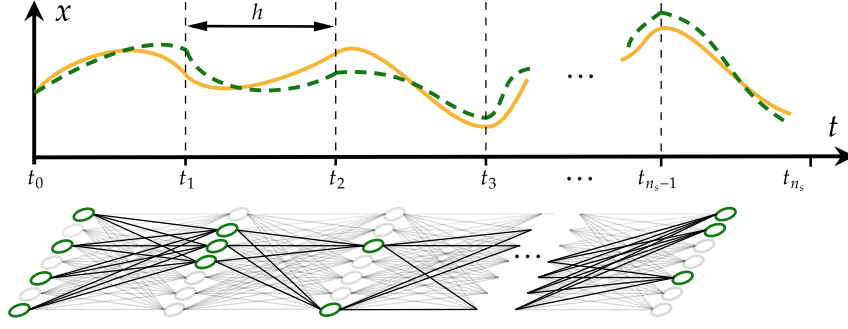


FIGURE 1. Top: Trajectories generated by the full model (FM) (orange) and the random model (RM) (green). Bottom: Vector fields $\mathbf{F}^{(w_{k_t})}$ obtained by masking, on each interval $[t_{k-1}, t_k]$, the subset of neurons in (2.1) selected by ω .

Here, each $\mathbf{f}_i : \mathbb{R}^d \times \Theta_i \rightarrow \mathbb{R}^d$ is a single-neuron perceptron with activation function $\sigma \in \mathcal{C}^{0,1}(\mathbb{R})$ and parameters $\vartheta_i = (\mathbf{w}_i, \mathbf{a}_i, b_i) \in L^\infty(0, T; \mathbb{R}^{2d+1})$, so that $\vartheta = (\mathbf{w}_i, \mathbf{a}_i, b_i)_{i \in [p]}$ and $\Theta = (\mathbb{R}^{2d+1})^p$. Although we focus on (NODE) for the numerical experiments, the generality of (FM) allows the extension of our analytical results to other deep learning models.

Well-posedness. We shall assume that every \mathbf{f}_i is continuous in θ_i and Lipschitz in \mathbf{x} , uniformly on θ_i over bounded subsets of Θ_i . Thus, for each $\vartheta \in L^\infty(0, T; \Theta)$ there exists a constant $\lambda_{\mathbf{F}, \mathbf{x}, \vartheta} \geq 0$ such that

$$\sup_{t \in [0, T]} \|\mathbf{F}(\mathbf{x}, \vartheta_t) - \mathbf{F}(\mathbf{y}, \vartheta_t)\| \leq \lambda_{\mathbf{F}, \mathbf{x}, \vartheta} \|\mathbf{x} - \mathbf{y}\|, \quad \text{for all } \mathbf{x}, \mathbf{y} \in \mathbb{R}^d. \quad (2.2)$$

Moreover, the quantity $\lambda_{\mathbf{F}, 0, \vartheta} := \sum_{i \in [p]} \|\mathbf{f}_i(0, \vartheta_{i, \cdot})\|_{L^\infty(0, T)}$ is finite (see Remark 8.2), whence

$$\sup_{t \in [0, T]} \|\mathbf{F}(\mathbf{x}, \vartheta_t)\| \leq \lambda_{\mathbf{F}, \mathbf{x}, \vartheta} \|\mathbf{x}\| + \lambda_{\mathbf{F}, 0, \vartheta}, \quad \text{for all } \mathbf{x} \in \mathbb{R}^d. \quad (2.3)$$

Thanks to Lemma 8.1, we deduce that for any $\mathbf{x}_0 \in \mathbb{R}^d$ and $\vartheta \in L^\infty(0, T; \Theta)$ there exists a unique solution $\mathbf{x} : [0, T] \rightarrow \mathbb{R}^d$ to (FM) in the Carathéodory sense—that is, $\mathbf{x} \in \mathcal{AC}([0, T]; \mathbb{R}^d)$.

Standing assumptions. Throughout, additional Lipschitz assumptions on the functions \mathbf{f}_i will be invoked and stated where used. For the reader's convenience and to fix notation, we collect them here:

Assumption. Fix compacts $\mathbf{K} \subset \mathbb{R}^d$ and $\mathbf{B}_i \subset \Theta_i$. For each $i \in [p]$ we list the following Lipschitz assumptions (in the sense of Section 1.4):

$$0 \leq \lambda_{\mathbf{f}_i, \theta, \mathbf{K}} < \infty \quad (\mathbf{f}_i \text{ Lipschitz in } \theta_i, \text{ uniform for } \mathbf{x} \in \mathbf{K}). \quad (\text{A1})$$

$$0 \leq \lambda_{\nabla_{\mathbf{x}} \mathbf{f}_i, \mathbf{x}, \mathbf{B}_i} < \infty \quad (\nabla_{\mathbf{x}} \mathbf{f}_i \text{ Lipschitz in } \mathbf{x}, \text{ uniform for } \theta_i \in \mathbf{B}_i). \quad (\text{A2})$$

$$0 \leq \lambda_{\nabla_{\mathbf{x}} \mathbf{f}_i, \theta, \mathbf{K}} < \infty \quad (\nabla_{\mathbf{x}} \mathbf{f}_i \text{ Lipschitz in } \theta_i, \text{ uniform for } \mathbf{x} \in \mathbf{K}). \quad (\text{A3})$$

$$0 \leq \lambda_{\nabla_{\theta} \mathbf{f}_i, \mathbf{x}, \mathbf{B}_i} < \infty \quad (\nabla_{\theta} \mathbf{f}_i \text{ Lipschitz in } \mathbf{x}, \text{ uniform for } \theta_i \in \mathbf{B}_i). \quad (\text{A4})$$

$$0 \leq \lambda_{\nabla_{\theta} \mathbf{f}_i, \theta, \mathbf{K}} < \infty \quad (\nabla_{\theta} \mathbf{f}_i \text{ Lipschitz in } \theta_i, \text{ uniform for } \mathbf{x} \in \mathbf{K}). \quad (\text{A5})$$

We do not assume (A1)–(A5) simultaneously; each result will state the specific items it uses. When $\vartheta \in L^\infty(0, T; \Theta)$, one can take $\mathbf{B}_i = \text{range}(\vartheta_i)$, and write ϑ in the subscript instead of \mathbf{B}_i , as in (2.2).

Analogously to (2.2), whenever any of (A1)–(A5) holds for every \mathbf{f}_i , the same item holds for \mathbf{F} , with the corresponding constant bounded by the sum of the individual ones.

Remark 2.1. A single umbrella hypothesis implying (A1)–(A5) is that each $\mathbf{f}_i \in \mathcal{C}^1(\mathbb{R}^d \times \Theta_i; \mathbb{R}^d)$ has full Jacobian $(\nabla_{\mathbf{x}} \mathbf{f}_i, \nabla_{\theta_i} \mathbf{f}_i)$ locally Lipschitz in (\mathbf{x}, θ_i) .

2.2. Random batch methods. We formalize the standard framework for random batch methods. Fix a number of batches $n_b \geq 1$ and a number of time steps $n_s \geq 1$. Consider a covering

$$\mathcal{B}_1, \dots, \mathcal{B}_{n_b} \subseteq \{1, \dots, p\}, \quad \text{with} \quad \bigcup_{j \in [n_b]} \mathcal{B}_j = \{1, \dots, p\},$$

and a random variable $\omega \in \{1, \dots, n_b\}$ that follows some probability distribution \mathbb{P} . For each $j \in [n_b]$, denote

$$q_j := \mathbb{P}(\omega = j) \in (0, 1], \quad (2.4) \quad \text{def:qj}$$

thus satisfying $\sum_{j \in [n_b]} q_j = 1$, and define

$$\mathbf{F}^{(j)}(\mathbf{x}, \theta) := \sum_{i \in \mathcal{B}_j} \frac{1}{\pi_i} \mathbf{f}_i(\mathbf{x}, \theta_i). \quad (2.5) \quad \text{eq:Fomega j}$$

Here, π_i is the i -th inclusion probability, i.e., the probability that neuron i is included in any batch:

$$\pi_i = \sum_{\mathcal{B}_\ell \ni i} q_\ell = \sum_{\ell \in [n_b]} q_\ell \mathbf{1}_{\{i \in \mathcal{B}_\ell\}}, \quad \text{for } i \in [p]. \quad (2.6) \quad \text{eq:definition}$$

Because the batches \mathcal{B}_j form a covering of $[p]$, we have that $\pi_{\min} := \min_{i \in [p]} \pi_i > 0$. Now, consider a partition of $[0, T]$ into n_s subintervals $[t_{k-1}, t_k)$ defined for $k \in [n_s] \cup \{0\}$ by

$$t_k = kh, \quad \text{with} \quad h := \frac{T}{n_s} \in (0, T].$$

Let $\omega_1, \dots, \omega_{n_s} \in [n_b]$ be a sequence of i.i.d. random variables following the distribution of ω . For the same values of $\mathbf{x}_0 \in \mathbb{R}^d$ and $\vartheta \in L^\infty(0, T; \Theta)$ used in (FM), we define the random model

$$\begin{cases} \dot{\hat{\mathbf{x}}}_t = \hat{\mathbf{F}}_t(\hat{\mathbf{x}}_t, \vartheta_t), & t \in [0, T], \\ \hat{\mathbf{x}}_0 = \mathbf{x}_0, \end{cases} \quad (\text{RM}) \quad \text{eq:random_no}$$

where

$$\hat{\mathbf{F}}_t(\hat{\mathbf{x}}, \theta) := \mathbf{F}^{(\omega_{k_t})}(\hat{\mathbf{x}}, \theta) = \sum_{i \in \mathcal{B}_{\omega_{k_t}}} \frac{1}{\pi_i} \mathbf{f}_i(\hat{\mathbf{x}}, \theta_i), \quad k_t := 1 + \lfloor t/h \rfloor. \quad (2.7) \quad \text{eq:hatFkt}$$

If \mathbf{f}_i satisfy (2.2), (2.3), or (A1)–(A5), then $\hat{\mathbf{F}}$ satisfies the same Lipschitz bounds as \mathbf{F} , with the constants multiplied by $\pi_{\min}^{-1} \in [1, +\infty)$. For instance, the analogue of (2.2) is

$$\|\hat{\mathbf{F}}_t(\mathbf{x}, \theta) - \hat{\mathbf{F}}_t(\mathbf{y}, \theta)\| \leq \sum_{i \in \mathcal{B}_{\omega_{k_t}}} \frac{1}{\pi_i} \|\mathbf{f}_i(\mathbf{x}, \theta_i) - \mathbf{f}_i(\mathbf{y}, \theta_i)\| \leq \frac{1}{\pi_{\min}} \lambda_{\mathbf{F}, \mathbf{x}, \vartheta} \|\mathbf{x} - \mathbf{y}\|.$$

Hence, Lemma 8.1 again guarantees the existence of a unique solution $\hat{\mathbf{x}} \in \mathcal{AC}([0, T]; \mathbb{R}^d)$ to (RM).

Interpretation. The piecewise-constant-in-time dynamics of the random model (RM) replicate the effect of dropout regularization in discrete neural networks. When each ω_k is sampled, the corresponding neuron batch \mathcal{B}_{ω_k} remains active on the fixed subinterval $[t_{k-1}, t_k)$, while all other neurons are masked.

3. MAIN RESULTS

3.1. Trajectory-level. By construction (see (2.5) and (2.7)), $\hat{\mathbf{F}}$ is unbiased. For a.e. $t \in [0, T]$,

$$\mathbb{E}_\omega[\hat{\mathbf{F}}_t(\mathbf{x}_t, \vartheta_t)] = \sum_{j \in [n_b]} \mathbf{F}^{(j)}(\mathbf{x}_t, \vartheta_t) q_j = \sum_{i \in [p]} \frac{\mathbf{f}_i(\mathbf{x}_t, \vartheta_{i,t})}{\pi_i} \sum_{j \in [n_b]} q_j \mathbf{1}_{\{i \in \mathcal{B}_j\}} = \mathbf{F}(\mathbf{x}_t, \vartheta_t). \quad (3.1) \quad \text{eq:expFrb}$$

To track the variability along trajectories, define $\Lambda : [0, T] \times \mathbb{R}^d \times L^\infty(0, T; \Theta) \rightarrow \mathbb{R}_{\geq 0}$ by

$$\Lambda_t(\mathbf{x}_0, \vartheta) := \mathbb{E}_\omega \left[\|\mathbf{F}(\mathbf{x}_t, \vartheta_t) - \hat{\mathbf{F}}_t(\mathbf{x}_t, \vartheta_t)\|^2 \right] = \sum_{j \in [n_b]} \|\mathbf{F}(\mathbf{x}_t, \vartheta_t) - \mathbf{F}^{(j)}(\mathbf{x}_t, \vartheta_t)\|^2 q_j, \quad (3.2) \quad \text{def:Lambda}$$

where \mathbf{x}_t solves (FM) with initial data \mathbf{x}_0 and control ϑ . The quantity Λ is independent of h and

$$\Lambda(\mathbf{x}_0, \vartheta) \in L^1(0, T), \quad \text{for all } \mathbf{x}_0 \in \mathbb{R}^d \text{ and } \vartheta \in L^\infty(0, T; \Theta), \quad (3.3) \quad \text{eq: uniform}$$

follows from a Grönwall estimate applied to $\|\mathbf{F}(\mathbf{x}_t, \vartheta_t) - \hat{\mathbf{F}}_t(\mathbf{x}_t, \vartheta_t)\|^2 \leq 2(1 + \pi_{\min}^{-2})(\lambda_{\mathbf{F}, \mathbf{x}, \vartheta} \|\mathbf{x}_t\| + \lambda_{\mathbf{F}, 0, \vartheta})^2$, which is derived from (2.3) and (2.5).

Our first theorem shows that, for any decomposition in random batches, the expected squared error between \mathbf{x}_t and $\hat{\mathbf{x}}_t$ decays linearly in h (or, equivalently, with n_s^{-1}). Consequently, if h is sufficiently small—corresponding to rapid switching in the random dynamics—the two systems behave similarly.

Theorem 3.1. *For any $\mathbf{x}_0 \in \mathbb{R}^d$ and $\vartheta \in L^\infty(0, T; \Theta)$ there exists*

$$S(\mathbf{x}_0, \vartheta) \geq 0 \quad \text{with} \quad \sup_{0 < h \leq T} S(\mathbf{x}_0, \vartheta) < +\infty, \quad (3.4)$$

such that the solutions \mathbf{x}_t of (FM) and $\hat{\mathbf{x}}_t$ of (RM) satisfy for all $0 < h \leq T$

$$\max_{t \in [0, T]} \mathbb{E}_\omega [\|\mathbf{x}_t - \hat{\mathbf{x}}_t\|^2] \leq S(\mathbf{x}_0, \vartheta) h.$$

The factor S is affine in $\|\Lambda\|_{L^1(0, T)}$ and in $\|\mathbf{x}_0\|$. Its explicit expression is given later in (4.1), where we analyze its expression with detail.

While Theorem 3.1 is valid when the same control ϑ is applied to both full and random models, in practice one often uses different controls. Under an additional mild assumption, the result extends directly by including an additional term that quantifies the distance between the two controls:

Corollary 3.2. *Assume (A1), let $\mathbf{x}_0 \in \mathbb{R}^d$ and $\vartheta_1, \vartheta_2 \in L^\infty(0, T; \Theta)$ be fixed. Then there exists $C(\vartheta_1, \vartheta_2) > 0$, independent of h , such that for all $0 < h \leq T$,*

$$\max_{t \in [0, T]} \mathbb{E}_\omega [\|\mathbf{x}_{\vartheta_1, t} - \hat{\mathbf{x}}_{\vartheta_2, t}\|^2] \leq S(\mathbf{x}_0, \vartheta_1) \wedge S(\mathbf{x}_0, \vartheta_2) h + C(\vartheta_1, \vartheta_2) \|\vartheta_1 - \vartheta_2\|_{L^1(0, T; \Theta)}^2, \quad (3.5)$$

where S is given by Theorem 3.1, \mathbf{x}_{ϑ_1} solves (FM) with $\vartheta = \vartheta_1$, and $\hat{\mathbf{x}}_{\vartheta_2}$ solves (RM) with $\vartheta = \vartheta_2$.

We conclude this section with a simple consequence of Theorem 3.1 via Markov's inequality.

Remark 3.3 (Concentration of trajectories). *Markov's inequality gives, for any $\varepsilon > 0$ and $t \in [0, T]$,*

$$\mathbb{P}(\|\mathbf{x}_t - \hat{\mathbf{x}}_t\|^2 > \varepsilon) \leq \frac{\mathbb{E}_\omega [\|\mathbf{x}_t - \hat{\mathbf{x}}_t\|^2]}{\varepsilon} \leq \frac{S(\mathbf{x}_0, \vartheta)}{\varepsilon} h.$$

Thus, as h and ε decrease with $h/\varepsilon \rightarrow 0$, the realizations of $\hat{\mathbf{x}}_t$ concentrate increasingly around \mathbf{x}_t . In other words, for fixed parameters and batch decomposition, each realization behaves like a “winning lottery ticket” [19] in the regime of small h .

3.2. Distribution-level. We have just quantified how dropout perturbs the forward evolution of a single data point \mathbf{x}_0 . We now assume that this point is drawn from a probability distribution with density ρ_B . When the trajectory evolves according to (FM), its density ρ_t solves the continuity equation

$$\begin{cases} \partial_t \rho_t(\mathbf{x}) + \nabla_{\mathbf{x}} \cdot (\mathbf{F}(\mathbf{x}, \vartheta_t) \rho_t(\mathbf{x})) = 0, & \text{in } [0, T] \times \mathbb{R}^d \\ \rho_0(\mathbf{x}) = \rho_B(\mathbf{x}), & \text{on } \mathbb{R}^d. \end{cases} \quad (3.6)$$

Besides (2.2), we shall assume (A2) holds. Consequently, for any $\rho_B \in \mathcal{C}^{0,1}(\mathbb{R}^d)$, there exists a unique weak solution $\rho \in \mathcal{C}^0([0, T]; \mathcal{C}^{0,1}(\mathbb{R}^d))$ to (3.6). Indeed, let Φ_t be the flow of (FM)—a \mathcal{C}^1 -diffeomorphism with $\Phi_0 = \text{Id}$ and $\Phi_t(\mathbf{x}_0) = \mathbf{x}_t$. Then the method of characteristics yields

$$\rho_t(\mathbf{x}) = \rho_B(\Phi_t^{-1}(\mathbf{x})) \exp \left(- \int_0^t \nabla_{\mathbf{x}} \cdot \mathbf{F}(\Phi_s(\Phi_t^{-1}(\mathbf{x})), \vartheta_s) ds \right), \quad \text{for all } (t, \mathbf{x}) \in [0, T] \times \mathbb{R}^d. \quad (3.7)$$

This immediately implies mass conservation and, by the assumptions on \mathbf{F} , propagation of spatial regularity. The dropout analogue of (3.6) replaces \mathbf{F} by $\hat{\mathbf{F}}$:

$$\begin{cases} \partial_t \hat{\rho}_t(\mathbf{x}) + \nabla_{\mathbf{x}} \cdot (\hat{\mathbf{F}}_t(\mathbf{x}, \vartheta_t) \hat{\rho}_t(\mathbf{x})) = 0, & \text{in } [0, T] \times \mathbb{R}^d \\ \hat{\rho}_0(\mathbf{x}) = \rho_B(\mathbf{x}). \end{cases} \quad (3.8)$$

Existence and uniqueness for (3.8) follow verbatim from the same hypotheses, with flow $\hat{\Phi}_t$ and representation analogous to (3.7).

Remark 3.4. *For probability measures $\mu, \nu \in \mathcal{P}(\mathbb{R}^d)$ with finite second moments, the 2-Wasserstein distance is defined by*

$$W_2^2(\mu, \nu) := \inf_{\pi \in \Pi(\mu, \nu)} \int_{\mathbb{R}^d \times \mathbb{R}^d} |\mathbf{x} - \mathbf{y}|^2 d\pi(\mathbf{x}, \mathbf{y}),$$

with $\Pi(\mu, \nu) := \{\pi \in \mathcal{P}(\mathbb{R}^d \times \mathbb{R}^d) : \pi(\cdot, \mathbb{R}^d) = \mu, \pi(\mathbb{R}^d, \cdot) = \nu\}$. For $d\mu_B := \rho_B dx$, $\mu_t := (\Phi_t)_\# \mu_B$ and $\hat{\mu}_t := (\hat{\Phi}_t)_\# \mu_B$, the coupling $(\Phi_t, \hat{\Phi}_t)_\# \mu_B \in \Pi(\mu_t, \hat{\mu}_t)$ yields

$$W_2^2(\mu_t, \hat{\mu}_t) \leq \int_{\mathbb{R}^d} \|\Phi_t(\mathbf{x}_0) - \hat{\Phi}_t(\mathbf{x}_0)\|^2 \rho_B(\mathbf{x}_0) d\mathbf{x}_0.$$

By virtue of [Theorem 3.1](#) it holds $\mathbb{E}_\omega[\|\Phi_t(\mathbf{x}_0) - \hat{\Phi}_t(\mathbf{x}_0)\|^2] \leq hS(\mathbf{x}_0, \vartheta)$, so we deduce

$$\mathbb{E}_\omega[W_2(\rho_t, \hat{\rho}_t)] \leq \sqrt{h} \left(\int_{\mathbb{R}^d} S(\mathbf{x}_0, \vartheta) \rho_B(\mathbf{x}_0) d\mathbf{x}_0 \right)^{1/2}$$

and, in particular, $\mathbb{E}_\omega[W_2(\rho_t, \hat{\rho}_t)] < +\infty$ if $S(\cdot, \vartheta) \in L^1(\rho_B)$.

The next result provides a pointwise error estimate, obtained by tracing backward in time the two characteristics that originate at any \mathbf{x} :

Theorem 3.5. Assume [\(A2\)](#). For any $\rho_B \in \mathcal{C}^{0,1}(\mathbb{R}^d)$ and $\vartheta \in L^\infty(0, T; \Theta)$ there exists $C(\rho_B, \vartheta) > 0$, independent of h , such that ρ and $\hat{\rho}$ solving [\(3.6\)](#)–[\(3.8\)](#) satisfy for all $(t, \mathbf{x}) \in [0, T] \times \mathbb{R}^d$ and $h > 0$,

$$\mathbb{E}_\omega[|\rho_t(\mathbf{x}) - \hat{\rho}_t(\mathbf{x})|^2] \leq C(\rho_B, \vartheta) (S(\mathbf{x}, \vartheta_{t-\cdot}) + 1) h, \quad (3.9)$$

where S is given by [Theorem 3.1](#), and $s \in [0, t] \mapsto \vartheta_{t-s}$ denotes the time-reversed control on $[0, t]$.

The explicit value of $C(\rho_B, \vartheta)$ can be found in the proof of the theorem.

Although [\(3.9\)](#) is pointwise, its RHS grows at most linearly on $\|\mathbf{x}\|$ through $S(\mathbf{x}, \vartheta_{t-\cdot})$ —see [\(4.1\)](#)—which allows extension to global metrics like total variation (equivalently, L^1 -distance between densities) under additional support/moment control:

Corollary 3.6. Assume [\(A2\)](#). If ρ_B has finite q -th moment for some $q > 0$, then there exists $K(\rho_B, \vartheta, T, q) > 0$, independent of h , such that for all $t \in [0, T]$,

$$\mathbb{E}_\omega[\|\rho_t - \hat{\rho}_t\|_{L^1(\mathbb{R}^d)}] \leq K h^{\frac{q}{2q+2d+2}}. \quad (3.10)$$

In particular, as $q \rightarrow \infty$, the exponent tends to $1/2$.

3.3. Training. Supervised learning is essentially an optimal control problem. Consider the system

$$\begin{cases} \dot{\mathbf{x}}_{m,t} = \sum_{i \in [p]} \mathbf{f}_i(\mathbf{x}_{m,t}, \vartheta_{i,t}) & t \in [0, T], \\ \mathbf{x}_{m,0} = \mathbf{x}_m, \end{cases} \quad (3.11)$$

for $m \in [n_d]$ and fixed inputs $\mathbf{x}_m \in \mathbb{R}^d$. The admissible controls are $\vartheta \in L^\infty(0, T; \Theta) \subset L^2(0, T; \Theta)$ so that the well-posedness in [Section 2.1](#) holds for any ϑ . We denote by $\mathbf{x}_{m,t} \equiv \mathbf{x}_{m,\vartheta,t}$ the corresponding solutions. The training objective is

$$\min_{\vartheta \in L^\infty(0, T; \Theta)} J(\vartheta) := \frac{\alpha}{2} \|\vartheta\|_{L^2(0, T; \Theta)}^2 + \sum_{m \in [n_d]} g_m(\mathbf{x}_{m,T}) + \beta \sum_{m \in [n_d]} \int_0^T \ell_m(\mathbf{x}_{m,t}) dt. \quad (3.12)$$

with $\alpha > 0$ and $\beta \geq 0$ fixed, and $\ell_m, g_m \in \mathcal{C}_{\text{loc}}^{1,1}(\mathbb{R}^d; \mathbb{R}_{\geq 0})$ are convex functions for each $m \in [n_d]$. The first two terms in [\(3.12\)](#) are standard in supervised learning: a quadratic Tikhonov regularization on the control and a terminal loss on the network outputs. The third term is a running cost that promotes accuracy along the entire trajectory (i.e. across layers in the neural network view); see [\[18\]](#) for analysis and further discussion.

We assume

$$\{\mathbf{f}_i(\mathbf{x}, \theta_i) : \theta_i \in \Theta_i\} \text{ is convex for each } \mathbf{x} \in \mathbb{R}^d \text{ and } i \in [p]. \quad (3.13)$$

By the direct method in the calculus of variations, together with [\(3.13\)](#), there exists $\vartheta^* \in L^\infty(0, T; \Theta)$ minimizing J (see [\[62, Chapter 2\]](#) and [Remark 3.9](#) below).

Following [Section 2](#), we incorporate dropout into [\(3.11\)](#). This yields

$$\begin{cases} \dot{\hat{\mathbf{x}}}_{m,t} = \sum_{i \in \mathcal{B}_{\omega_{k_t}}} \frac{1}{\pi_i} \mathbf{f}_i(\hat{\mathbf{x}}_{m,t}, \vartheta_{i,t}), & t \in [0, T], \\ \hat{\mathbf{x}}_{m,0} = \mathbf{x}_m. \end{cases} \quad (3.14)$$

The objective function is

$$\min_{\vartheta \in L^\infty(0, T; \Theta)} \hat{J}(\vartheta) := \frac{\alpha}{2} \|\vartheta\|_{L^2(0, T; \Theta)}^2 + \sum_{m \in [n_d]} g_m(\hat{\mathbf{x}}_{m,T}) + \beta \sum_{m \in [n_d]} \int_0^T \ell_m(\hat{\mathbf{x}}_{m,t}) dt. \quad (3.15)$$

Again, there exists $\hat{\vartheta}^* \in L^\infty(0, T; \Theta)$ minimizing \hat{J} . The deviation between the respective optimal trajectories that solve [\(3.11\)](#) and [\(3.14\)](#) can be quantified via [Corollary 3.2](#)—provided that [\(A1\)](#) is satisfied—as

$$\max_{t \in [0, T]} \mathbb{E}_\omega[\|\mathbf{x}_{m,\vartheta^*,t} - \hat{\mathbf{x}}_{m,\hat{\vartheta}^*,t}\|^2] \leq S(\mathbf{x}_m, \vartheta^*) \wedge S(\mathbf{x}_m, \hat{\vartheta}^*) h + C(\vartheta^*, \hat{\vartheta}^*) \|\vartheta^* - \hat{\vartheta}^*\|_{L^1(0, T; \Theta)}^2.$$

The second term in the RHS is independent of h and scales with the L^1 -distance between ϑ^* and $\hat{\vartheta}^*$. However, the two minima get close as h decays:

Proposition 3.7. *Let J and \hat{J} be given by (3.12) and (3.15), and let $\vartheta^*, \hat{\vartheta}^* \in L^\infty(0, T; \Theta)$ be respective optimal controls. Then*

$$\mathbb{E}_\omega \left[|J(\vartheta^*) - \hat{J}(\hat{\vartheta}^*)|^2 \right] \leq 4 \sum_{m \in [n_d]} (\beta^2 \lambda_{\ell_m, B_R}^2 T^2 + \lambda_{g_m, B_R}^2) \left(S(\mathbf{x}_m, \vartheta^*) + S(\mathbf{x}_m, \hat{\vartheta}^*) \right) h,$$

where $B_R \subset \mathbb{R}^d$ contains all trajectories \mathbf{x}_m and $\hat{\mathbf{x}}_m$ for $m \in [n_d]$, and S is given by Theorem 3.1.

A cornerstone in optimal control is Pontryagin's Maximum Principle (PMP). We will use this result to quantify the distance between ϑ^* and $\hat{\vartheta}^*$. First, we define the Hamiltonian $H : \mathbb{R}^{2dn_d} \times \Theta \rightarrow \mathbb{R}$ associated with (3.12):

$$H((\mathbf{x}_m, \mathbf{p}_m)_{m \in [n_d]}, \theta) = \sum_{m \in [n_d]} (\langle \mathbf{F}(\mathbf{x}_m, \theta), \mathbf{p}_m \rangle + \beta \ell_m(\mathbf{x}_m)) + \frac{\alpha}{2} \|\theta\|^2. \quad (3.16)$$

For each $m \in [n_d]$, the forward equation (3.11) can then be expressed compactly as

$$\dot{\mathbf{x}}_{m,t} = \nabla_{\mathbf{p}_m} H((\mathbf{x}_m, \mathbf{p}_m)_{m \in [n_d]}, \vartheta_t), \quad \mathbf{x}_{m,0} = \mathbf{x}_m, \quad (3.17)$$

where $\mathbf{p}_{m,t}$ is the solution of the adjoint equation defined by

$$\dot{\mathbf{p}}_{m,t} = -\nabla_{\mathbf{x}_m} H((\mathbf{x}_m, \mathbf{p}_m)_{m \in [n_d]}, \vartheta_t), \quad \mathbf{p}_{m,T} = \nabla_{g_m}(\mathbf{x}_m, T).$$

More precisely, by inserting (3.16) into the adjoint equation we arrive at

$$\begin{cases} \dot{\mathbf{p}}_{m,t} &= -\nabla_{\mathbf{x}} \mathbf{F}(\mathbf{x}_{m,t}, \vartheta_t)^\top \mathbf{p}_{m,t} - \beta \nabla \ell_m(\mathbf{x}_{m,t}), & t \in [0, T], \\ \mathbf{p}_{m,T} &= \nabla g_m(\mathbf{x}_m, T). \end{cases} \quad (3.18)$$

Note that $t \mapsto \nabla_{\mathbf{x}} \mathbf{F}(\cdot, \vartheta_t)$ is defined a.e. and uniformly bounded for all $t \in [0, T]$ thanks to (2.2). Consequently, Lemma 8.1 guarantees a unique adjoint $\mathbf{p}_m \in \mathcal{AC}([0, T]; \mathbb{R}^d)$, because:

- (1) the map $t \mapsto \nabla \ell_m(\mathbf{x}_{m,t})$ is continuous in $[0, T]$, for being $\ell_m \in \mathcal{C}^1$ and $\mathbf{x}_m \in \mathcal{AC}([0, T]; \mathbb{R}^d)$;
- (2) $\|\nabla_{\mathbf{x}} \mathbf{F}(\mathbf{x}_{m,t}, \vartheta_t)\| \leq \lambda_{\mathbf{F}, \mathbf{x}, \vartheta}$ for almost every $t \in [0, T]$, by Rademacher's theorem applied to (2.2).

Similarly, we define the Hamiltonian $\hat{H} : \mathbb{R}^{2dn_d} \times \Theta \rightarrow \mathbb{R}$ associated with (3.15):

$$\hat{H}((\mathbf{x}_m, \mathbf{p}_m)_{m \in [n_d]}, \theta) = \sum_{m \in [n_d]} \left(\langle \hat{\mathbf{F}}(\mathbf{x}_m, \theta), \mathbf{p}_m \rangle + \beta \ell_m(\mathbf{x}_m) \right) + \frac{\alpha}{2} \|\theta\|^2,$$

and the adjoint equation for each $m \in [n_d]$,

$$\begin{cases} \dot{\hat{\mathbf{p}}}_{m,t} &= -\nabla_{\mathbf{x}} \hat{\mathbf{F}}(\hat{\mathbf{x}}_{m,t}, \vartheta_t)^\top \hat{\mathbf{p}}_{m,t} - \beta \nabla \ell_m(\hat{\mathbf{x}}_{m,t}), & t \in [0, T], \\ \hat{\mathbf{p}}_{m,T} &= \nabla g_m(\hat{\mathbf{x}}_m, T). \end{cases} \quad (3.19)$$

Here, $\hat{\mathbf{x}}_m$ solves (3.14) with the same control $\vartheta \in L^\infty(0, T; \Theta)$ used in (3.11). Again, Lemma 8.1 ensures existence and uniqueness of a solution $\hat{\mathbf{p}}_m \in \mathcal{AC}([0, T]; \mathbb{R}^d)$ to (3.19).

We assume $\hat{\mathbf{F}}$ takes the same batch values as in (3.14): the sequence $(\omega_k)_{k \in [n_s]}$ is sampled in (3.14) and then kept fixed for all forward-adjoint passes and across all training iterations. The case of per-iteration resampling—drawing an independent schedule at each iteration—will be discussed in Section 7.

To quantify variance of $\nabla_{\mathbf{x}} \hat{\mathbf{F}}$ along trajectories, we now define $\Gamma : [0, T] \times \mathbb{R}^d \times L^\infty(0, T; \Theta) \rightarrow \mathbb{R}_{\geq 0}$ by

$$\Gamma_t(\mathbf{x}_0, \vartheta) := \mathbb{E}_\omega \left[\left\| \nabla_{\mathbf{x}} \mathbf{F}(\mathbf{x}_t, \vartheta_t) - \nabla_{\mathbf{x}} \hat{\mathbf{F}}_t(\mathbf{x}_t, \vartheta_t) \right\|^2 \right], \quad (3.20)$$

where \mathbf{x}_t solves (FM) with control ϑ and initial value \mathbf{x}_0 . Assuming (A2), a similar argument to (3.3) gives

$$\Gamma(\mathbf{x}_0, \vartheta) \in L^1(0, T), \quad \text{for all } \mathbf{x}_0 \in \mathbb{R}^d \text{ and } \vartheta \in L^\infty(0, T; \Theta).$$

The following result is the analogous to Corollary 3.2 for backward dynamics: it bounds the expected squared distance between the two adjoint states taking different controls.

Proposition 3.8. Assume (A2), (A3). Let $\mathbf{x}_0 \in \mathbb{R}^d$ and $\ell, g \in \mathcal{C}_{\text{loc}}^{1,1}(\mathbb{R}^d)$ convex. For $j = 1, 2$, let \mathbf{x}_{ϑ_j} and $\hat{\mathbf{x}}_{\vartheta_j}$ be the solutions of (FM) and (RM) with initial condition \mathbf{x}_0 and control $\vartheta_j \in L^\infty(0, T; \Theta)$, and let \mathbf{p}_{ϑ_j} and $\hat{\mathbf{p}}_{\vartheta_j}$ solve the adjoint systems (3.18)–(3.19). Then there exists $C > 0$, independent of h , such that for all $0 < h \leq T$,

$$\max_{t \in [0, T]} \mathbb{E}_\omega [\|\mathbf{p}_{\vartheta_1, t} - \hat{\mathbf{p}}_{\vartheta_2, t}\|^2] \leq C \min_{j=1,2} \left(\sqrt{\|\Gamma(\mathbf{x}_0, \vartheta_j)\|_{L^1(0, T)}} + S(\mathbf{x}_0, \vartheta_j) \right) h + C \|\vartheta_1 - \vartheta_2\|_{L^1(0, T; \Theta)}^2,$$

where Γ, S are given by (3.20) and (3.4)–(4.1).

The extension to multiple data points follows by applying the bound to each initial condition and then taking a supremum or aggregating. The adjoint state yields an optimality condition via Pontryagin's Maximum Principle:

Pontryagin Maximum Principle (PMP). Let $\mathbf{x}_{m, \vartheta}$ and $\mathbf{p}_{m, \vartheta}$ solve (3.11)–(3.18) with control $\vartheta \in L^\infty(0, T; \Theta)$ for each $m \in [n_d]$. If $\vartheta^* \in L^2(0, T; \Theta)$ is optimal for (3.12) then, for a.e. $t \in [0, T]$,

$$H\left((\mathbf{x}_{m, \vartheta^*, t}, \mathbf{p}_{m, \vartheta^*, t})_{m \in [n_d]}, \vartheta_t^*\right) = \min_{\theta \in \Theta} H\left((\mathbf{x}_{m, \vartheta^*, t}, \mathbf{p}_{m, \vartheta^*, t})_{m \in [n_d]}, \theta\right), \quad (3.21)$$

and, a posteriori, $\vartheta^* \in L^\infty(0, T; \Theta)$.

A proof can be found in [45, Section 4] or [62, Section 2]. By the L^2 -regularization terms in (3.12) and (3.15), the first-order optimality conditions yield the following implicit relations, valid for a.e. $t \in [0, T]$:

$$\vartheta_t^* = -\frac{1}{\alpha} \sum_{m \in [n_d]} \nabla_\theta \mathbf{F}(\mathbf{x}_{m, \vartheta^*, t}, \vartheta_t^*)^\top \mathbf{p}_{m, \vartheta^*, t}, \quad \hat{\vartheta}_t^* = -\frac{1}{\alpha} \sum_{m \in [n_d]} \nabla_\theta \hat{\mathbf{F}}(\hat{\mathbf{x}}_{m, \hat{\vartheta}^*, t}, \hat{\vartheta}_t^*)^\top \hat{\mathbf{p}}_{m, \hat{\vartheta}^*, t}. \quad (3.22)$$

Remark 3.9 (A posteriori regularity). From (3.22), we deduce that $\vartheta^* \in L^\infty(0, T; \Theta)$ —the same holds for $\hat{\vartheta}^*$ —because:

- (1) By Rademacher's theorem and (A1), each term $\nabla_\theta \mathbf{F}(\mathbf{x}_{m, \vartheta^*, t}, \vartheta_t^*)$ is uniformly bounded in $[0, T]$;
- (2) Each trajectory $\mathbf{p}_{m, \vartheta^*, t}$ is bounded (see Lemma 8.5 in Section 8).

Remark 3.10. Whenever there exists $M \in [0, \alpha/n_d)$ such that, uniformly in $t \in [0, T]$ and $m \in [n_d]$,

$$\nabla_\theta^2 \langle \mathbf{F}(\mathbf{x}_{m, t}, \vartheta_t), \mathbf{p}_{m, t} \rangle + M \text{Id} \quad \text{is positive semidefinite}, \quad (3.23)$$

then the Hamiltonian (3.16) is $(\alpha - n_d M)$ -strongly convex in $\theta \in \Theta$, in the sense that for every $\theta_1, \theta_2 \in \Theta$ and a.e. $t \in [0, T]$,

$$H(\cdot, \theta_2) \geq H(\cdot, \theta_1) + \langle \nabla_\theta H(\cdot, \theta_1), \theta_2 - \theta_1 \rangle + \frac{\alpha - n_d M}{2} \|\theta_2 - \theta_1\|^2. \quad (3.24)$$

In particular, if \mathbf{F} is affine in θ then H is α -strongly convex because we can take $M = 0$. Condition (3.23) guarantees a unique minimizer in (3.21) for almost every t . We emphasize that it does not imply global (strong) convexity of the functional $J(\vartheta)$ without additional linear-quadratic structure.

In what follows, we rely on an estimate on the difference of gradients derived in Lemma 8.7. We use it to bound the expected squared distance between the optimal controls of (3.12) and (3.15).

Theorem 3.11. Suppose (A1)–(A5) hold, and

$$\theta \mapsto \mathbf{F}(\mathbf{x}, \theta) \text{ is affine}. \quad (3.25)$$

Let ϑ^* and $\hat{\vartheta}^*$ be minimizers of (3.12)–(3.15). Then there exist non-negative $C_1(\vartheta)$ and $C_2(\vartheta)$, independent of h , such that

$$\mathbb{E}_\omega \left[\|\vartheta^* - \hat{\vartheta}^*\|_{L^2(0, T; \Theta)}^2 \right] \leq \min_{\vartheta \in \{\vartheta^*, \hat{\vartheta}^*\}} \frac{C_1(\vartheta) + h C_2(\vartheta)}{\alpha^2}. \quad (3.26)$$

Explicit admissible expressions for $C_1(\vartheta^*)$ and $C_2(\vartheta^*)$ are provided at the end of the proof.

Remark 3.12 (Beyond affinity). The proof above only uses (3.25) to obtain strong monotonicity of $\nabla_\theta H$ in θ . If, more generally, (3.23) holds with some $M \in [0, \alpha/n_d)$, the same argument yields

$$\mathbb{E}_\omega \left[\|\vartheta^* - \hat{\vartheta}^*\|_{L^2(0, T; \Theta)}^2 \right] \leq \min_{\vartheta \in \{\vartheta^*, \hat{\vartheta}^*\}} \frac{C_1(\vartheta) + h C_2(\vartheta)}{(\alpha - n_d M)^2}.$$

Remark 3.13. We now discuss the numerical computation of the minimizers. In standard practice, one approximates ϑ^* via gradient-descent iterations

$$\vartheta_{k+1} = \vartheta_k - \eta \nabla J(\vartheta_k), \quad k \geq 0, \quad (3.27)$$

with $\eta > 0$, where the Riesz representative of the Fréchet derivative is

$$\nabla J(\vartheta)_t = \alpha \vartheta_t + \sum_{m \in [n_d]} \nabla_{\theta} \mathbf{F}(\mathbf{x}_{m,t}, \vartheta_t)^\top \mathbf{p}_{m,t} \in L^2(0, T; \Theta) \quad \text{for a.e. } t \in [0, T]. \quad (3.28)$$

We consider the analogous iteration for \hat{J} (same stepsize η) and compare the two sequences.

Under (A1)–(A5), the map ∇J is Lipschitz on $L^2(0, T; \Theta)$. For any $\eta \in (0, 2/\lambda_{\nabla J})$ the gradient-descent scheme satisfies $J(\vartheta_{k+1}) \leq J(\vartheta_k)$, which yields uniform L^2 bounds on the iterates. By Grönwall, all forward and adjoint trajectories stay in a common compact set, so the constants entering the gap estimate between ∇J and $\nabla \hat{J}$ are uniform along the iterations. Then subtracting the two updates leads to a one-step recursion of the form

$$\mathbb{E}_\omega [\|\vartheta_k - \hat{\vartheta}_k\|_{L^2(0, T; \Theta)}^2] \leq \text{factor}(\eta, \lambda_{\nabla J}) \cdot \mathbb{E}_\omega [\|\vartheta_k - \hat{\vartheta}_k\|_{L^2}^2] + C_1(\vartheta_0) + h C_2(\vartheta_0) \quad (3.29)$$

for all $k \geq 0$, with $C_1(\vartheta_0)$ and $C_2(\vartheta_0)$ positive and independent of h . Unrolling the recursion shows that the dependence on k is at most geometric, with a ratio determined solely by η and $\lambda_{\nabla J}$, while for fixed η and k the dependence on h is affine. The derivation of (3.29) follows the standard steps mentioned.

4. DESIGN

We have performed error analysis for the forward pass and training of the dropout model independently of the specific random batch scheme (batch sizes, number of batches, and sampling distribution). We now turn to the design of the random batch decomposition.

4.1. Rate vs Scheme. Fix $\mathbf{x}_0 \in \mathbb{R}^d$ and $\vartheta \in L^\infty(0, T; \Theta)$, and recall Theorem 3.1. An explicit choice of the factor S (see the proof in Section 8.3 for its derivation) is

$$S(\mathbf{x}_0, \vartheta) := \frac{2\lambda_{\mathbf{F}, \mathbf{x}, \vartheta}}{\pi_{\min}} e^{\frac{2\lambda_{\mathbf{F}, \mathbf{x}, \vartheta} T}{\pi_{\min}}} \left[T \|\Lambda(\mathbf{x}_0, \vartheta)\|_{L^1} \sqrt{\sum_{j \in [n_b]} q_j^{-1}} + \sqrt{T \|\Lambda(\mathbf{x}_0, \vartheta)\|_{L^1}} \left(\|\mathbf{x}_0\| + \frac{\lambda_{\mathbf{F}, 0, \vartheta}}{\lambda_{\mathbf{F}, \mathbf{x}, \vartheta}} \right) \right] \quad (4.1)$$

whenever $\lambda_{\mathbf{F}, \mathbf{x}, \vartheta} > 0$, and

$$S(\mathbf{x}_0, \vartheta) := 2 \frac{\lambda_{\mathbf{F}, 0, \vartheta}}{\pi_{\min}} \sqrt{T \|\Lambda(\mathbf{x}_0, \vartheta)\|_{L^1}}$$

whenever $\lambda_{\mathbf{F}, \mathbf{x}, \vartheta} = 0$. All quantities are defined in (2.2)–(2.6) and (3.2).

Following Theorem 3.1, reducing the trajectory error between (FM) and (RM) amounts to designing the batches and sampling so as to decrease S . The expression in (4.1) highlights three design levers:

- (1) the time-integrated variance $\|\Lambda\|_{L^1(0, T)}$;
- (2) the sampling imbalance $\sum_j q_j^{-1}$ (minimized by uniform $q_j \equiv 1/n_b$);
- (3) the minimal inclusion probability π_{\min} .

A sensible scheme should jointly lower $\|\Lambda\|_{L^1(0, T)}$, avoid highly unbalanced q_j , and keep π_{\min} bounded away from 0. For each canonical scheme below, we compute the three levers and estimate S .

(1) **Single-batch** ($n_b = 1$, $\mathcal{B}_1 = [p]$, $q_1 = 1$). Every neuron is always active.

(2) **Drop-one** ($n_b = p$, $\mathcal{B}_j = [p] \setminus \{j\}$). Neuron i is inactive if and only if $\omega = i$.

(3) **Pick-one** ($n_b = p$, $\mathcal{B}_j = \{j\}$). Neuron i is active if and only if $\omega = i$.

(4) **Balanced batches of fixed size.** Fix $r \in [p-1]$ and sample \mathcal{B}_j uniformly among all subsets of $[p]$ with size r , so $n_b = \binom{p}{r}$ and $q_j = \binom{p}{r}^{-1}$. Note that we get (2) when $r = p-1$, and (3) when $r = 1$.

(5) **Balanced disjoint batches of fixed size.** Partition $[p]$ into $n_b = p/r$ disjoint batches of size r (assume r divides p) and sample one batch uniformly at each subinterval.

(6) **All subsets uniformly** ($n_b = 2^p$). The batches \mathcal{B}_j range over all (possibly empty) subsets of $[p]$ with equal probability $q_j = 2^{-p}$.

(7) **Bernoulli dropout.** In the usual implementation of dropout, neurons are masked by i.i.d. random variables $b_i^{(k)} \sim \text{Bernoulli}(q_B)$ with $q_B \in (0, 1]$. In continuous-time setting, we write

$$\hat{\mathbf{F}}_t^{sd} = \frac{1}{q_B} \sum_{i \in [p]} b_i^{(k_t)} \mathbf{f}_{i,t}, \quad k_t := 1 + \lfloor t/h \rfloor. \quad (4.2)$$

From an RBM perspective, this scheme corresponds to “all subsets” with a specific sampling law:

Proposition 4.1. *Within the RBM framework (2.5)–(2.7), let the batches \mathcal{B}_j range over all (possibly empty) subsets of $[p]$ with sampling probability*

$$\mathbb{P}(\omega = j) = q_B^{|\mathcal{B}_j|} (1 - q_B)^{p - |\mathcal{B}_j|}.$$

Then $\pi_i = q_B$ for every i , and (RM) coincides with the standard Bernoulli dropout field (4.2), i.e.

$$\hat{\mathbf{F}}_t = \hat{\mathbf{F}}_t^{sd} \quad \text{for all } t \in [0, T].$$

In particular, at $q_B = 2^{-1}$ the sampling law is uniform over all subsets: $q_j = 2^{-p}$, i.e. we recover (6).

To compute the three design levers on the canonical schemes we have considered, it is convenient to introduce the neuron-wise mean and variance along the trajectory,

$$\mu_t(\mathbf{x}_0, \vartheta) := \left\| \frac{1}{p} \sum_{i \in [p]} \mathbf{f}_i(\mathbf{x}_t, \vartheta_{i,t}) \right\|, \quad \sigma_t^2(\mathbf{x}_0, \vartheta) := \frac{1}{p} \sum_{j \in [p]} \left\| \mathbf{f}_j(\mathbf{x}_t, \vartheta_{j,t}) - \frac{1}{p} \sum_{i \in [p]} \mathbf{f}_i(\mathbf{x}_t, \vartheta_{i,t}) \right\|^2.$$

Since $\sup_{t \in [0, T]} \|\mathbf{x}_t\| < \infty$ (see Lemma 8.4 ahead) and $\vartheta \in L^\infty$, we get

$$\mu_\star(\mathbf{x}_0, \vartheta) := \sup_{t \in [0, T]} \left\| \frac{1}{p} \sum_{i \in [p]} \mathbf{f}_i(\mathbf{x}_t, \vartheta_{i,t}) \right\| < \infty, \quad \sigma_\star^2(\mathbf{x}_0, \vartheta) := \sup_{t \in [0, T]} \sigma_t^2(\mathbf{x}_0, \vartheta) < \infty. \quad (4.3)$$

In Table 1 we summarize the results for uniform sampling $q_j = n_b^{-1}$, and the growth of S as $p \rightarrow \infty$. Complete derivations are in Section 8.6.

Scheme	Λ_t	$\sum_j q_j^{-1}$	π_{\min}	Order of S in p
Single-batch	0	1	1	0
Drop-one	$\frac{p^2}{(p-1)^2} \sigma_t^2$	p^2	$1 - 1/p$	$\mathcal{O}(\lambda p e^{2\lambda T})$
Pick-one	$p^2 \sigma_t^2$	p^2	$1/p$	$\mathcal{O}(\lambda p^4 e^{2\lambda p T})$
Balanced size r (all r -subsets)	$\frac{p^2(p-r)}{(p-1)r} \sigma_t^2$	$\binom{p}{r}^2$	r/p	$\mathcal{O}(\lambda \frac{p^{r+3}}{r^2} e^{2\lambda p T/r})$
Balanced size r (disjoint)	$\frac{p^2(p-r)}{(p-1)r} \sigma_t^2$	$\left(\frac{p}{r}\right)^2$	r/p	$\mathcal{O}(\lambda \frac{p^4}{r^3} e^{2\lambda p T/r})$
All subsets	$p(\sigma_t^2 + \mu_t^2)$	2^{2p}	$1/2$	$\mathcal{O}(\lambda p e^{4\lambda + p \log 2})$
Bernoulli dropout (q_B)	$\frac{1-q_B}{q_B} p(\sigma_t^2 + \mu_t^2)$	$\frac{1}{q_B^p (1-q_B)^p}$	q_B	$\mathcal{O}(\frac{\lambda p}{(q_B(1-q_B))^{p/2}} e^{2\lambda T/q_B})$

TABLE 1. Design levers and scaling of S as $p \rightarrow \infty$ for uniform $q_j = n_b^{-1}$. Note that $\lambda \equiv \lambda_{\mathbf{F}, \mathbf{x}, \vartheta}$ also depends on p .

For balanced batches of size r , S decreases monotonically as r increases, but the per-step computational cost grows with r , so larger batches are not necessarily better. This motivates a cost–accuracy trade-off analysis, which we carry out in the next subsection.

4.2. A cost–accuracy trade-off. The dropout model (RM) is useful only if it attains a prescribed accuracy at a lower computational cost than the full model (FM). We quantify cost with the total expected number of elementary neuron evaluations over $[0, T]$:

$$C = (\text{number of discretization steps}) \times (\text{mean number of neurons evaluated per step}). \quad (4.4)$$

To keep the model transparent, we take the following simplifications:

- (1) Ignore hardware-dependent effects (cache, vectorization, etc.), so C is a machine-independent proxy for running time.

- (2) One call to \mathbf{F} costs p neuron operations; one call to $\hat{\mathbf{F}}$ costs the corresponding batch size $|\mathcal{B}_{\omega_{k_t}}|$. Let $r \in [p]$ be the mean batch size,

$$r := \sum_{j \in [n_b]} q_j |\mathcal{B}_j|.$$

- (3) Integrate the model with explicit Euler of fixed step $\Delta t > 0$. To ensure the solver takes at least one step per interval and to prevent numerical instabilities, impose

$$\Delta t = \gamma h, \quad 0 < \gamma \leq 1 \wedge \frac{c_{\text{stab}} \pi_{\min}}{\lambda_{\mathbf{F}, \mathbf{x}, \vartheta}}, \quad (4.5)$$

where $c_{\text{stab}} > 0$ is the stability constant of (RM) for the Euler method.

Therefore (4.4) becomes, for (RM),

$$\mathbf{C}_{\text{RM}} = \frac{T}{\Delta t} \times r = \frac{T}{\gamma h} \times r. \quad (4.6)$$

Let $\hat{\mathbf{x}}^{\Delta t}$ be the Euler trajectory for (RM) with step Δt . By Theorem 3.1 and explicit-Euler global error, the RMS (root mean square) error can be decomposed as

$$\begin{aligned} \sqrt{\max_{t \in [0, T]} \mathbb{E}_{\omega} [\|\mathbf{x}_t - \hat{\mathbf{x}}_t^{\Delta t}\|^2]} &\leq \underbrace{\sqrt{\max_{t \in [0, T]} \mathbb{E}_{\omega} [\|\mathbf{x}_t - \hat{\mathbf{x}}_t\|^2]}}_{\text{model error}} + \underbrace{\max_{t \in [0, T]} \|\hat{\mathbf{x}}_t - \hat{\mathbf{x}}_t^{\Delta t}\|}_{\text{integration error}} \\ &\leq \sqrt{S(\mathbf{x}_0, \vartheta) h} + c_{\text{int}} \gamma h =: \mathcal{E}(h), \end{aligned} \quad (4.7)$$

where we have introduced the first-order integration constant for (RM) along the trajectory,

$$c_{\text{int}} = \frac{\lambda_{\nabla_{\mathbf{x}} \mathbf{F}, \mathbf{x}, \vartheta}}{2 \pi_{\min}} \exp\left(\frac{\lambda_{\mathbf{F}, \mathbf{x}, \vartheta}}{\pi_{\min}} T\right) \left[\exp\left(\frac{\lambda_{\mathbf{F}, \mathbf{x}, \vartheta}}{\pi_{\min}} T\right) - 1 \right] \left(\|\mathbf{x}_0\| + \frac{\lambda_{\mathbf{F}, 0, \vartheta}}{\lambda_{\mathbf{F}, \mathbf{x}, \vartheta}} \right). \quad (4.8)$$

It follows:

Proposition 4.2. Fix $\mathbf{x}_0 \in \mathbb{R}^d$ and $\vartheta \in L^\infty(0, T; \Theta)$ and let \mathbf{x} solve (FM) and $\hat{\mathbf{x}}^{\Delta t}$ be the Euler trajectory for (RM) with step Δt and γ as in (4.5). For a prescribed tolerance $\varepsilon > 0$,

$$h^*(\varepsilon) := \arg \min_{h > 0} \{\mathbf{C}_{\text{RM}} : \mathcal{E}(h) \leq \varepsilon\} = \frac{4\varepsilon^2}{S} \left(1 + \sqrt{1 + \frac{4c_{\text{int}}\gamma\varepsilon}{S}} \right)^{-2}, \quad (4.9)$$

where $S \equiv S(\mathbf{x}_0, \vartheta)$ is defined in (4.1) and $c_{\text{int}} \geq 0$ is the first-order integration constant for (RM). Moreover, the minimal cost is

$$\mathbf{C}_{\text{RM}}^*(\varepsilon) = \frac{T r}{\gamma h^*} = \frac{T r S}{4 \gamma \varepsilon^2} \left(1 + \sqrt{1 + \frac{4c_{\text{int}}\gamma\varepsilon}{S}} \right)^2. \quad (4.10)$$

From (4.9) we get two asymptotic regimes. Define the critical tolerance

$$\varepsilon_c := \frac{S(\mathbf{x}_0, \vartheta)}{c_{\text{int}} \gamma} \quad \text{with} \quad h^*(\varepsilon_c) = \frac{\varepsilon_c^2}{S} \cdot \frac{4}{(1 + \sqrt{5})^2} \approx 0.382 \frac{\varepsilon_c^2}{S}.$$

Then, using $(1 + \sqrt{1 + 4\varepsilon/\varepsilon_c})^2 \sim 4\varepsilon/\varepsilon_c$:

- (1) **High tolerance / discretization-limited** ($\varepsilon \gg \varepsilon_c$)

$$h^*(\varepsilon) \sim \frac{\varepsilon}{c_{\text{int}} \gamma}, \quad \mathbf{C}_{\text{RM}}^*(\varepsilon) \sim \frac{T r c_{\text{int}}}{\varepsilon}.$$

- (2) **High accuracy / variance-limited** ($\varepsilon \ll \varepsilon_c$)

$$h^*(\varepsilon) \sim \frac{\varepsilon^2}{S}, \quad \mathbf{C}_{\text{RM}}^*(\varepsilon) \sim \frac{T r S}{\gamma \varepsilon^2}.$$

Remark 4.3. If we simultaneously impose model error $\leq \varepsilon/2$ and integration error $\leq \varepsilon/2$, then

$$\bar{h} := \begin{cases} \frac{\varepsilon}{2 c_{\text{int}} \gamma}, & \text{if } \varepsilon \geq 2\varepsilon_c \quad (\text{discretization-limited}), \\ \frac{\varepsilon^2}{4 S(\mathbf{x}_0, \vartheta)}, & \text{if } \varepsilon \leq 2\varepsilon_c \quad (\text{variance-limited}), \end{cases} \quad (4.11)$$

ensures that $\mathcal{E}(\bar{h}) \leq \varepsilon$. Although \bar{h} is suboptimal, it is algebraically simpler than h^* .

We analyze now the relative cost between the random and the full models. For the latter, and given a tolerance $\varepsilon > 0$, the cost C_{FM} takes its optimal value at

$$C_{\text{FM}}^* = \frac{T p c_{\text{int,FM}}}{\varepsilon}, \quad (4.12)$$

being $c_{\text{int,FM}} \geq 0$ exactly as (4.8) but taking $\pi_{\min} = 1$. We deduce:

Proposition 4.4. *Let $\mathbf{x}^{\Delta t_{\text{FM}}}$ and $\hat{\mathbf{x}}^{\Delta t_{\text{RM}}}$ be Euler trajectories for (FM) and (RM) with steps Δt_{FM} and Δt_{RM} constrained as in (4.5). For a tolerance $\varepsilon > 0$, the optimal cost ratio is*

$$\frac{C_{\text{FM}}^*(\varepsilon)}{C_{\text{RM}}^*(\varepsilon)} = \frac{4 p c_{\text{int,FM}} \gamma \varepsilon}{r S \left(1 + \sqrt{1 + \frac{4 c_{\text{int,RM}} \gamma \varepsilon}{S}} \right)^2}. \quad (4.13)$$

Moreover, letting $\varepsilon_c := S/(c_{\text{int,RM}}\gamma)$ and $\kappa = \kappa(\pi_{\min}, \lambda_{\mathbf{F}, \mathbf{x}, \vartheta}, T) := \frac{1}{\pi_{\min}} \frac{e^{(\lambda_{\mathbf{F}, \mathbf{x}, \vartheta} / \pi_{\min})T} - 1}{e^{\lambda_{\mathbf{F}, \mathbf{x}, \vartheta} T} - 1} \geq \frac{1}{\pi_{\min}}$,

$$\frac{C_{\text{FM}}^*(\varepsilon)}{C_{\text{RM}}^*(\varepsilon)} \geq \begin{cases} \frac{p}{r \kappa}, & \text{if } \varepsilon \gg \varepsilon_c \quad (\text{discretization-limited}), \\ \frac{p c_{\text{int,FM}} \gamma \varepsilon}{r S}, & \text{if } \varepsilon \ll \varepsilon_c \quad (\text{variance-limited}). \end{cases}$$

Corollary 4.5. *Under the balanced choice of Remark 4.3 (model and integration errors $\leq \varepsilon/2$),*

$$\varepsilon \geq 2\varepsilon_c : \quad \frac{C_{\text{FM}}^*(\varepsilon)}{C_{\text{RM}}(\bar{h})} = \frac{p}{2 r \kappa}, \quad \varepsilon \leq 2\varepsilon_c : \quad \frac{C_{\text{FM}}^*(\varepsilon)}{C_{\text{RM}}(\bar{h})} = \frac{p c_{\text{int,FM}} \gamma \varepsilon}{4 r S},$$

where $C_{\text{RM}}(\bar{h}) = Tr/(\gamma \bar{h})$.

To conclude the comparative analysis, we note:

- (1) *Discretization-limited regime* ($\varepsilon \geq \varepsilon_c$): the random model is more cost-efficient than the full model whenever $r \ll p$ and κ is moderate (equivalently, π_{\min} is not too small), consistently with the ratio in (4.13).
- (2) *Variance-limited regime* ($\varepsilon \leq \varepsilon_c$): the full model becomes asymptotically more cost-efficient, since it does not incur the model-error term governed by S .

Practical rule. To minimize cost given a target tolerance ε , define $\varepsilon_c(r) := S(r)/(c_{\text{int}}(r) \gamma(r))$ and choose

$$r^* = \min\{r \in [p] : \varepsilon \geq 2\varepsilon_c(r)\} \quad (\text{if the set is empty, set } r^* = p).$$

Then, with \bar{h} from Remark 4.3, integrate using $\Delta t = \gamma(r^*) \bar{h}$.

Qualitative modeling. When the goal is to capture the qualitative behavior of the dynamics rather than fine details (as in the dropout context), very small tolerances are unnecessary. Thus, one typically operates in the $\varepsilon \geq \varepsilon_c$ regime, thereby gaining computational advantages.

5. EXAMPLE: NEURAL ODES

We now particularize the results of Section 3 to (NODE) and its random version (see (2.7)),

$$\dot{\hat{\mathbf{x}}}_t = \sum_{i \in \mathcal{B}_{\omega_{k_t}}} \frac{1}{\pi_i} \mathbf{w}_{i,t} \sigma(\langle \mathbf{a}_{i,t}, \hat{\mathbf{x}}_t \rangle + b_{i,t}), \quad t \in [0, T]. \quad (\text{rNODE})$$

(NODE) can be seen as a continuous-depth analog for single-layer residual networks, with $\sigma \in \mathcal{C}^{0,1}(\mathbb{R})$ and the time-dependent parameters are

$$\vartheta \equiv (\mathbf{w}_i, \mathbf{a}_i, b_i)_{i \in [p]} \in L^\infty(0, T; \Theta), \quad \Theta \subseteq \mathbb{R}^{p(2d+1)}.$$

Fix a compact $K \subset \mathbb{R}^d$ containing the trajectories of (NODE) and (rNODE) on $[0, T]$. For concreteness, by (2.3) and Grönwall there exists $R > 0$ such that

$$\|\mathbf{x}_t\| \leq R, \quad \|\hat{\mathbf{x}}_t\| \leq R, \quad t \in [0, T],$$

so we can take $K = B_R$. For simplicity, denote $\|\cdot\|_\infty \equiv \|\cdot\|_{L^\infty(0, T)}$ and define

$$R_K := \max_{\mathbf{x} \in K} \|\mathbf{x}\|, \quad M_\theta := \sup_{\theta \in \Theta} \|\theta\|,$$

the Lipschitz moduli λ_σ and $\lambda_{\sigma'}$ of σ and σ' , and the bounds

$$M_\sigma := \sup_{\substack{\mathbf{x} \in \mathbf{K} \\ i \in [p]}} |\sigma(\langle \mathbf{a}_i, \mathbf{x} \rangle + b_i)|, \quad M_{\sigma'} := \sup_{\substack{\mathbf{x} \in \mathbf{K} \\ i \in [p]}} |\sigma'(\langle \mathbf{a}_i, \mathbf{x} \rangle + b_i)|.$$

Table 2 records sufficient conditions on σ and ϑ guaranteeing the assumptions in Section 2 for (NODE).

TABLE 2. (NODE) with full control $\theta = (\mathbf{w}_i, \mathbf{a}_i, b_i)_{i \in [p]} \in L^\infty(0, T; \Theta)$. Top: sufficient conditions that ensure each structural assumption from Section 2, with one admissible Lipschitz bound. Bottom: minimal conditions on σ and Θ required for each result.

(A) Structural assumptions and admissible Lipschitz bounds (full parameters).

Assumption	Hypotheses	Lipschitz bound
(2.2)	$\sigma \in \mathcal{C}^{0,1}(\mathbb{R})$	$\lambda_\sigma \sum_{i \in [p]} \ \mathbf{w}_i\ _\infty \ \mathbf{a}_i\ _\infty$
(A1) (on K)	Θ bounded; $\sigma \in \mathcal{C}^{0,1}(\mathbb{R})$	$p M_\sigma + p \lambda_\sigma (R_K + 1) M_\theta$
(A2)	$\sigma \in \mathcal{C}^{1,1}(\mathbb{R})$	$\lambda_{\sigma'} \sum_{i \in [p]} \ \mathbf{w}_i\ _\infty \ \mathbf{a}_i\ _\infty^2$
(A3) (on K)	Θ bounded; $\sigma \in \mathcal{C}^{1,1}(\mathbb{R})$	$\sum_{i \in [p]} \left[M_{\sigma'} \ \mathbf{a}_i\ _\infty + \ \mathbf{w}_i\ _\infty (M_{\sigma'} + \lambda_{\sigma'} (R_K + 1) \ \mathbf{a}_i\ _\infty) \right]$
(A4) (on K)	$\sigma \in \mathcal{C}^{1,1}(\mathbb{R})$	$\sum_{i \in [p]} \left[\lambda_\sigma \ \mathbf{a}_i\ _\infty + \ \mathbf{w}_i\ _\infty (M_{\sigma'} + \lambda_{\sigma'} R_K \ \mathbf{a}_i\ _\infty) \right]$
(A5) (on K)	Θ bounded; $\sigma \in \mathcal{C}^{1,1}(\mathbb{R})$	$\sum_{i \in [p]} \left[M_{\sigma'} R_K + \ \mathbf{w}_i\ _\infty \lambda_{\sigma'} (R_K^2 + R_K) \right]$

(B) Assumptions per result (full parameters).

Theorem 3.1	Corollary 3.2	Theorem 3.5	Proposition 3.7	Proposition 3.8	Theorem 3.11
$\sigma \in \mathcal{C}^{0,1}$	$\sigma \in \mathcal{C}^{0,1}; \Theta$ bounded	$\sigma \in \mathcal{C}^{1,1}$	$\sigma \in \mathcal{C}^{0,1}$	$\sigma \in \mathcal{C}^{1,1}; \Theta$ bounded	$\sigma \in \mathcal{C}^{1,1}; \Theta$ bounded

We remark:

(i) Bounds are stated on the compact \mathbf{K} fixed above because, e.g.

$$\nabla_{\mathbf{a}_i} \mathbf{F}(\mathbf{x}, \theta) = \mathbf{w}_{i,t} \sigma'(\langle \mathbf{a}_{i,t}, \mathbf{x} \rangle + b_{i,t}) \mathbf{x}^\top$$

is linear in \mathbf{x} and thus unbounded on \mathbb{R}^d .

(ii) (A2)–(A5) require $\sigma \in \mathcal{C}^{1,1}(\mathbb{R})$. Hence ReLU is non-valid, while smooth activations such as tanh, sigmoid, or GeLU are admissible. Results that rely only on (2.2), (A1) allow ReLU.

When we consider $\theta = (\mathbf{w}_i)_{i \in [p]}$ (with (\mathbf{a}_i, b_i) fixed), the assumptions can be relaxed, since

$$\nabla_\theta \mathbf{F}(\mathbf{x}, \theta) = (\partial_{\mathbf{w}_i} \mathbf{F}(\mathbf{x}, \theta))_{i \in [p]} = (\sigma(\langle \mathbf{a}_i, \mathbf{x} \rangle + b_i))_{i \in [p]}$$

does not depend on θ , so (A5) holds trivially. Moreover, $\partial_{\mathbf{w}_i} \mathbf{F}$ is globally Lipschitz in \mathbf{x} with constant $\lambda_\sigma \|\mathbf{a}_i\|$, hence (A4) holds on all of \mathbb{R}^d (no restriction to compacts is needed). No boundedness of Θ is required in the weights-only setting. Table 3 summarizes the exact regularity of σ needed for each structural assumption and for each result.

Remark 5.1. For (NODE) with full parameters $\theta = (\mathbf{w}_i, \mathbf{a}_i, b_i)_{i=1}^p$, assumption (3.13) fails because of the nonlinear dependence of \mathbf{f}_i on (\mathbf{a}_i, b_i) . A standard remedy to ensure the existence of minimizer is to keep (\mathbf{a}_i, b_i) fixed and optimize \mathbf{w}_i , so that \mathbf{F} becomes control-affine. This simplification is known to keep good expressivity for large enough p , see [34, 11, 1].

6. NUMERICS

We validate our theoretical results on (NODE) and analyze the effect of dropout on wall-clock time, memory usage, and trajectory error as a function of batch size and resampling step size.

6.1. Forward pass. We first validate Theorem 3.1. We implement (NODE) in PyTorch with $T = 2$, $p = 24$, and activation $\sigma(\cdot) = (\cdot)_+$. We consider two cases:

- (1) *Time-independent:* $\vartheta = (\mathbf{w}_i, \mathbf{a}_i, b_i)_{i \in [p]} \in \mathbb{R}^{(2d+1)p}$.
- (2) *Time-dependent:* $\vartheta = (\mathbf{w}_i, \mathbf{a}_i, b_i)_{i \in [p]} : [0, T] \rightarrow \mathbb{R}^{(2d+1)p}$ parameterized by a two-layer tanh-NN.

TABLE 3. (NODE) with weights-only control $\theta = (\mathbf{w}_i)_{i \in [p]} \in L^\infty(0, T; \Theta)$ and (\mathbf{a}_i, b_i) fixed. Top: hypotheses on σ that ensure each structural assumption, with an admissible bound. Bottom: minimal regularity on σ required for each main result (two-row horizontal layout, one column per result). No boundedness of Θ is required.

(A) Structural assumptions and admissible bounds (weights-only).

Assumption	Hypotheses on σ	Lipschitz bound
(2.2)	$\sigma \in \mathcal{C}^{0,1}(\mathbb{R})$	$\lambda_\sigma \sum_{i \in [p]} \ \mathbf{w}_i\ _\infty \ \mathbf{a}_i\ _\infty$
(A1)	$\sigma \in \mathcal{C}(\mathbb{R})$	$M_\sigma \sqrt{p}$
(A2)	$\sigma \in \mathcal{C}^{1,1}(\mathbb{R})$	$\lambda_{\sigma'} \sum_{i \in [p]} \ \mathbf{w}_i\ _\infty \ \mathbf{a}_i\ _\infty^2$
(A3)	$\sigma \in \mathcal{C}^1(\mathbb{R})$	$M_{\sigma'} \left(\sum_{i \in [p]} \ \mathbf{a}_i\ _\infty^2 \right)^{1/2}$
(A4)	$\sigma \in \mathcal{C}^{0,1}(\mathbb{R})$	$\lambda_\sigma \max_{i \in [p]} \ \mathbf{a}_i\ _\infty$
(A5)	none	0

(B) Assumptions per result (weights-only).

Theorem 3.1	Corollary 3.2	Theorem 3.5	Proposition 3.7	Proposition 3.8	Theorem 3.11
$\sigma \in \mathcal{C}^{0,1}$	$\sigma \in \mathcal{C}^{0,1}$	$\sigma \in \mathcal{C}^{1,1}$	$\sigma \in \mathcal{C}^{0,1}$	$\sigma \in \mathcal{C}^{1,1}$	$\sigma \in \mathcal{C}^{1,1}$

Integration over $[0, T]$ uses a fourth-order Runge–Kutta (RK4) solver with step $\Delta t = 0.002$. We train on `make_circles` (scikit-learn) with one-hot targets $(-1, 0)$ and $(0, 1)$ using MSE at $t = T$.

We fix three disjoint batches $(\mathcal{B}_1, \mathcal{B}_2, \mathcal{B}_3)$ of size 8 containing neurons from a trained model, sampled with $q_j = 1/3$. Each batch sampled is held on a subinterval of length $h = \Delta t$. At each solver step we identify the active subinterval and mask the non-selected neurons. Figure 2 illustrates the full and random dynamics.

Convergence. We approximate the expectation in Theorem 3.1 via Monte Carlo: for each h we draw $K = 20$ realizations, compute $\max_{t \in [0, T]} \|\mathbf{x}_t - \hat{\mathbf{x}}_t\|^2$, and average over realizations. As $h \rightarrow 0$, the error decays with slope ≥ 0.5 in log-log scale, as predicted. The observed slope actually exceeds the theoretical rate, suggesting a potentially faster convergence in practice; see Figure 3.

Decision boundary. Figure 4 shows that dropout widens the decision boundary (white level set), and the widening increases with h , consistent with the regularization effect of dropout [66]. Accuracies are reported below each panel.

Use of memory and computational time. We now benchmark peak memory and forward-pass wall-clock time versus dataset size (same architecture and solver settings). For small datasets, (rNODE) can be slightly slower due to the per-step masking overhead; for larger datasets, it becomes faster and more memory-efficient because each step evaluates only $r < p$ neurons (fewer matrix-vector products). See Figure 5 and Table 4.

6.2. Application to transport of measures. Given ρ_B and a target ρ_T , we train the control ϑ in (NODE) so that the solution ρ_t of (3.6) transports ρ_B to ρ_T on $[0, T]$. We use the parameterization

$$W_t = W_0, \quad A_t = A_0, \quad b_t = b_0 + b_1 t,$$

with $W_0 \in \mathbb{R}^{d \times p}$, $A_0 \in \mathbb{R}^{p \times d}$, $b_0, b_1 \in \mathbb{R}^p$. Since (A2) fails when $\sigma(\cdot) = (\cdot)_+$, we use $\sigma(\cdot) = \tanh(\cdot)$.

Numerical scheme.

- (1) **Flow matching (training).** Draw pairs $\{(\mathbf{x}_0^\tau, \mathbf{x}_T^\tau)\}_{\tau \in [\mathcal{T}]} \sim \rho_B \times \rho_T$, sample $t \sim \mathcal{U}([0, T])$, and minimize

$$\mathcal{L}_\vartheta = \frac{1}{\mathcal{T}} \sum_{\tau \in [\mathcal{T}]} \mathbb{E}_t \left\| \mathbf{F}((1-t)\mathbf{x}_0^\tau + t\mathbf{x}_T^\tau, \vartheta_t) - (\mathbf{x}_T^\tau - \mathbf{x}_0^\tau) \right\|_2^2.$$

Optimization uses Adam with a fixed learning rate (autodiff in PyTorch).

- (2) **Particle discretization.** Given particles $\{\mathbf{x}_i\}_{i \in [N]} \subset \mathbb{R}^d$, approximate

$$\rho_t^N = \sum_{i \in [N]} \alpha_{i,t} \delta_{\mathbf{x}_{i,t}}, \quad \dot{\mathbf{x}}_{i,t} = \mathbf{F}(\mathbf{x}_{i,t}, \vartheta_t), \quad \frac{d}{dt} \log \alpha_{i,t} = -\nabla_{\mathbf{x}} \cdot \mathbf{F}(\mathbf{x}_{i,t}, \vartheta_t).$$

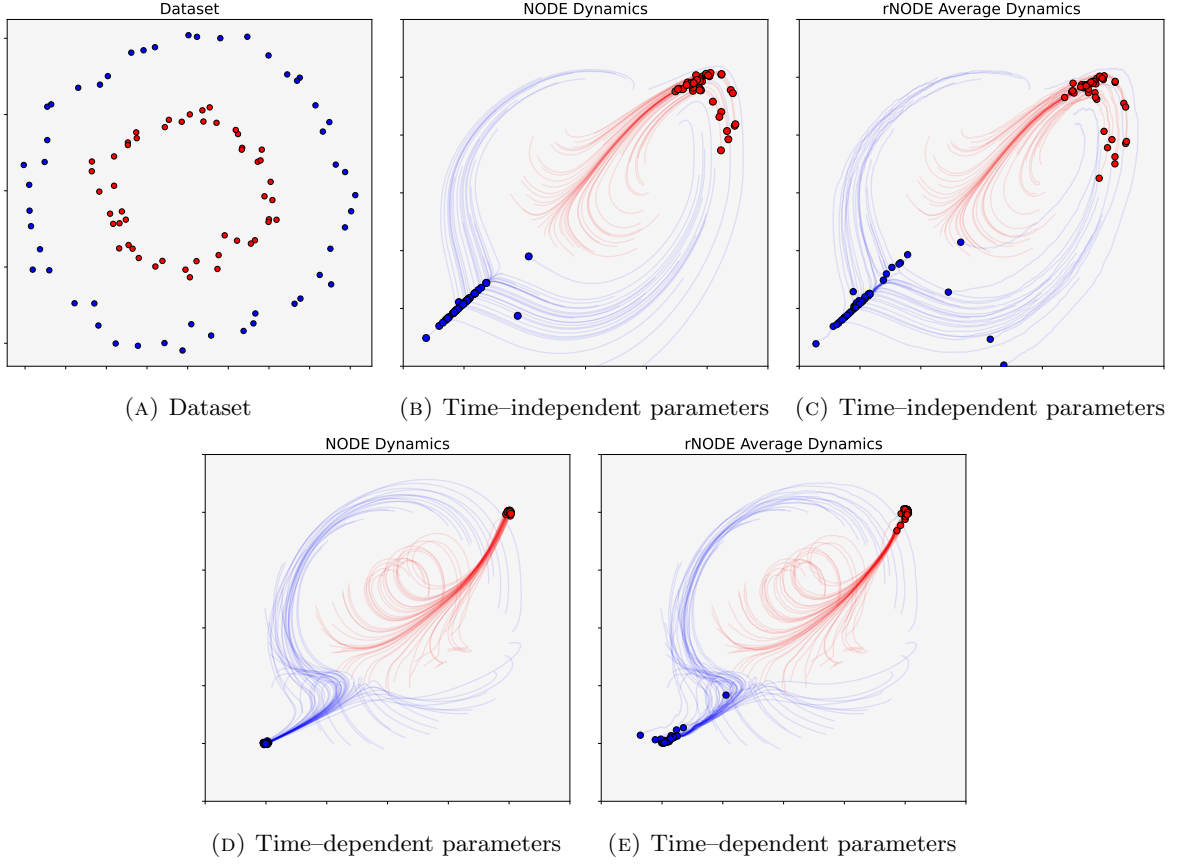


FIGURE 2. Point trajectories for (NODE) and (rNODE).

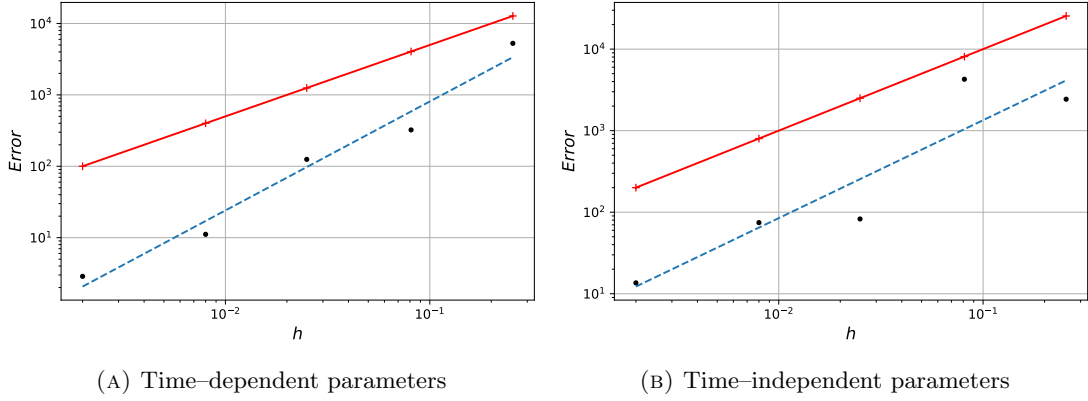


FIGURE 3. Error $\max_t \mathbb{E}_\omega[\|\mathbf{x}_t - \hat{\mathbf{x}}_t\|^2]$ vs. h on a log-log scale. Red line: reference slope from [Theorem 3.1](#). Black dots: numerical errors averaged over 20 realizations for several values of h . Blue dashed line: linear-regression fit. Estimated slopes—time-dependent case: 1.53; time-independent case: 1.20.

We use midpoint Runge-Kutta RK2:

$$\mathbf{x}_{i,n+1} = \mathbf{x}_{i,n} + \Delta t \mathbf{F}(\mathbf{x}_{i,\text{mid}}, \vartheta_{t_{\text{mid}}}), \quad \alpha_{i,n+1} = \alpha_{i,n} \exp\left(-\Delta t \mathbb{E}_e[e^\top (\nabla_{\mathbf{x}} \mathbf{F}) e] \Big|_{(\mathbf{x}_{i,\text{mid}}, \vartheta_{t_{\text{mid}}})}\right),$$

where $\mathbf{x}_{i,\text{mid}} = \mathbf{x}_{i,n} + \frac{1}{2}\Delta t \mathbf{F}(\mathbf{x}_{i,n}, \vartheta_{t_n})$, $t_{\text{mid}} = t_n + \frac{1}{2}\Delta t$, and $\mathbb{E}_e[e^\top (\nabla_{\mathbf{x}} \mathbf{F}) e]$ is the Hutchinson trace estimator with $e \sim \mathcal{N}(0, \text{Id})$. Diracs are rendered via Gaussian KDE on a uniform grid.

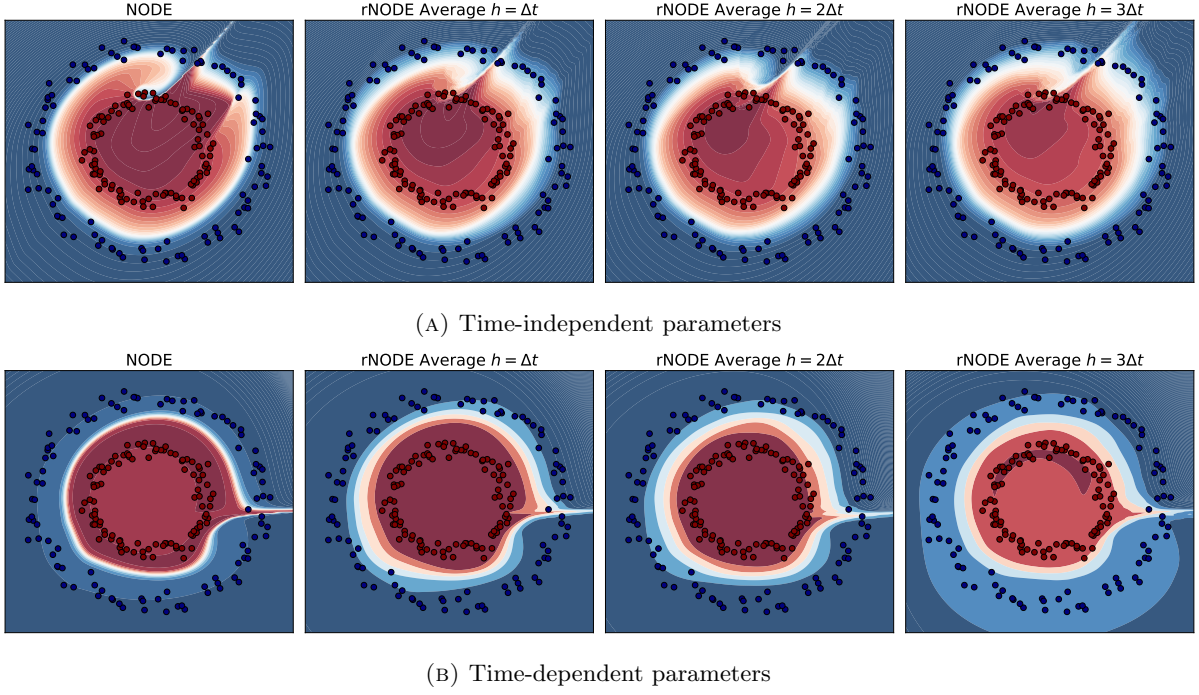


FIGURE 4. Decision boundary for full vs random models at different $h/\Delta t$. Test accuracies (left to right) in (A): 98.50%, 100.0%, 98.00%, 99.00%. In (B): all 99.50%.

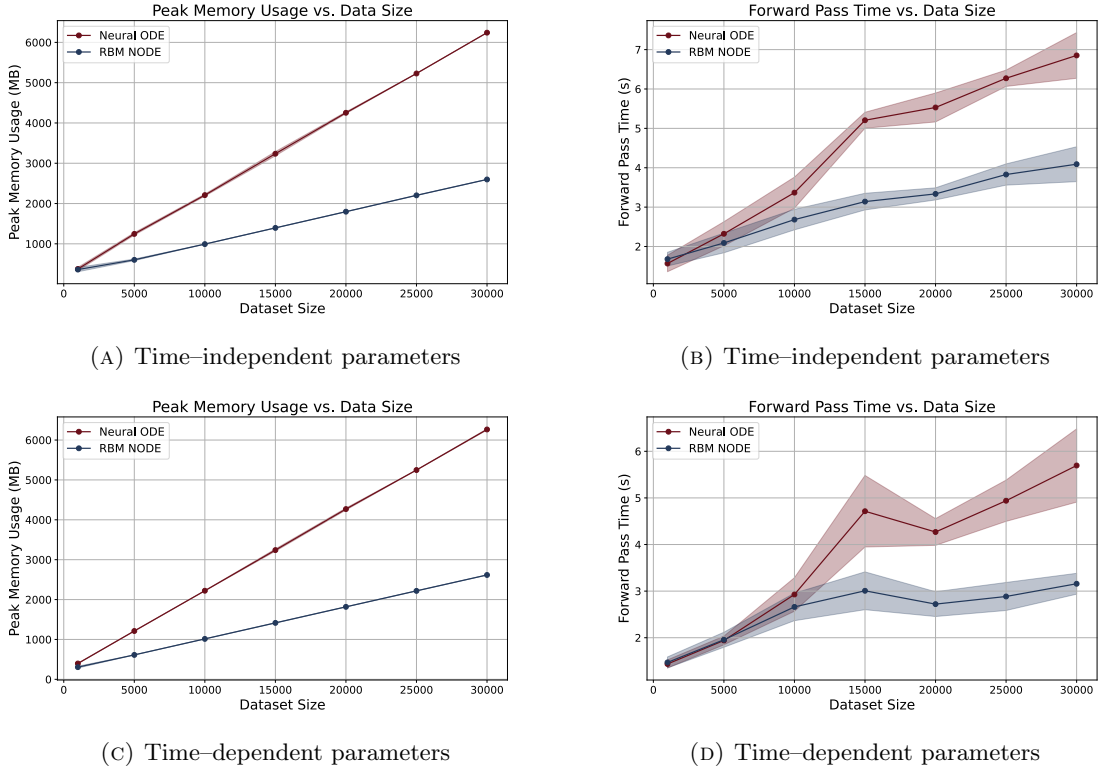


FIGURE 5. Peak memory and forward-pass time vs dataset size.

Setup and results. We take

$$\rho_B(x, y) = \begin{cases} 1 - (x + 1)^2 - (y + 1)^2, & \text{if } (x + 1)^2 + (y + 1)^2 < 1, \\ 0 & \text{otherwise,} \end{cases}$$

Metric	(NODE)	(rNODE) (batches)							
		2 batches	3 batches	4 batches	5 batches	6 batches	7 batches	8 batches	9 batches
<i>Time-independent parameters</i>									
Train Loss	0.0276	0.0769	0.0479	0.1464	0.0943	0.1421	0.1892	0.7183	0.7504
Test Loss	0.1133	0.0986	0.0672	0.1539	0.1120	0.1533	0.1915	0.7361	0.7414
Train Accuracy	100.00%	100.00%	100.00%	100.00%	100.00%	100.00%	99.00%	75.00%	84.00%
Test Accuracy	96.80%	99.13%	99.53%	99.63%	100.00%	98.93%	98.33%	75.43%	84.80%
Test Time (s)	2.3539	1.9503	1.8923	1.9429	1.7842	1.7760	1.6889	1.6715	1.6885
Test Memory (MB)	745.2617	714.36	641.73	590.56	552.38	535.75	524.48	515.05	507.65
<i>Time-dependent parameters</i>									
Train Loss	0.0001	0.0079	0.0033	2.3955	0.0417	10.6097	2.5717	23.5554	74.7088
Test Loss	0.0090	0.0180	0.0145	3.6248	0.0463	14.5793	3.9496	24.0698	85.0768
Train Accuracy	100.00%	100.00%	100.00%	98.00%	100.00%	99.00%	97.00%	94.00%	94.00%
Test Accuracy	99.80%	99.80%	99.70%	98.07%	99.93%	98.10%	96.00%	94.70%	92.10%
Test Time (s)	2.7680	2.5263	2.5958	2.5135	2.5093	2.6779	2.4950	2.6225	2.5371
Test Memory (MB)	3767.2148	3306.30	1075.07	914.79	889.04	823.97	804.57	792.65	765.15

TABLE 4. Performance of (NODE) vs (rNODE) across batch counts.

and target $\rho_T = \sum_{k \in [3]} \mathcal{N}(\mu_k, \Sigma_k)$ with $\mu_1 = (6, 0)$, $\mu_2 = (4.5, 3)$, $\mu_3 = (6, 2)$ and

$$\Sigma_1 = \Sigma_2 = \begin{bmatrix} 0.2 & 0.05 \\ 0.05 & 0.2 \end{bmatrix}, \quad \Sigma_3 = 0.05 \text{ Id}.$$

We set $\mathcal{T} = 250$, $N = 200$, $T = 1$, $\Delta t = 0.01$, and a 300×300 spatial grid. Figure 6 (top row) shows snapshots and flow lines.

We repeat with the continuity equation using (rNODE), averaging over 3 uniform batches and $K = 10$ realizations; see Figure 6 (bottom row) and timings in Table 5. The solver exhibits lower time/memory as the number of batches increases.

Metric	Continuity Equation	Random Continuity Equation			
		2 batches	3 batches	4 batches	5 batches
Time (ms)	74.9691	42.4881	31.2689	24.2228	18.8842
Memory (MB)	109.1180	82.13	74.00	68.82	67.06

TABLE 5. Full vs random continuity equation: performance for different batch counts.

To quantify convergence, we compute the expected L^1 -error, over 20 realizations. The log-log slope is ≈ 0.5 in line with Corollary 3.6 (note that the initial density is compactly supported); see Figure 7.

6.3. Training. We solve (3.12) with time-dependent parameters as in Section 6.1, and GeLU activation $\sigma(x) = x(1 + \text{erf}(x/\sqrt{2}))/2$. Data $(\mathbf{x}_m, \mathbf{y}_m)$ come from the `make_circles` dataset, with $n_d = 100$.

For the RBM version (3.15), we fix a (sampled) dropout schedule across epochs (same realization throughout training), as in the analysis. This fixed schedule induces a time-sparse architecture that is constant across epochs. Operationally, it behaves like a structured pruning mask repeated in time.

We set $T = 2$, $p = 24$, $\alpha = 0.01$, $\beta = 0.5$, and costs

$$\ell_m(\mathbf{x}) = g_m(\mathbf{x}) = \|\mathbf{x} - \mathbf{y}_m\|^2.$$

Optimization uses Adam; time integration uses `rk4` via the module `odeint_adjoint` from `torchdiffeq`.

For training, we use the Adam optimizer and integrate with `rk4` Runge-Kutta scheme through the module `odeint_adjoint` from `torchdiffeq`.

Decision Boundary. We compare the decision boundary obtained by solving (3.12) with the one that solves (3.15) taking three batches of 8 neurons, $K = 10$ realizations, 1000 epochs, $\Delta t = 0.1$.

Figure 8 shows that averaging realizations of (rNODE) smooths the “tails” typical of (NODE) flows (the preimage of a simple classifier by the bijective flow map is a smooth, non-self-intersecting boundary

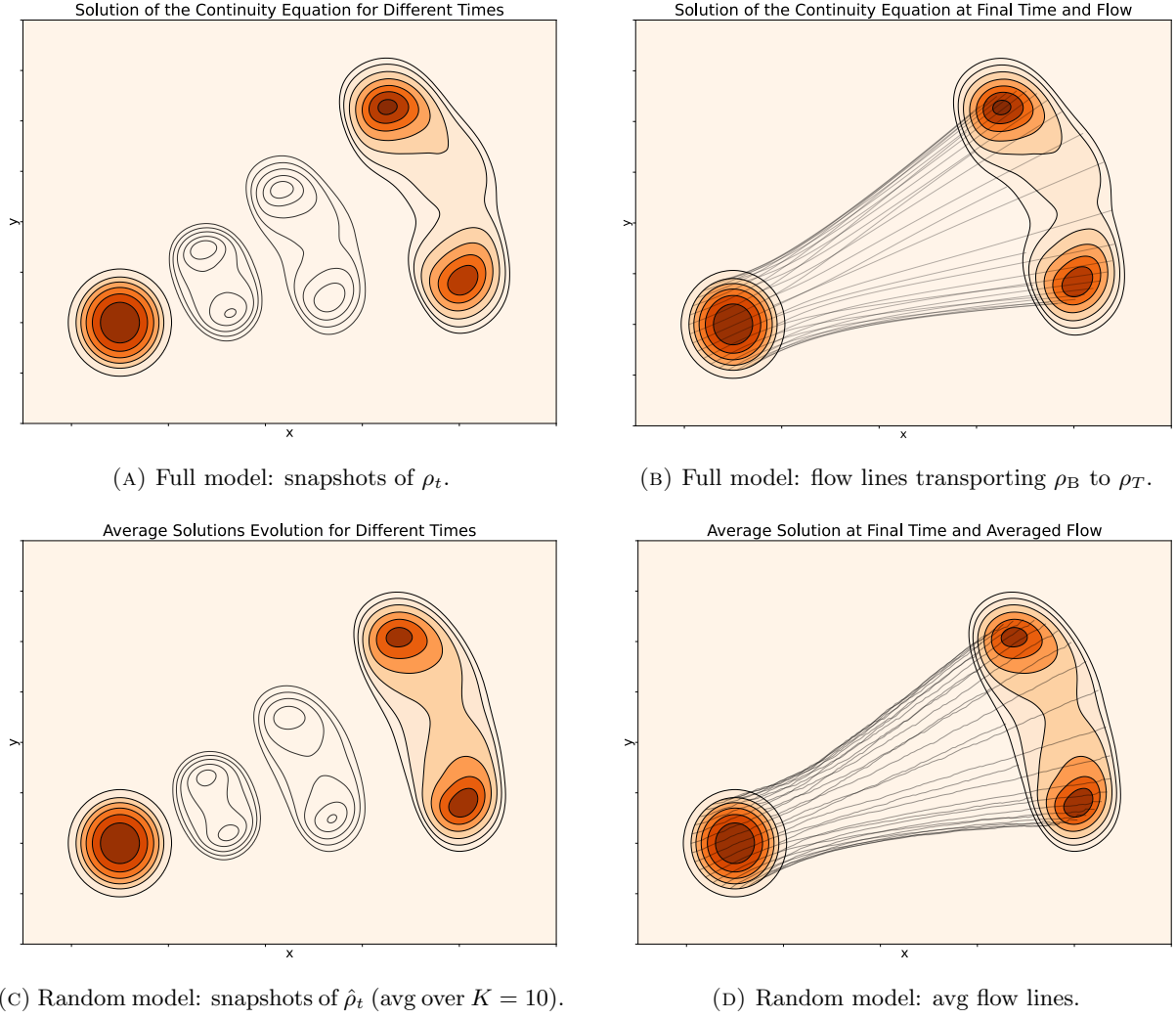
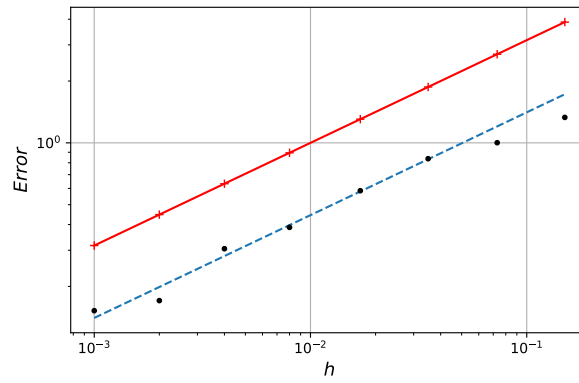
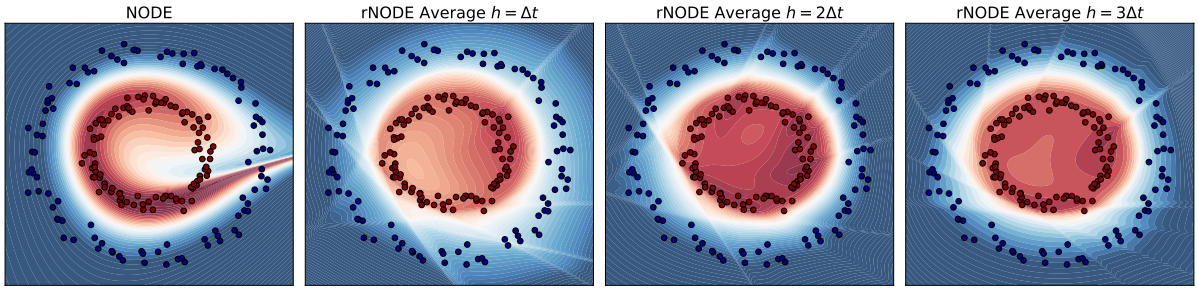


FIGURE 6. Comparison of the full model (top row) and the random model (bottom row).

FIGURE 7. Error $\max_t \mathbb{E}_\omega[\|\rho_t - \hat{\rho}_t\|_{L^1}]$ vs. $h^{1/2}$ in log-log scale. Red line: reference slope from Corollary 3.6. Black dots: numerical errors averaged over 20 realizations. Blue dashed line: linear-regression fit slope=0.5.

decision). Therefore it acts as a regularizer (as in Section 6.1): multiple runs of (rNODE) with different orientations makes these tails point in different directions and largely cancel, yielding a smoother boundary that aligns more closely with the data.

FIGURE 8. Decision boundary of (NODE) vs (rNODE) for several h .

Performance in training. We report averages over $K = 15$ realizations of (rNODE) in the same setting. Table 6 shows how average training time, memory and performance metrics after training evolve when the number of batches increases. In particular, the usage of memory and time is reduced as the number of batches increases. With 2 batches we get similar memory usage, lower time and higher train/test accuracy that (NODE). Moreover, with 4 batches we get better train accuracy, a similar test accuracy, and less memory usage and training time (consistent with the cost–accuracy trade–off in Section 4.2). Consequently, RBM with a fixed schedule is a practical proxy to assess prune–ability: if performance remains stable with $r \ll p$, the model likely admits a pruned realization with comparable accuracy and lower footprint.

Metric	(NODE)	(rNODE)			
		2 Batches	3 Batches	4 Batches	6 Batches
Train Loss	0.63	0.12	52.54	0.33	43.24
Test Loss	0.56	0.67	68.15	0.71	56.69
Train Accuracy	0.98	1.00	0.67	1.00	0.50
Test Accuracy	0.79	0.72	0.58	0.80	0.50
Training Time (s)	233.23	210.54	208.29	207.99	224.01
Training Memory Usage (MB)	286.25	282.13	287.66	285.72	281.48

TABLE 6. Training (1000 epochs): (NODE) vs (rNODE) with different batch sizes. (rNODE) entries are averages over 15 realizations (fixed schedule).

Computational setup. AMD Ryzen 9 5900HS @ 3.30 GHz, 16 GB RAM (15.4 GB usable). Python + NumPy/SciPy/PyTorch. Wall–clock measured via `time.perf_counter`; peak memory via OS–level RSS (Python `resource`).

7. CONCLUSIONS AND DISCUSSION

Summary. We have introduced a continuous–time dropout framework for controlled differential systems (under standard Lipschitz assumptions) via random batch methods (RBMs). We proved: (i) linear–in– h convergence in expected squared error of the forward dynamics; (ii) analogous rates in the optimal–control training setting (with explicit conditions ensuring stability of adjoints and controls), and (iii) error bounds for measure transport under the continuity equation (pointwise L^2 and L^1 errors with optimal $\mathcal{O}(\sqrt{h})$ scaling). These results indicate that randomized pruning can approximate the full model accurately while offering computational and memory advantages in parallel implementations.

Beyond rates, we conducted a design analysis (Section 4.1): we derived optimal–bound surrogates across canonical schemes, identifying how the batch scheme parameters control the convergence constants. Classical Bernoulli dropout emerges as a special case of our continuous–time RBM (with explicit variance and sampling factors), opening the door to principled improvements and analysis beyond the standard keep–probability rule. We further quantified the cost–accuracy trade–off (Section 4.2), providing an explicit expression for the cost–minimizing h at a target tolerance.

Finally, we specialized all results to a single-layer neural ODE as a worked example, which we used in the numerical section. When the sampling schedule is fixed across epochs, RBM behaves as a continuous-time analogue of structured pruning. Our experiments indicate that modest active widths already achieve accuracy close to the full model.

Discussion. The following summarizes extensions of the framework and some observations.

- **Non-uniform switching grids.** All forward/transport estimates remain valid for partitions with variable subintervals $\{h_k\}$ upon replacing h with $\max_k h_k$.
- **Training beyond the single-layer model.** The results of Section 3.3 carry over to vector fields \mathbf{f}_i that satisfy the standing assumptions (A1)–(A5). For existence of optimal controls, convexity of the admissible velocity set $\{\mathbf{F}(\mathbf{x}, \theta) : \theta \in \Theta\}$ is sufficient (see, e.g., [62, Chapter 2], [6, Chapter 9.3]). When global optimal controls may fail to exist by non-convexity, one can still analyze gradient-based iterates and their deviations under RBM as done in Remark 3.13.
- **Relation to mean-field RBM analyses.** Mean-field RBM studies (e.g., [36]) obtain $\mathcal{O}(h)$ Wasserstein errors for diffusive Fokker–Planck limits. Our setting is pure transport (no diffusion) and works at finite width without a mean-field limit; hence their diffusion-based arguments do not transfer directly.
- **Design guidelines.** Keep q_j balanced, with a lower bound for q_j , and pick batch size r to reduce Λ using the trade-off in Section 4.2: under balanced r -batches, Λ is inversely proportional to r , while the per-step cost increases proportionally with r . Combine this with Proposition 4.2 to pick (h, r) as a target error. Numerics in Section 6 match the predicted speedups in the integration-dominated regime.
- **Practical limitation.** Transport results (Section 3.2) require (A2); with non-smooth activations (e.g., ReLU) we used tanh in experiments. Extending transport bounds to non-smooth flows is natural but nontrivial.

Open problems. We conclude by presenting a list of future directions.

- **Per-iteration resampling vs. fixed schedules.** Our analysis adopts a fixed dropout schedule across epochs, yielding a deterministic control-to-state map that deactivates a subset of neurons. In practice, per-iteration (or epoch) resampling alters the gradient noise and can improve generalization. It is therefore important to quantify the resulting bias–variance trade-off and to establish convergence-in-expectation guarantees for training under per-iteration resampling, as well as to compare it with the fixed-schedule scheme studied here. A very recent study [9] analyzes the different regimes for gradient descent-optimization dynamics arising in the mean-field limit as hyperparameters (width, learning rate and dropout rate) scale in two-layer networks.
- **Data-aware/adaptive sampling and switching.** Design q_j and batches $\{\mathcal{B}_j\}$ using importance criteria (e.g., neuron influence on \mathbf{F} or on $\nabla_\theta H$) to reduce Λ along actual trajectories at fixed compute. Provide guarantees that couple sampling to Λ (or Γ) in (3.2)–(3.20).

Replace fixed h by adaptive or random switching (e.g. Poisson process jump times) to concentrate compute where dynamics are stiff. For Poisson, prove scalings of the form $\mathbb{E}_\omega[\max_t \|\mathbf{x}_t - \hat{\mathbf{x}}_t\|^2] \propto \lambda^{-1}$ and $\mathbb{E}_\omega[\|\rho_t - \hat{\rho}_t\|_{L^1}] \propto \lambda^{-1/2}$ (with $h \simeq \lambda^{-1}$), and extend to adjoint/training estimates and higher-order integrators with their stability constraints.

- **Generalization under pruned dynamics.** We control trajectory and cost deviations, but not generalization. Derive data-dependent generalization bounds for continuous-time dropout (cf. results for discrete MLPs such as [52]), clarifying when random masking improves test performance.
- **Existence and regularity under weak assumptions.** Establish transport and training bounds with non-smooth vector fields (e.g., ReLU, BV in x), replacing (A2) by weaker conditions while preserving well-posedness of characteristics/adjoints. Identify minimal conditions (convex/closed control families, compact Θ , coercive costs) ensuring existence of optimal controls compatible with RBM bounds. In our baseline setting, existence of optimal controls is not guaranteed a priori (see [22, Remark 13.2]). Analyze relaxed controls (H^1/BV , Young measures) and the corresponding Pontryagin systems.
- **Post-training distillation.** Combining randomized pruning during training with post-training distillation may further reduce parameters at negligible extra cost.

- **Numerics beyond first order.** Analyze how higher-order solvers interact with switching—stability constraints, and the cost–accuracy trade-off in [Section 4.2](#). We expect the two-regime conclusion to persist; however, a formal analysis remains to be carried out.

8. PROOFS

Whenever the parameter ϑ has been fixed or is clear from context, for simplicity we will omit its explicit dependence and write

$$\mathbf{F}_t(\cdot) \equiv \mathbf{F}(\cdot, \vartheta_t) \quad \text{and} \quad \hat{\mathbf{F}}_t(\cdot) \equiv \hat{\mathbf{F}}(\cdot, \vartheta_t).$$

This convention also applies to other functions depending on t only through ϑ .

8.1. Classical results. The following result establishes the existence of absolutely continuous solutions for parameterized ODEs that need not be continuous in t . It is a generalization of the classical Carathéodory conditions, which impose the stronger assumption that, in [\(8.1\)](#), the right-hand side does not depend on \mathbf{x} . A proof can be found in [\[26, Theorem 6.2\]](#).

Lemma 8.1. *Let $\mathbf{F} : \mathbb{R}^d \times \Theta \rightarrow \mathbb{R}^d$ and $\vartheta : [0, T] \rightarrow \Theta$ satisfy the following Carathéodory conditions:*

- (1) *For almost every $t \in [0, T]$, the map $\mathbf{x} \mapsto \mathbf{F}(\mathbf{x}, \vartheta_t)$ is continuous.*
- (2) *For each \mathbf{x} , the map $t \mapsto \mathbf{F}(\mathbf{x}, \vartheta_t)$ is measurable in $[0, T]$.*
- (3) *There exists a function $m \in L^1(0, T)$ such that for almost every $t \in [0, T]$:*

$$\|\mathbf{F}(\mathbf{x}, \vartheta_t)\| \leq m_t(\|\mathbf{x}\| + 1), \quad \text{for all } \mathbf{x} \in \mathbb{R}^d. \quad (8.1)$$

Then, there exists a solution $\mathbf{x} \in \mathcal{SC}([0, T]; \mathbb{R}^d)$ to the initial value problem

$$\begin{cases} \dot{\mathbf{x}}_t = \mathbf{F}(\mathbf{x}_t, \vartheta_t), & t \in [0, T], \\ \mathbf{x}_0 \in \mathbb{R}^d, \end{cases}$$

Furthermore, if there exists a function $\lambda(\vartheta) \in L^1(0, T)$ such that for almost every $t \in [0, T]$

$$\|\mathbf{F}(\mathbf{x}, \vartheta_t) - \mathbf{F}(\mathbf{y}, \vartheta_t)\| \leq \lambda_t(\vartheta) \|\mathbf{x} - \mathbf{y}\|, \quad \text{for all } \mathbf{x}, \mathbf{y} \in \mathbb{R}^d, \quad (8.2)$$

then the solution \mathbf{x} is unique.

Remark 8.2. *Assume that the Lipschitz condition [\(8.2\)](#) holds. Then, the following statements are equivalent:*

- (1) *The linear growth bound [\(8.1\)](#) is satisfied for some $m \in L^1(0, T)$.*
- (2) *The map $t \mapsto \|\mathbf{F}(0, \vartheta_t)\|$ belongs to $L^1(0, T)$.*

If either holds, [\(8.1\)](#) is satisfied with

$$m_t = \lambda_t + \|\mathbf{F}(0, \vartheta_t)\|.$$

We also state an extension of Grönwall's lemma as a direct application of [\[3, Lemma 3.3\]](#):

Lemma 8.3. *Let $x \in \mathcal{C}^1([t_0, t_1]; \mathbb{R}_{\geq 0})$, $\alpha \in \mathcal{C}^0([t_0, t_1]; \mathbb{R}_{\geq 0})$ and $\beta \in \mathcal{C}^0([t_0, t_1])$. Suppose that*

$$\frac{1}{2} \frac{d}{dt} x_t^2 \leq \alpha_t x_t^2 + \beta_t x_t,$$

holds for all $t \in [t_0, t_1]$. Then, for any $t \in [t_0, t_1]$, we have:

$$x_t \leq x_{t_0} \exp \left(\int_{t_0}^t \alpha_s ds \right) + \int_{t_0}^t \beta_s \exp \left(\int_s^t \alpha_\tau d\tau \right) ds.$$

8.2. Technical lemmas. We shall prove three lemmas that will be useful in the upcoming proofs. The first one follows directly from the linear growth condition [\(2.3\)](#):

Lemma 8.4. *For any $\mathbf{x}_0 \in \mathbb{R}^d$ and $\vartheta \in L^\infty(0, T; \Theta)$, the respective solutions \mathbf{x}_t and $\hat{\mathbf{x}}_t$ of [\(FM\)](#) and [\(RM\)](#) for satisfy*

$$\max_{t \in [0, T]} \|\mathbf{x}_t\| \leq \|\mathbf{x}_0\| e^{\lambda_{\mathbf{F}, \mathbf{x}, \vartheta} T} + \frac{\lambda_{\mathbf{F}, 0, \vartheta}}{\lambda_{\mathbf{F}, \mathbf{x}, \vartheta}} (e^{\lambda_{\mathbf{F}, \mathbf{x}, \vartheta} T} - 1), \quad (8.3)$$

and

$$\max_{t \in [0, T]} \|\mathbf{x}_t - \hat{\mathbf{x}}_t\| \leq e^{\frac{\lambda_{\mathbf{F}, \mathbf{x}, \vartheta}}{\pi_{\min}} T} \left(T \|\Lambda(\mathbf{x}_0, \vartheta)\|_{L^1(0, T)} \sum_{j \in [n_b]} q_j^{-1} \right)^{1/2}, \quad (8.4)$$

where $\lambda_{\mathbf{F}, \mathbf{x}, \vartheta}$ and $\lambda_{\mathbf{F}, 0, \vartheta}$ are defined in (2.2) and (2.3), $\pi_{\min} = \min_{i \in [p]} \pi_i$ as in (2.6), Λ as in (3.2), and q_j in (2.4). Moreover, assume (A1) and let $\tilde{\vartheta} \in L^\infty(0, T; \Theta)$. Then it holds:

$$\max_{t \in [0, T]} \|\mathbf{x}_{\vartheta, t} - \mathbf{x}_{\tilde{\vartheta}, t}\| \leq \lambda_{\mathbf{F}, \theta, K} e^{\lambda_{\mathbf{F}, \mathbf{x}, \vartheta} \vee \lambda_{\mathbf{F}, \mathbf{x}, \tilde{\vartheta}} T} \|\vartheta - \tilde{\vartheta}\|_{L^1(0, T; \Theta)}, \quad (8.5)$$

eq:constant_

where $K \subset \mathbb{R}^d$ is compact and contains the trajectories \mathbf{x}_ϑ and $\mathbf{x}_{\tilde{\vartheta}}$ associated with the controls ϑ , $\tilde{\vartheta}$, respectively.

Proof of Lemma 8.4. Let $t \in [0, T]$. From (FM) and using (2.3), we get

$$\frac{1}{2} \frac{d}{dt} \|\mathbf{x}_t\|^2 = \langle \mathbf{F}_t(\mathbf{x}_t), \mathbf{x}_t \rangle \leq \|\mathbf{F}_t(\mathbf{x}_t)\| \cdot \|\mathbf{x}_t\| \leq \lambda_{\mathbf{F}, \mathbf{x}, \vartheta} \|\mathbf{x}_t\|^2 + \lambda_{\mathbf{F}, 0, \vartheta} \|\mathbf{x}_t\|.$$

By Lemma 8.3, for all $t \in [0, T]$

$$\|\mathbf{x}_t\| \leq \|\mathbf{x}_0\| e^{\lambda_{\mathbf{F}, \mathbf{x}, \vartheta} t} + \lambda_{\mathbf{F}, 0, \vartheta} \int_0^t e^{\lambda_{\mathbf{F}, \mathbf{x}, \vartheta} (t-s)} ds = \|\mathbf{x}_0\| e^{\lambda_{\mathbf{F}, \mathbf{x}, \vartheta} T} + \frac{\lambda_{\mathbf{F}, 0, \vartheta}}{\lambda_{\mathbf{F}, \mathbf{x}, \vartheta}} (e^{\lambda_{\mathbf{F}, \mathbf{x}, \vartheta} T} - 1).$$

To show (8.4), let $t \in [0, T]$ and assume $k \equiv k_t$. From (FM) and (RM), we get

$$\begin{aligned} \frac{1}{2} \frac{d}{dt} \|\mathbf{x}_t - \hat{\mathbf{x}}_t\|^2 &= \langle \dot{\mathbf{x}}_t - \dot{\hat{\mathbf{x}}}_t, \mathbf{x}_t - \hat{\mathbf{x}}_t \rangle = \langle \mathbf{F}_t(\mathbf{x}_t) - \mathbf{F}_t^{(\omega_k)}(\hat{\mathbf{x}}_t), \mathbf{x}_t - \hat{\mathbf{x}}_t \rangle \\ &= \langle \mathbf{F}_t(\mathbf{x}_t) - \mathbf{F}_t^{(\omega_k)}(\mathbf{x}_t), \mathbf{x}_t - \hat{\mathbf{x}}_t \rangle + \langle \mathbf{F}_t^{(\omega_k)}(\mathbf{x}_t) - \mathbf{F}_t^{(\omega_k)}(\hat{\mathbf{x}}_t), \mathbf{x}_t - \hat{\mathbf{x}}_t \rangle \\ &\stackrel{(1)}{\leq} \|\mathbf{F}_t(\mathbf{x}_t) - \mathbf{F}_t^{(\omega_k)}(\mathbf{x}_t)\| \cdot \|\mathbf{x}_t - \hat{\mathbf{x}}_t\| + \|\mathbf{F}_t^{(\omega_k)}(\mathbf{x}_t) - \mathbf{F}_t^{(\omega_k)}(\hat{\mathbf{x}}_t)\| \cdot \|\mathbf{x}_t - \hat{\mathbf{x}}_t\| \\ &\leq \sum_{j \in [n_b]} \|\mathbf{F}_t(\mathbf{x}_t) - \mathbf{F}_t^{(j)}(\mathbf{x}_t)\| q_j^{1/2} q_j^{-1/2} \|\mathbf{x}_t - \hat{\mathbf{x}}_t\| + \frac{\lambda_{\mathbf{F}, \mathbf{x}, \vartheta}}{\pi_{\min}} \|\mathbf{x}_t - \hat{\mathbf{x}}_t\|^2 \\ &\stackrel{(2)}{\leq} \left(\Lambda_t(\mathbf{x}_0, \vartheta) \sum_{j \in [n_b]} q_j^{-1} \right)^{1/2} \|\mathbf{x}_t - \hat{\mathbf{x}}_t\| + \frac{\lambda_{\mathbf{F}, \mathbf{x}, \vartheta}}{\pi_{\min}} \|\mathbf{x}_t - \hat{\mathbf{x}}_t\|^2 \end{aligned} \quad (8.6)$$

eq:alignprop

$$= \beta_t \|\mathbf{x}_t - \hat{\mathbf{x}}_t\| + \frac{\lambda_{\mathbf{F}, \mathbf{x}, \vartheta}}{\pi_{\min}} \|\mathbf{x}_t - \hat{\mathbf{x}}_t\|^2, \quad (8.7)$$

where we have used (2.2) and (2.5), applied the Cauchy-Schwarz inequality in (1) and (2), and denoted

$$\beta_t = \left(\Lambda_t(\mathbf{x}_0, \vartheta) \sum_{j \in [n_b]} q_j^{-1} \right)^{1/2}.$$

Application of Lemma 8.3 in (8.6) then gives

$$\|\mathbf{x}_t - \hat{\mathbf{x}}_t\| \leq \|\mathbf{x}_{t_{k-1}} - \hat{\mathbf{x}}_{t_{k-1}}\| e^{\lambda_{\mathbf{F}, \mathbf{x}, \vartheta} (t-t_{k-1})/\pi_{\min}} + \int_{t_{k-1}}^t \beta_s e^{\lambda_{\mathbf{F}, \mathbf{x}, \vartheta} (t-s)/\pi_{\min}} ds.$$

Since $\hat{\mathbf{x}}_0 = \mathbf{x}_0$, we have for $t \in [0, t_1]$

$$\|\mathbf{x}_t - \hat{\mathbf{x}}_t\| \leq \int_0^t \beta_s e^{\lambda_{\mathbf{F}, \mathbf{x}, \vartheta} (t-s)/\pi_{\min}} ds \leq e^{\lambda_{\mathbf{F}, \mathbf{x}, \vartheta} h/\pi_{\min}} \int_0^{t_1} \beta_s ds.$$

Proceeding inductively and applying Cauchy-Schwarz, we deduce that for all $t \in [0, T]$

$$\|\mathbf{x}_t - \hat{\mathbf{x}}_t\| \leq e^{\lambda_{\mathbf{F}, \mathbf{x}, \vartheta} T/\pi_{\min}} \int_0^t \beta_s ds \leq e^{\lambda_{\mathbf{F}, \mathbf{x}, \vartheta} T/\pi_{\min}} \left(T \|\Lambda(\mathbf{x}_0, \vartheta)\|_{L^1(0, T)} \sum_{j \in [n_b]} q_j^{-1} \right)^{1/2}.$$

Finally, by (8.3) there exists a compact $K \subset \mathbb{R}^d$ containing the two trajectories \mathbf{x}_ϑ and $\mathbf{x}_{\tilde{\vartheta}}$. We compute:

$$\begin{aligned} \frac{1}{2} \frac{d}{dt} \|\mathbf{x}_{\vartheta, t} - \mathbf{x}_{\tilde{\vartheta}, t}\|^2 &\leq \left(\|\mathbf{F}(\mathbf{x}_{\vartheta, t}, \vartheta_t) - \mathbf{F}(\mathbf{x}_{\tilde{\vartheta}, t}, \vartheta_t)\| + \|\mathbf{F}(\mathbf{x}_{\tilde{\vartheta}, t}, \vartheta_t) - \mathbf{F}(\mathbf{x}_{\tilde{\vartheta}, t}, \tilde{\vartheta}_t)\| \right) \|\mathbf{x}_{\vartheta, t} - \mathbf{x}_{\tilde{\vartheta}, t}\| \\ &\leq \lambda_{\mathbf{F}, \mathbf{x}, \vartheta} \|\mathbf{x}_{\vartheta, t} - \mathbf{x}_{\tilde{\vartheta}, t}\|^2 + \lambda_{\mathbf{F}, \theta, K} \|\vartheta_t - \tilde{\vartheta}_t\| \|\mathbf{x}_{\vartheta, t} - \mathbf{x}_{\tilde{\vartheta}, t}\|. \end{aligned} \quad (8.8)$$

eq: comp

Applying Lemma 8.3 and doing the symmetric computation with $\tilde{\vartheta}$, the third estimation follows and we complete the proof. \square

inform_bounds

Lemma 8.5. Fix $\mathbf{x}_0 \in \mathbb{R}^d$ and $\vartheta \in L^\infty(0, T; \Theta)$. Let $\mathbf{x}, \hat{\mathbf{x}}$ solve (FM)–(RM) and let $R > 0$ be such that $\mathbf{x}_t, \hat{\mathbf{x}}_t \in B_R$ for all $t \in [0, T]$ (e.g. defined by (8.3)). For any convex $\ell, g \in \mathcal{C}_{\text{loc}}^{1,1}(\mathbb{R}^d)$, set

$$\lambda_{\ell, B_R} := \sup_{\mathbf{x} \in B_R} \|\nabla \ell(\mathbf{x})\|, \quad \lambda_{g, B_R} := \sup_{\mathbf{x} \in B_R} \|\nabla g(\mathbf{x})\|.$$

Let $\mathbf{p}, \hat{\mathbf{p}}$ solve (3.18)–(3.19). Then there exists $C_p > 0$ depending on $T, \beta, \lambda_{\mathbf{F}, \mathbf{x}, \vartheta}, \pi_{\min}^{-1}, \lambda_{\ell, B_R}$ and λ_{g, B_R} , but independent of h , such that

$$\|\mathbf{p}\|_{L^\infty(0, T)} \leq C_p, \quad \|\hat{\mathbf{p}}\|_{L^\infty(0, T)} \leq C_p, \quad \|\dot{\hat{\mathbf{p}}}\|_{L^\infty(0, T)} \leq C_p. \quad (8.9)$$

eq:adjoint_L

Proof. For the first bound in (8.9), differentiate along (3.18) applying Rademacher's theorem in (2.2):

$$\frac{1}{2} \frac{d}{dt} \|\mathbf{p}_t\|^2 = -\langle \nabla_{\mathbf{x}} \mathbf{F}_t(\mathbf{x}_t)^\top \mathbf{p}_t, \mathbf{p}_t \rangle - \beta \langle \nabla \ell(\mathbf{x}_t), \mathbf{p}_t \rangle \leq \lambda_{\mathbf{F}, \mathbf{x}, \vartheta} \|\mathbf{p}_t\|^2 + \beta \lambda_{\ell, B_R} \|\mathbf{p}_t\|.$$

This is exactly the setup of Lemma 8.3. Using the terminal condition $\|\mathbf{p}_T\| = \|\nabla g(\mathbf{x}_T)\| \leq \lambda_{g, B_R}$ yields $\|\mathbf{p}\|_{L^\infty(0, T)} \leq C_1$ with C_1 depending only on the listed quantities. The same computation for (3.19), together with $\|\nabla_{\mathbf{x}} \hat{\mathbf{F}}_t\| \leq \pi_{\min}^{-1} \lambda_{\mathbf{F}, \mathbf{x}, \vartheta}$, gives $\|\hat{\mathbf{p}}\|_{L^\infty(0, T)} \leq C_2$.

Finally, the bound on the derivative follows directly from (3.19) and the previous bounds:

$$\|\dot{\hat{\mathbf{p}}}_t\| \leq \|\nabla_{\mathbf{x}} \hat{\mathbf{F}}_t(\hat{\mathbf{x}}_t)\| \cdot \|\hat{\mathbf{p}}_t\| + \beta \|\nabla \ell(\hat{\mathbf{x}}_t)\| \leq \pi_{\min}^{-1} \lambda_{\mathbf{F}, \mathbf{x}, \vartheta} \|\hat{\mathbf{p}}\|_{L^\infty(0, T)} + \beta \lambda_{\ell, B_R} \leq C_3.$$

Take $C_p = \max\{C_1, C_2, C_3\}$, and thus independent of h and of the particular realization of the batches. \square

The third lemma will be useful to prove Theorem 3.5:

lem:scrS

Lemma 8.6. For any $\omega \in [n_b]$ it holds

$$\sum_{i, \ell \in [p]} \mathbb{E}_\omega \left[\left(1 - \frac{\mathbf{1}_{\{i \in \mathcal{B}_\omega\}}}{\pi_i} \right) \left(1 - \frac{\mathbf{1}_{\{\ell \in \mathcal{B}_\omega\}}}{\pi_\ell} \right) \right] = \sum_{j \in [n_b]} q_j \left(\sum_{i \in \mathcal{B}_j} \frac{1}{\pi_i} \right)^2 - p^2.$$

Proof. For each $i, \ell \in [p]$, we expand the product as

$$\begin{aligned} \left(1 - \frac{\mathbf{1}_{\{i \in \mathcal{B}_\omega\}}}{\pi_i} \right) \left(1 - \frac{\mathbf{1}_{\{\ell \in \mathcal{B}_\omega\}}}{\pi_\ell} \right) &= 1 - \frac{\mathbf{1}_{\{i \in \mathcal{B}_\omega\}}}{\pi_i} - \frac{\mathbf{1}_{\{\ell \in \mathcal{B}_\omega\}}}{\pi_\ell} + \frac{\mathbf{1}_{\{i \in \mathcal{B}_\omega\}} \mathbf{1}_{\{\ell \in \mathcal{B}_\omega\}}}{\pi_i \pi_\ell} \\ &= 1 - \frac{\mathbf{1}_{\{i \in \mathcal{B}_\omega\}}}{\pi_i} - \frac{\mathbf{1}_{\{\ell \in \mathcal{B}_\omega\}}}{\pi_\ell} + \frac{\mathbf{1}_{\{i, \ell \in \mathcal{B}_\omega\}}}{\pi_i \pi_\ell}. \end{aligned}$$

By the definition of π_i in (2.6), we have $\mathbb{E}_\omega[\mathbf{1}_{\{i \in \mathcal{B}_\omega\}}] = \sum_{j \in [n_b]} q_j \mathbf{1}_{\{i \in \mathcal{B}_j\}} = \pi_i$. Thus, we compute

$$\begin{aligned} \mathbb{E}_\omega \left[\left(1 - \frac{\mathbf{1}_{\{i \in \mathcal{B}_\omega\}}}{\pi_i} \right) \left(1 - \frac{\mathbf{1}_{\{\ell \in \mathcal{B}_\omega\}}}{\pi_\ell} \right) \right] &= 1 - \frac{\mathbb{E}_\omega[\mathbf{1}_{\{i \in \mathcal{B}_\omega\}}]}{\pi_i} - \frac{\mathbb{E}_\omega[\mathbf{1}_{\{\ell \in \mathcal{B}_\omega\}}]}{\pi_\ell} + \frac{\mathbb{E}_\omega[\mathbf{1}_{\{i, \ell \in \mathcal{B}_\omega\}}]}{\pi_i \pi_\ell} \\ &= \frac{\sum_{j \in [n_b]} q_j \mathbf{1}_{\{i, \ell \in \mathcal{B}_j\}}}{\pi_i \pi_\ell} - 1. \end{aligned}$$

Summing over all indices $(i, \ell) \in [p]^2$, we get

$$\sum_{i, \ell \in [p]} \mathbb{E}_\omega \left[\left(1 - \frac{\mathbf{1}_{\{i \in \mathcal{B}_\omega\}}}{\pi_i} \right) \left(1 - \frac{\mathbf{1}_{\{\ell \in \mathcal{B}_\omega\}}}{\pi_\ell} \right) \right] = \sum_{j \in [n_b]} q_j \sum_{i, \ell \in [p]} \frac{\mathbf{1}_{\{i, \ell \in \mathcal{B}_j\}}}{\pi_i \pi_\ell} - p^2. \quad (8.10)$$

eq2:lema3

For each $j \in [n_b]$, the term $\mathbf{1}_{\{i, \ell \in \mathcal{B}_j\}}$ is nonzero only when $i, \ell \in \mathcal{B}_j$, so that

$$\sum_{i, \ell \in [p]} \frac{\mathbf{1}_{\{i, \ell \in \mathcal{B}_j\}}}{\pi_i \pi_\ell} = \sum_{i, \ell \in \mathcal{B}_j} \frac{1}{\pi_i \pi_\ell} = \sum_{i \in \mathcal{B}_j} \frac{1}{\pi_i} \sum_{\ell \in \mathcal{B}_j} \frac{1}{\pi_\ell} = \left(\sum_{i \in \mathcal{B}_j} \frac{1}{\pi_i} \right)^2. \quad (8.11)$$

eq3:lema3

By inserting (8.11) into (8.10), the proof follows. \square

ss:prfs1

8.3. Proofs of Section 3.1.

Proof of Theorem 3.1. Let $t \in [0, T]$ be fixed. Similarly to (8.6), we have that

$$\begin{aligned}
\frac{1}{2} \frac{d}{dt} \|\mathbf{x}_t - \hat{\mathbf{x}}_t\|^2 &= \langle \mathbf{F}_t(\mathbf{x}_t) - \mathbf{F}_t^{(\omega_{k_t})}(\hat{\mathbf{x}}_t), \mathbf{x}_t - \hat{\mathbf{x}}_t \rangle \\
&= \langle \mathbf{F}_t(\mathbf{x}_t) - \mathbf{F}_t^{(\omega_{k_t})}(\mathbf{x}_t), \mathbf{x}_t - \hat{\mathbf{x}}_{t_{k_t-1}} \rangle \\
&\quad + \langle \mathbf{F}_t(\mathbf{x}_t) - \mathbf{F}_t^{(\omega_{k_t})}(\mathbf{x}_t), \hat{\mathbf{x}}_{t_{k_t-1}} - \hat{\mathbf{x}}_t \rangle + \langle \mathbf{F}_t^{(\omega_{k_t})}(\mathbf{x}_t) - \mathbf{F}_t^{(\omega_{k_t})}(\hat{\mathbf{x}}_t), \mathbf{x}_t - \hat{\mathbf{x}}_t \rangle \\
&\leq \langle \mathbf{F}_t(\mathbf{x}_t) - \mathbf{F}_t^{(\omega_{k_t})}(\mathbf{x}_t), \mathbf{x}_t - \hat{\mathbf{x}}_{t_{k_t-1}} \rangle \\
&\quad + \|\mathbf{F}_t(\mathbf{x}_t) - \mathbf{F}_t^{(\omega_{k_t})}(\mathbf{x}_t)\| \cdot \|\hat{\mathbf{x}}_{t_{k_t-1}} - \hat{\mathbf{x}}_t\| + \frac{\lambda_{\mathbf{F}, \mathbf{x}, \vartheta}}{\pi_{\min}} \|\mathbf{x}_t - \hat{\mathbf{x}}_t\|^2.
\end{aligned} \tag{8.12}$$

eq:ddtexxrb0

with $\lambda_{\mathbf{F}, \mathbf{x}, \vartheta}$ given by (2.2) and $\pi_{\min} = \min_{i \in [p]} \pi_i$. Now, observe that

$$\mathbb{E}_{\omega} [\langle \mathbf{F}_t(\mathbf{x}_t) - \mathbf{F}_t^{(\omega_{k_t})}(\mathbf{x}_t), \mathbf{x}_t - \hat{\mathbf{x}}_{t_{k_t-1}} \rangle] = \langle \mathbb{E}_{\omega} [\mathbf{F}_t(\mathbf{x}_t) - \mathbf{F}_t^{(\omega_{k_t})}(\mathbf{x}_t)], \mathbb{E}_{\omega} [\mathbf{x}_t - \hat{\mathbf{x}}_{t_{k_t-1}}] \rangle = 0,$$

holds from the unbiasedness of $\hat{\mathbf{F}}$ and the independence between $\mathbf{x}_t - \hat{\mathbf{x}}_{t_{k_t-1}}$ and $\mathbf{F}_t(\mathbf{x}_t) - \mathbf{F}_t^{(\omega_{k_t})}(\mathbf{x}_t)$. Taking the expectation,

$$\begin{aligned}
\frac{1}{2} \frac{d}{dt} \mathbb{E}_{\omega} [\|\mathbf{x}_t - \hat{\mathbf{x}}_t\|^2] &\leq \mathbb{E}_{\omega} [\|\mathbf{F}_t(\mathbf{x}_t) - \mathbf{F}_t^{(\omega_{k_t})}(\mathbf{x}_t)\| \cdot \|\hat{\mathbf{x}}_{t_{k_t-1}} - \hat{\mathbf{x}}_t\|] + \frac{\lambda_{\mathbf{F}, \mathbf{x}, \vartheta}}{\pi_{\min}} \mathbb{E}_{\omega} [\|\mathbf{x}_t - \hat{\mathbf{x}}_t\|^2] \\
&\leq \mathbb{E}_{\omega} [\|\mathbf{F}_t(\mathbf{x}_t) - \mathbf{F}_t^{(\omega_{k_t})}(\mathbf{x}_t)\|^2]^{1/2} \mathbb{E}_{\omega} [\|\hat{\mathbf{x}}_{t_{k_t-1}} - \hat{\mathbf{x}}_t\|^2]^{1/2} + \frac{\lambda_{\mathbf{F}, \mathbf{x}, \vartheta}}{\pi_{\min}} \mathbb{E}_{\omega} [\|\mathbf{x}_t - \hat{\mathbf{x}}_t\|^2] \\
&\leq \Lambda_t(\mathbf{x}_0, \vartheta)^{1/2} \mathbb{E}_{\omega} [\|\hat{\mathbf{x}}_{t_{k_t-1}} - \hat{\mathbf{x}}_t\|^2]^{1/2} + \frac{\lambda_{\mathbf{F}, \mathbf{x}, \vartheta}}{\pi_{\min}} \mathbb{E}_{\omega} [\|\mathbf{x}_t - \hat{\mathbf{x}}_t\|^2].
\end{aligned} \tag{8.13}$$

eq:ddtexxrb0

We integrate (8.13) on $[t_{k_t-1}, t]$ to get

$$\begin{aligned}
\mathbb{E}_{\omega} [\|\mathbf{x}_t - \hat{\mathbf{x}}_t\|^2] &\leq \mathbb{E}_{\omega} [\|\mathbf{x}_{t_{k_t-1}} - \hat{\mathbf{x}}_{t_{k_t-1}}\|^2] \\
&\quad + 2 \int_{t_{k_t-1}}^t \left\{ \Lambda_s(\mathbf{x}_0, \vartheta)^{1/2} \mathbb{E}_{\omega} [\|\hat{\mathbf{x}}_{t_{k_t-1}} - \hat{\mathbf{x}}_s\|^2]^{1/2} + \frac{\lambda_{\mathbf{F}, \mathbf{x}, \vartheta}}{\pi_{\min}} \mathbb{E}_{\omega} [\|\mathbf{x}_s - \hat{\mathbf{x}}_s\|^2] \right\} ds \\
&\leq \mathbb{E}_{\omega} [\|\mathbf{x}_{t_{k_t-1}} - \hat{\mathbf{x}}_{t_{k_t-1}}\|^2] \\
&\quad + 2 \left(\int_{t_{k_t-1}}^t \Lambda_s(\mathbf{x}_0, \vartheta) ds \int_{t_{k_t-1}}^t \mathbb{E}_{\omega} [\|\hat{\mathbf{x}}_{t_{k_t-1}} - \hat{\mathbf{x}}_s\|^2] ds \right)^{1/2} + \frac{\lambda_{\mathbf{F}, \mathbf{x}, \vartheta}}{\pi_{\min}} \int_{t_{k_t-1}}^t \mathbb{E}_{\omega} [\|\mathbf{x}_s - \hat{\mathbf{x}}_s\|^2] ds.
\end{aligned}$$

Applying this bound recursively on the term $\mathbb{E}_{\omega} [\|\mathbf{x}_{t_{k_t-1}} - \hat{\mathbf{x}}_{t_{k_t-1}}\|^2]$, and noting that $\mathbf{x}_0 = \hat{\mathbf{x}}_0$, we get

$$\begin{aligned}
\mathbb{E}_{\omega} [\|\mathbf{x}_t - \hat{\mathbf{x}}_t\|^2] &\leq 2 \sum_{k \in [k_t-1]} \left(\int_{t_{k-1}}^{t_k} \Lambda_s(\mathbf{x}_0, \vartheta) ds \int_{t_{k-1}}^{t_k} \mathbb{E}_{\omega} [\|\hat{\mathbf{x}}_{t_{k-1}} - \hat{\mathbf{x}}_s\|^2] ds \right)^{1/2} \\
&\quad + 2 \left(\int_{t_{k_t-1}}^t \Lambda_s(\mathbf{x}_0, \vartheta) ds \int_{t_{k_t-1}}^t \mathbb{E}_{\omega} [\|\hat{\mathbf{x}}_{t_{k_t-1}} - \hat{\mathbf{x}}_s\|^2] ds \right)^{1/2} + \frac{\lambda_{\mathbf{F}, \mathbf{x}, \vartheta}}{\pi_{\min}} \int_0^t \mathbb{E}_{\omega} [\|\mathbf{x}_s - \hat{\mathbf{x}}_s\|^2] ds \\
&\stackrel{(1)}{\leq} 2 \left(\int_0^t \Lambda_s(\mathbf{x}_0, \vartheta) ds \right)^{1/2} \left(\int_0^t \mathbb{E}_{\omega} [\|\hat{\mathbf{x}}_{t_{k_s-1}} - \hat{\mathbf{x}}_s\|^2] ds \right)^{1/2} + \frac{\lambda_{\mathbf{F}, \mathbf{x}, \vartheta}}{\pi_{\min}} \int_0^t \mathbb{E}_{\omega} [\|\mathbf{x}_s - \hat{\mathbf{x}}_s\|^2] ds,
\end{aligned}$$

where (1) follows from the Cauchy-Schwarz inequality applied to the sum. A standard Grönwall estimate now gives us:

$$\mathbb{E}_{\omega} [\|\mathbf{x}_t - \hat{\mathbf{x}}_t\|^2] \leq 2 \|\Lambda(\mathbf{x}_0, \vartheta)\|_{L^1(0, T)}^{1/2} \left(\int_0^T \mathbb{E}_{\omega} [\|\hat{\mathbf{x}}_{t_{k_s-1}} - \hat{\mathbf{x}}_s\|^2] ds \right)^{1/2} e^{\lambda_{\mathbf{F}, \mathbf{x}, \vartheta} T / \pi_{\min}}. \tag{8.14}$$

eq:estimation

Since $\hat{\mathbf{x}}$ is absolutely continuous, for any $s \in [0, T]$ it holds

$$\mathbb{E}_{\omega} [\|\hat{\mathbf{x}}_{t_{k_s-1}} - \hat{\mathbf{x}}_s\|^2] = \mathbb{E}_{\omega} \left[\left\| \int_{t_{k_s-1}}^s \hat{\mathbf{F}}_{\tau}(\hat{\mathbf{x}}_{\tau}) d\tau \right\|^2 \right] \leq \mathbb{E}_{\omega} \left[\left(\int_{t_{k_s-1}}^s \|\hat{\mathbf{F}}_{\tau}(\hat{\mathbf{x}}_{\tau})\| d\tau \right)^2 \right]$$

$$\leq \mathbb{E}_\omega \left[\int_{t_{k_s-1}}^s d\tau \int_{t_{k_s-1}}^s \|\hat{\mathbf{F}}_\tau(\hat{\mathbf{x}}_\tau)\|^2 d\tau \right] \leq h \int_{t_{k_s-1}}^{t_{k_s}} \mathbb{E}_\omega \left[\|\hat{\mathbf{F}}_\tau(\hat{\mathbf{x}}_\tau)\|^2 \right] d\tau. \quad (8.15)$$

Replacing (8.15) into (8.14), we get

$$\begin{aligned} \mathbb{E}_\omega [\|\mathbf{x}_t - \hat{\mathbf{x}}_t\|^2] &\leq 2\|\Lambda(\mathbf{x}_0, \vartheta)\|_{L^1(0,T)}^{1/2} \left(\int_0^T h \int_{t_{k_s-1}}^{t_{k_s}} \mathbb{E}_\omega [\|\hat{\mathbf{F}}_\tau(\hat{\mathbf{x}}_\tau)\|^2] d\tau ds \right)^{1/2} e^{\lambda_{\mathbf{F},\mathbf{x},\vartheta} T / \pi_{\min}} \\ &= 2\|\Lambda(\mathbf{x}_0, \vartheta)\|_{L^1(0,T)}^{1/2} \left(\int_0^T h^2 \mathbb{E}_\omega [\|\hat{\mathbf{F}}_s(\hat{\mathbf{x}}_s)\|^2] ds \right)^{1/2} e^{\lambda_{\mathbf{F},\mathbf{x},\vartheta} T / \pi_{\min}} \\ &= 2\|\Lambda(\mathbf{x}_0, \vartheta)\|_{L^1(0,T)}^{1/2} \left(\int_0^T \mathbb{E}_\omega [\|\hat{\mathbf{F}}_s(\hat{\mathbf{x}}_s)\|^2] ds \right)^{1/2} h e^{\lambda_{\mathbf{F},\mathbf{x},\vartheta} T / \pi_{\min}}. \end{aligned} \quad (8.16)$$

It only remains to verify that $\|\hat{\mathbf{F}}_t(\hat{\mathbf{x}}_t)\|$ is bounded above by a quantity independent of h . By (2.3), we have for every $t \in [0, T]$

$$\|\hat{\mathbf{F}}_t(\hat{\mathbf{x}}_t)\| \leq \frac{\lambda_{\mathbf{F},\mathbf{x},\vartheta}}{\pi_{\min}} \|\hat{\mathbf{x}}_t\| + \frac{\lambda_{\mathbf{F},0,\vartheta}}{\pi_{\min}} \leq \frac{\lambda_{\mathbf{F},\mathbf{x},\vartheta}}{\pi_{\min}} \|\hat{\mathbf{x}}_t - \mathbf{x}_t\| + \frac{\lambda_{\mathbf{F},\mathbf{x},\vartheta}}{\pi_{\min}} \|\mathbf{x}_t\| + \frac{\lambda_{\mathbf{F},0,\vartheta}}{\pi_{\min}}.$$

So, using (8.3), (8.4) and $\pi_{\min} \leq 1$, we get for $\lambda_{\mathbf{F},\mathbf{x},\vartheta} \neq 0$:

$$\begin{aligned} \|\hat{\mathbf{F}}_t(\hat{\mathbf{x}}_t)\| &\leq \frac{\lambda_{\mathbf{F},\mathbf{x},\vartheta}}{\pi_{\min}} e^{\lambda_{\mathbf{F},\mathbf{x},\vartheta} T / \pi_{\min}} \left(T \|\Lambda(\mathbf{x}_0, \vartheta)\|_{L^1(0,T)} \sum_{j \in [n_b]} q_j^{-1} \right)^{1/2} + \frac{\lambda_{\mathbf{F},\mathbf{x},\vartheta}}{\pi_{\min}} \|\mathbf{x}_0\| e^{\lambda_{\mathbf{F},\mathbf{x},\vartheta} T} + \frac{\lambda_{\mathbf{F},0,\vartheta}}{\pi_{\min}} e^{\lambda_{\mathbf{F},\mathbf{x},\vartheta} T} \\ &\leq \frac{\lambda_{\mathbf{F},\mathbf{x},\vartheta}}{\pi_{\min}} e^{\lambda_{\mathbf{F},\mathbf{x},\vartheta} T / \pi_{\min}} \left[\left(T \|\Lambda(\mathbf{x}_0, \vartheta)\|_{L^1(0,T)} \sum_{j \in [n_b]} q_j^{-1} \right)^{1/2} + \|\mathbf{x}_0\| + \frac{\lambda_{\mathbf{F},0,\vartheta}}{\lambda_{\mathbf{F},\mathbf{x},\vartheta}} \right] \end{aligned} \quad (8.17)$$

and, for $\lambda_{\mathbf{F},\mathbf{x},\vartheta} = 0$:

$$\|\hat{\mathbf{F}}_t(\hat{\mathbf{x}}_t)\| \leq \frac{\lambda_{\mathbf{F},0,\vartheta}}{\pi_{\min}}.$$

We conclude the proof by substituting (8.17) into (8.16). \square

Proof of Corollary 3.2. Let \mathbf{x}_i and $\hat{\mathbf{x}}_i$ be the respective solutions of (FM) and (RM) with $\vartheta = \vartheta_i$ for $i = 1, 2$. Consider the compact set

$$\mathbf{K} = \{\mathbf{x}_{\vartheta_i,t} : t \in [0, T], i = 1, 2\} \cup \{\hat{\mathbf{x}}_{\vartheta_i,t} : t \in [0, T], i = 1, 2\} \subset \mathbb{R}^d.$$

By assumption, there is $\lambda_{\mathbf{F},\mathbf{x},\vartheta} \geq 0$ and $\lambda_{\mathbf{F},\mathbf{x},\vartheta_2}$ with

$$\begin{aligned} \frac{1}{2} \frac{d}{dt} \|\mathbf{x}_{\vartheta_1,t} - \mathbf{x}_{\vartheta_2,t}\|^2 &= \langle \mathbf{F}(\mathbf{x}_{\vartheta_1,t}, \vartheta_{1,t}) - \mathbf{F}(\mathbf{x}_{\vartheta_2,t}, \vartheta_{2,t}), \mathbf{x}_{\vartheta_1,t} - \mathbf{x}_{\vartheta_2,t} \rangle \\ &= \langle \mathbf{F}(\mathbf{x}_{\vartheta_1,t}, \vartheta_{1,t}) - \mathbf{F}(\mathbf{x}_{\vartheta_1,t}, \vartheta_{2,t}), \mathbf{x}_{\vartheta_1,t} - \mathbf{x}_{\vartheta_2,t} \rangle + \langle \mathbf{F}(\mathbf{x}_{\vartheta_1,t}, \vartheta_{2,t}) - \mathbf{F}(\mathbf{x}_{\vartheta_2,t}, \vartheta_{2,t}), \mathbf{x}_{\vartheta_1,t} - \mathbf{x}_{\vartheta_2,t} \rangle \\ &\leq \lambda_{\mathbf{F},\theta,\mathbf{K}} \|\vartheta_{1,t} - \vartheta_{2,t}\| \cdot \|\mathbf{x}_{\vartheta_1,t} - \mathbf{x}_{\vartheta_2,t}\| + \lambda_{\mathbf{F},\mathbf{x},\vartheta_2} \|\mathbf{x}_{\vartheta_1,t} - \mathbf{x}_{\vartheta_2,t}\|^2. \end{aligned}$$

Lemma 8.3 then yields

$$\begin{aligned} \|\mathbf{x}_{\vartheta_1,t} - \mathbf{x}_{\vartheta_2,t}\| &\leq \|\mathbf{x}_{\vartheta_1,0} - \mathbf{x}_{\vartheta_2,0}\| e^{\lambda_{\mathbf{F},\mathbf{x},\vartheta_2} T} + \lambda_{\mathbf{F},\theta,\mathbf{K}} e^{\lambda_{\mathbf{F},\mathbf{x},\vartheta_2} T} \|\vartheta_1 - \vartheta_2\|_{L^1(0,T;\Theta)} \\ &= \lambda_{\mathbf{F},\theta,\mathbf{K}} e^{\lambda_{\mathbf{F},\mathbf{x},\vartheta_2} T} \|\vartheta_1 - \vartheta_2\|_{L^1(0,T;\Theta)}, \end{aligned}$$

and symmetrically with ϑ_1 . Hence

$$\|\mathbf{x}_{\vartheta_1,t} - \mathbf{x}_{\vartheta_2,t}\|^2 \leq (\lambda_{\mathbf{F},\theta,\mathbf{K}} e^{\lambda_{\mathbf{F},\mathbf{x},\vartheta_1} T})^2 \|\vartheta_1 - \vartheta_2\|_{L^1(0,T;\Theta)}^2 \wedge (\lambda_{\mathbf{F},\theta,\mathbf{K}} e^{\lambda_{\mathbf{F},\mathbf{x},\vartheta_2} T})^2 \|\vartheta_1 - \vartheta_2\|_{L^1(0,T;\Theta)}^2.$$

By the triangle inequality and Theorem 3.1,

$$\begin{aligned} \mathbb{E}_\omega [\|\mathbf{x}_{\vartheta_1,t} - \hat{\mathbf{x}}_{\vartheta_2,t}\|^2] &\leq 2\|\mathbf{x}_{\vartheta_1,t} - \mathbf{x}_{\vartheta_2,t}\|^2 + 2\mathbb{E}_\omega [\|\mathbf{x}_{\vartheta_2,t} - \hat{\mathbf{x}}_{\vartheta_2,t}\|^2] \\ &\leq 2\lambda_{\mathbf{F},\theta,\mathbf{K}}^2 e^{2\lambda_{\mathbf{F},\mathbf{x},\vartheta_1} \wedge \lambda_{\mathbf{F},\mathbf{x},\vartheta_2} T} \|\vartheta_1 - \vartheta_2\|_{L^1(0,T;\Theta)}^2 + 2S(\mathbf{x}_0, \vartheta_1) \wedge S(\mathbf{x}_0, \vartheta_2) h. \end{aligned} \quad (8.18)$$

Taking the maximum over $[0, T]$ proves (3.5), with

$$C(\vartheta_1, \vartheta_2) = 2\lambda_{\mathbf{F},\theta,\mathbf{K}}^2 e^{2(\lambda_{\mathbf{F},\mathbf{x},\vartheta_1} \wedge \lambda_{\mathbf{F},\mathbf{x},\vartheta_2}) T}.$$

\square

8.4. Proofs of Section 3.2.

Proof of Theorem 3.5. Fix $(t, \mathbf{x}) \in [0, T] \times \mathbb{R}^d$. Let $\mathbf{y} := \Phi_t^{-1}(\mathbf{x})$ and $\hat{\mathbf{y}} := \hat{\Phi}_t^{-1}(\mathbf{x})$, where Φ_t and $\hat{\Phi}_t$ are the flows of (FM) and (RM), respectively. Define

$$J_t(\mathbf{y}) := \exp \left(- \int_0^t \nabla_{\mathbf{x}} \cdot \mathbf{F}_s(\Phi_s(\mathbf{y})) ds \right), \quad \hat{J}_t(\mathbf{y}) := \exp \left(- \int_0^t \nabla_{\mathbf{x}} \cdot \hat{\mathbf{F}}_s(\hat{\Phi}_s(\mathbf{y})) ds \right).$$

From (3.7), we get for a.e. \mathbf{x}

$$\rho_t(\mathbf{x}) = \rho_B(\mathbf{y}) J_t(\mathbf{y}), \quad \hat{\rho}_t(\mathbf{x}) = \rho_B(\hat{\mathbf{y}}) \hat{J}_t(\hat{\mathbf{y}}).$$

Using the triangle inequality and $\rho_B \in \mathcal{C}^{0,1}(\mathbb{R}^d)$,

$$\begin{aligned} |\rho_t(\mathbf{x}) - \hat{\rho}_t(\mathbf{x})| &\leq |\rho_B(\mathbf{y}) - \rho_B(\hat{\mathbf{y}})| J_t(\mathbf{y}) + \rho_B(\hat{\mathbf{y}}) |J_t(\mathbf{y}) - \hat{J}_t(\hat{\mathbf{y}})| \\ &\leq \lambda_{\rho_B} \|\mathbf{y} - \hat{\mathbf{y}}\| J_t(\mathbf{y}) + \|\rho_B\|_{L^\infty(\mathbb{R}^d)} |J_t(\mathbf{y}) - \hat{J}_t(\hat{\mathbf{y}})|. \end{aligned}$$

By (2.2), it follows that $\|\nabla_{\mathbf{x}} \mathbf{F}_t\| \leq \lambda_{\mathbf{F}, \mathbf{x}, \vartheta}$ and $\|\nabla_{\mathbf{x}} \hat{\mathbf{F}}_t\| \leq \lambda_{\mathbf{F}, \mathbf{x}, \vartheta} / \pi_{\min}$ for a.e. t . Hence

$$|\nabla_{\mathbf{x}} \cdot \mathbf{F}| \leq d\lambda_{\mathbf{F}, \mathbf{x}, \vartheta}, \quad |\nabla_{\mathbf{x}} \cdot \hat{\mathbf{F}}| \leq \frac{d\lambda_{\mathbf{F}, \mathbf{x}, \vartheta}}{\pi_{\min}}, \quad |J_t(\mathbf{y})| \leq e^{d\lambda_{\mathbf{F}, \mathbf{x}, \vartheta} T}, \quad |\hat{J}_t(\mathbf{y})| \leq e^{d\lambda_{\mathbf{F}, \mathbf{x}, \vartheta} T / \pi_{\min}}. \quad (8.19)$$

eq: boundd1

Moreover, with

$$A = - \int_0^t \nabla_{\mathbf{x}} \cdot \mathbf{F}_s(\Phi_s(\mathbf{y})) ds, \quad B = - \int_0^t \nabla_{\mathbf{x}} \cdot \hat{\mathbf{F}}_s(\hat{\Phi}_s(\hat{\mathbf{y}})) ds,$$

the mean value theorem yields $e^A - e^B = e^\xi (A - B)$ for some ξ between A and B . Thus,

$$|e^A - e^B| \leq e^{d\lambda_{\mathbf{F}, \mathbf{x}, \vartheta} T / \pi_{\min}} |A - B|,$$

where we have used (8.19). We can deduce

$$|\rho_t(\mathbf{x}) - \hat{\rho}_t(\mathbf{x})|^2 \leq 2\lambda_{\rho_B}^2 e^{2d\lambda_{\mathbf{F}, \mathbf{x}, \vartheta} T} \|\mathbf{y} - \hat{\mathbf{y}}\|^2 + 2\|\rho_B\|_{L^\infty(\mathbb{R}^d)}^2 e^{2d\lambda_{\mathbf{F}, \mathbf{x}, \vartheta} T / \pi_{\min}} |A - B|^2. \quad (8.20)$$

eq: rho-diff-

After taking expectation, the first term on the RHS can be bounded using Theorem 3.1:

$$2\lambda_{\rho_B}^2 e^{2d\lambda_{\mathbf{F}, \mathbf{x}, \vartheta} T} \mathbb{E}_\omega [\|\mathbf{y} - \hat{\mathbf{y}}\|^2] \leq 2\lambda_{\rho_B}^2 e^{2d\lambda_{\mathbf{F}, \mathbf{x}, \vartheta} T} S(\mathbf{x}, \vartheta_{t-}) h. \quad (8.21)$$

eq: transport

Meanwhile, we decompose

$$A - B = \int_0^t \nabla_{\mathbf{x}} \cdot (\mathbf{F}_s(\Phi_s(\mathbf{y})) - \hat{\mathbf{F}}_s(\Phi_s(\mathbf{y}))) ds + \int_0^t \nabla_{\mathbf{x}} \cdot (\hat{\mathbf{F}}_s(\Phi_s(\mathbf{y})) - \hat{\mathbf{F}}_s(\hat{\Phi}_s(\hat{\mathbf{y}}))) ds$$

and use $(u + v)^2 \leq 2u^2 + 2v^2$ to bound the second term of (8.20) as

$$|A - B|^2 \leq 2 \left| \int_0^t \nabla_{\mathbf{x}} \cdot (\mathbf{F}_s(\Phi_s(\mathbf{y})) - \hat{\mathbf{F}}_s(\Phi_s(\mathbf{y}))) ds \right|^2 + 2 \left| \int_0^t \nabla_{\mathbf{x}} \cdot (\hat{\mathbf{F}}_s(\Phi_s(\mathbf{y})) - \hat{\mathbf{F}}_s(\hat{\Phi}_s(\hat{\mathbf{y}}))) ds \right|^2.$$

For the term with different trajectories, we use Cauchy-Schwarz, (A2) and Theorem 3.1 (applied to the time-reversed control $s \mapsto \vartheta_{t-s}$ and field $-\mathbf{F}$):

$$\begin{aligned} \left| \int_0^t \nabla_{\mathbf{x}} \cdot (\hat{\mathbf{F}}_s(\Phi_s(\mathbf{y})) - \hat{\mathbf{F}}_s(\hat{\Phi}_s(\hat{\mathbf{y}}))) ds \right|^2 &\leq \frac{d^2 \lambda_{\nabla_{\mathbf{x}} \mathbf{F}, \mathbf{x}, \vartheta}^2 T}{\pi_{\min}^2} \int_0^t \|\Phi_s(\mathbf{y}) - \hat{\Phi}_s(\hat{\mathbf{y}})\|^2 ds \\ &\leq \frac{d^2 \lambda_{\nabla_{\mathbf{x}} \mathbf{F}, \mathbf{x}, \vartheta}^2 T^2}{\pi_{\min}^2} S(\mathbf{x}, \vartheta_{t-}) h. \end{aligned} \quad (8.22)$$

eq: bound11tr

For the term with the same spatial trajectory, we get

$$\begin{aligned} \left| \int_0^t \nabla_{\mathbf{x}} \cdot (\mathbf{F}_s(\Phi_s(\mathbf{y})) - \hat{\mathbf{F}}_s(\Phi_s(\mathbf{y}))) ds \right|^2 &\leq \left| \sum_{k \in [n_s]} \int_{t_{k-1}}^{t_k} \nabla_{\mathbf{x}} \cdot (\mathbf{F}_s(\Phi_s(\mathbf{y})) - \mathbf{F}_s^{(\omega_k)}(\Phi_s(\mathbf{y}))) ds \right|^2 \\ &= \left| \sum_{k \in [n_s]} \sum_{i \in [p]} \left(1 - \frac{\mathbf{1}_{\{i \in \mathcal{B}_{\omega_k}\}}}{\pi_i} \right) \int_{t_{k-1}}^{t_k} \nabla_{\mathbf{x}} \cdot \mathbf{f}_i(\Phi_s(\mathbf{y}), \vartheta_{i,s}) ds \right|^2 \\ &\leq \left| \sum_{k \in [n_s]} \sum_{i \in [p]} \left(1 - \frac{\mathbf{1}_{\{i \in \mathcal{B}_{\omega_k}\}}}{\pi_i} \right) h d\lambda_{\mathbf{F}, \mathbf{x}, \vartheta} \right|^2 \end{aligned}$$

$$= h^2 d^2 \lambda_{\mathbf{F}, \mathbf{x}, \vartheta}^2 \sum_{k, \ell \in [n_s]} \sum_{i, j \in [p]} \left(1 - \frac{\mathbf{1}_{\{i \in \mathcal{B}_{\omega_k}\}}}{\pi_i}\right) \left(1 - \frac{\mathbf{1}_{\{j \in \mathcal{B}_{\omega_\ell}\}}}{\pi_j}\right).$$

Because the random variables ω_k are independent and $\mathbb{E}_\omega[\mathbf{1}_{\{i \in \mathcal{B}_{\omega_k}\}}] = \pi_i$,

$$\begin{aligned} \mathbb{E}_\omega \left[\sum_{i, j \in [p]} \left(1 - \frac{\mathbf{1}_{\{i \in \mathcal{B}_{\omega_k}\}}}{\pi_i}\right) \left(1 - \frac{\mathbf{1}_{\{j \in \mathcal{B}_{\omega_\ell}\}}}{\pi_j}\right) \right] &= \mathbb{E}_\omega \left[\sum_{i \in [p]} \left(1 - \frac{\mathbf{1}_{\{i \in \mathcal{B}_{\omega_k}\}}}{\pi_i}\right) \right] \mathbb{E}_\omega \left[\sum_{j \in [p]} \left(1 - \frac{\mathbf{1}_{\{j \in \mathcal{B}_{\omega_\ell}\}}}{\pi_j}\right) \right] \\ &= 0. \end{aligned}$$

Thus, taking the expectation,

$$\begin{aligned} \mathbb{E}_\omega \left[\left| \int_0^t \nabla_{\mathbf{x}} \cdot (\mathbf{F}_s(\Phi_s(\mathbf{y})) - \hat{\mathbf{F}}_s(\Phi_s(\mathbf{y}))) \, ds \right|^2 \right] &\leq h^2 d^2 \lambda_{\mathbf{F}, \mathbf{x}, \vartheta}^2 \sum_{k \in [n_s]} \mathbb{E}_\omega \left[\sum_{i, j \in [p]} \left(1 - \frac{\mathbf{1}_{\{i \in \mathcal{B}_{\omega_k}\}}}{\pi_i}\right) \left(1 - \frac{\mathbf{1}_{\{j \in \mathcal{B}_{\omega_k}\}}}{\pi_j}\right) \right] \\ &\leq h^2 d^2 \lambda_{\mathbf{F}, \mathbf{x}, \vartheta}^2 \sum_{k \in [n_s]} \left(\sum_{j \in [n_b]} q_j \left(\sum_{i \in \mathcal{B}_j} \pi_i^{-1} \right)^2 - p^2 \right) \\ &= h d^2 \lambda_{\mathbf{F}, \mathbf{x}, \vartheta}^2 T \left(\sum_{j \in [n_b]} q_j \left(\sum_{i \in \mathcal{B}_j} \pi_i^{-1} \right)^2 - p^2 \right), \end{aligned}$$

where we have applied [Lemma 8.6](#) and $hn_s = T$. All in all, we can bound

$$\mathbb{E}_\omega \left[|A - B|^2 \right] \leq 2d^2 \lambda_{\mathbf{F}, \mathbf{x}, \vartheta}^2 T \left(\sum_{j \in [n_b]} q_j \left(\sum_{i \in \mathcal{B}_j} \pi_i^{-1} \right)^2 - p^2 \right) h + \frac{2d^2 \lambda_{\nabla_{\mathbf{x}} \mathbf{F}, \mathbf{x}, \vartheta}^2 T^2}{\pi_{\min}^2} S(\mathbf{x}, \vartheta_{t-}) h. \quad (8.23)$$

Combining (8.20) with (8.21) and (8.23), we conclude that (3.9) holds for all $t \in [0, T]$ and $\mathbf{x} \in \mathbb{R}^d$, with

$$C(\rho_B, \vartheta) = e^{2d\lambda_{\mathbf{F}, \mathbf{x}, \vartheta} T} \left[2\lambda_{\rho_B}^2 + 4d^2 T \|\rho_B\|_{L^\infty(\mathbb{R}^d)}^2 \left(\frac{\lambda_{\nabla_{\mathbf{x}} \mathbf{F}, \mathbf{x}, \vartheta}^2 T}{\pi_{\min}^2} + \lambda_{\mathbf{F}, \mathbf{x}, \vartheta}^2 \left(\sum_{j \in [n_b]} q_j \left(\sum_{i \in \mathcal{B}_j} \pi_i^{-1} \right)^2 - p^2 \right) \right) \right].$$

□

Proof of Corollary 3.6. For $q > 0$, using (8.3) we get for some constants $c_1, c_2 \geq 0$:

$$\|\mathbf{x}_t\|^q \leq e^{c_1 T} \|\mathbf{x}_0\|^q + \frac{c_2}{c_1} (e^{c_1 T} - 1). \quad (8.24)$$

Integrating (8.24) against ρ_B gives a bound

$$\int_{\mathbb{R}^d} \|\mathbf{x}\|^q \rho_t(\mathbf{x}) \, d\mathbf{x} \leq e^{c_1 T} \int_{\mathbb{R}^d} \|\mathbf{x}\|^q \rho_B(\mathbf{x}) \, d\mathbf{x} + \frac{c_2}{c_1} (e^{c_1 T} - 1) =: M_q, \quad (8.25)$$

and the same holds for $\hat{\rho}_t$ with c_1 and c_2 rescaled by π_{\min}^{-1} . Thus for all $R > 0$,

$$\int_{\mathbb{R}^d \setminus B_R} \rho_t + \int_{\mathbb{R}^d \setminus B_R} \hat{\rho}_t \leq \int_{\mathbb{R}^d \setminus B_R} \|\mathbf{x}\|^q \rho_t(\mathbf{x}) / R^q + \int_{\mathbb{R}^d \setminus B_R} \|\mathbf{x}\|^q \hat{\rho}_t(\mathbf{x}) / R^q \leq \frac{2M_q}{R^q}. \quad (8.26)$$

Next, by (3.9),

$$\mathbb{E}_\omega \left[|\rho_t(\mathbf{x}) - \hat{\rho}_t(\mathbf{x})|^2 \right] \leq C(\rho_B, \vartheta) (1 + S(\mathbf{x}, \vartheta_{t-})) h. \quad (8.27)$$

By (3.2) and (2.2)–(2.3), there exists $K_\Lambda \geq 0$, independent of t and h , such that

$$\Lambda_t(\mathbf{x}, \vartheta) = \sum_j q_j \|\mathbf{F}(\mathbf{x}, \vartheta_t) - \mathbf{F}^{(j)}(\mathbf{x}, \vartheta_t)\|^2 \leq K_\Lambda (1 + \|\mathbf{x}\|)^2.$$

Applying (8.3) to the backward characteristic \mathbf{y}_s with $\mathbf{y}_0 = \mathbf{x}$ (where Φ_t is the flow of (FM)) yields

$$\max_{s \in [0, t]} \|\mathbf{y}_s\| \leq \|\mathbf{x}\| e^{\lambda_{\mathbf{F}, \mathbf{x}, \vartheta} t} + \frac{\lambda_{\mathbf{F}, 0, \vartheta}}{\lambda_{\mathbf{F}, \mathbf{x}, \vartheta}} (e^{\lambda_{\mathbf{F}, \mathbf{x}, \vartheta} t} - 1). \quad (8.28)$$

Hence,

$$\|\Lambda(\mathbf{x}, \vartheta_{t-})\|_{L^1(0, t)} \leq t K_\Lambda (1 + \max_{s \in [0, t]} \|\mathbf{y}_s\|)^2 \quad (8.29)$$

admits an upper bound quadratic in $\|\mathbf{x}\|$. Substituting (8.29) into the explicit formula (4.1) shows that $\mathbf{S}(\mathbf{x}, \vartheta_{t-})$ also admits an upper bound quadratic in $\|\mathbf{x}\|$. Using Cauchy–Schwarz in space and Jensen in expectation, together with $\int_{B_R} d\mathbf{x} = C_d R^d$, we get

$$\mathbb{E}_\omega \left[\int_{B_R} |\rho_t - \hat{\rho}_t| \right] \leq \sqrt{C_d R^d} \left(\int_{B_R} \mathbb{E}_\omega [|\rho_t - \hat{\rho}_t|^2] \right)^{1/2}.$$

Combining with (8.27) and the quadratic bound for \mathbf{S} , we obtain, for all $R \geq 1$,

$$\mathbb{E}_\omega \left[\int_{B_R} |\rho_t - \hat{\rho}_t| \right] \leq K \sqrt{h} R^{d+1},$$

with $K \geq 0$ constant and independent of h . Decomposing $\mathbb{R}^d = B_R \cup (\mathbb{R}^d \setminus B_R)$ and combining with (8.26) gives

$$\mathbb{E}_\omega [\|\rho_t - \hat{\rho}_t\|_{L^1}] \leq K \sqrt{h} R^{d+1} + \frac{2M_q}{R^q}.$$

Optimizing at $R^* = \left(\frac{2M_q}{K\sqrt{h}} \right)^{1/(q+d+1)}$ finally yields

$$\mathbb{E}_\omega [\|\rho_t - \hat{\rho}_t\|_{L^1(\mathbb{R}^d)}] \leq K(\rho_B, \vartheta, T, q) h^{\frac{q}{2q+2d+2}},$$

which is (3.10). □

8.5. Proofs of Section 3.3.

Proof of Proposition 3.7. Using $(a+b)^2 \leq 2a^2 + 2b^2$,

$$\mathbb{E}_\omega \left[|\hat{J}(\hat{\vartheta}^*) - J(\vartheta^*)|^2 \right] \leq 2\mathbb{E}_\omega \left[|\hat{J}(\hat{\vartheta}^*) - J(\hat{\vartheta}^*)|^2 \right] + 2\mathbb{E}_\omega \left[|\hat{J}(\vartheta^*) - J(\vartheta^*)|^2 \right]. \quad (8.30)$$

eq:estimation

We bound the first term (the second is identical with ϑ^* in place of $\hat{\vartheta}^*$). Let $\mathbf{x}_{m,t}$ and $\hat{\mathbf{x}}_{m,t}$ solve (3.11) and (3.14) with $\vartheta = \hat{\vartheta}^*$. Using Lipschitz continuity of ℓ_m, g_m on B_R ,

$$\begin{aligned} |\hat{J}(\hat{\vartheta}^*) - J(\hat{\vartheta}^*)| &\leq \sum_{m \in [n_d]} \left| \beta \int_0^T (\ell_m(\hat{\mathbf{x}}_{m,t}) - \ell_m(\mathbf{x}_{m,t})) dt + g_m(\hat{\mathbf{x}}_{m,T}) - g_m(\mathbf{x}_{m,T}) \right| \\ &\leq \sum_{m \in [n_d]} \left(\beta \lambda_{\ell_m, B_R} \int_0^T \|\hat{\mathbf{x}}_{m,t} - \mathbf{x}_{m,t}\| dt + \lambda_{g_m, B_R} \|\hat{\mathbf{x}}_{m,T} - \mathbf{x}_{m,T}\| \right). \end{aligned}$$

Squaring and using again $(a+b)^2 \leq 2a^2 + 2b^2$,

$$|\hat{J}(\hat{\vartheta}^*) - J(\hat{\vartheta}^*)|^2 \leq 2 \sum_{m \in [n_d]} \left(\beta^2 \lambda_{\ell_m, B_R}^2 T^2 \max_{t \in [0, T]} \|\hat{\mathbf{x}}_{m,t} - \mathbf{x}_{m,t}\|^2 + \lambda_{g_m, B_R}^2 \|\hat{\mathbf{x}}_{m,T} - \mathbf{x}_{m,T}\|^2 \right).$$

Taking expectations, by Theorem 3.1 it follows that

$$\mathbb{E}_\omega \left[|\hat{J}(\hat{\vartheta}^*) - J(\hat{\vartheta}^*)|^2 \right] \leq 2 \sum_{m \in [n_d]} (\beta^2 \lambda_{\ell_m, B_R}^2 T^2 + \lambda_{g_m, B_R}^2) \mathbf{S}(\mathbf{x}_m, \hat{\vartheta}^*) h.$$

Repeating the argument for ϑ^* and substituting on (8.30), the proof concludes. □

Proof of Proposition 3.8. As in Theorem 3.1 and Corollary 3.2, we split the proof into (i) same control and (ii) different controls. Constants $C > 0$ below are independent of h and may change from line to line.

(i) *Same control.* Fix $\vartheta \in L^\infty(0, T; \Theta)$ and drop the explicit dependence of \mathbf{p} and \mathbf{x} on this parameter. For each $t \in [0, T]$,

$$\frac{1}{2} \|\mathbf{p}_t - \hat{\mathbf{p}}_t\|^2 \leq \|\mathbf{p}_t(\mathbf{x}) - \hat{\mathbf{p}}_t(\mathbf{x})\|^2 + \|\hat{\mathbf{p}}_t(\mathbf{x}) - \hat{\mathbf{p}}_t(\hat{\mathbf{x}})\|^2 =: A_t + B_t \quad (8.31)$$

eq: p_same

where $\mathbf{p}(\mathbf{x})$ and $\hat{\mathbf{p}}(\mathbf{x})$ solve (3.18) and (3.19), respectively, with forward trajectory $\mathbf{x}: [0, T] \rightarrow \mathbb{R}^d$.

Term A_t . On each $[t_{k-1}, t_k)$, differentiate A_t and expand as in (8.13), but with $\nabla_{\mathbf{x}} \mathbf{F}_t$ instead of \mathbf{F}_t , and use unbiasedness/independence of ω_{k_t} to cancel the cross term in expectation, exactly as in (8.12)–(8.13).

Using Γ (definition (3.20)), Lemma 8.5 and Grönwall gives

$$\mathbb{E}_\omega [A_t] \leq C e^{\lambda_{\mathbf{F}, \mathbf{x}, \vartheta} T / \pi_{\min}} \left(\int_0^T \Gamma_s(\mathbf{x}_0, \vartheta) ds \right)^{1/2} \left(\int_0^T \mathbb{E}_\omega [\|\hat{\mathbf{p}}_s - \hat{\mathbf{p}}_{t_{k_s-1}}\|^2] ds \right)^{1/2}.$$

By absolute continuity and Cauchy-Schwarz, for $s \in [t_{k_s-1}, t_{k_s})$ we get

$$\|\hat{\mathbf{p}}_s - \hat{\mathbf{p}}_{t_{k-1}}\|^2 \leq (s - t_{k-1}) \int_{t_{k-1}}^s \|\dot{\hat{\mathbf{p}}}_\tau\|^2 d\tau \leq h \int_{t_{k-1}}^{t_k} \|\dot{\hat{\mathbf{p}}}_\tau\|^2 d\tau.$$

Summing on k and using [Lemma 8.5](#),

$$\int_0^T \mathbb{E}_\omega \|\hat{\mathbf{p}}_s - \hat{\mathbf{p}}_{t_{k_s-1}}\|^2 ds \leq h \int_0^T \int_{t_{k-1}}^{t_k} \mathbb{E}_\omega \|\dot{\hat{\mathbf{p}}}_\tau\|^2 d\tau ds \leq C_p h^2.$$

Thus

$$\mathbb{E}_\omega [A_t] \leq C e^{\lambda_{\mathbf{F}, \mathbf{x}, \vartheta} T / \pi_{\min}} \|\Gamma(\mathbf{x}_0, \vartheta)\|_{L^1(0, T)}^{1/2} h. \quad (8.32)$$

Term B_t . Let $\lambda_{\nabla \ell, B_R}$ be the Lipschitz constant of $\nabla \ell$ on a ball $B_R \subset \mathbb{R}^d$ that contains the two trajectories \mathbf{x} and $\hat{\mathbf{x}}$. Thanks to [\(A2\)](#) and [Lemma 8.5](#), we can compute

$$\begin{aligned} \frac{dB_t}{dt} &\leq \|\nabla_{\mathbf{x}} \hat{\mathbf{F}}_t(\mathbf{x}_t) - \nabla_{\mathbf{x}} \hat{\mathbf{F}}_t(\hat{\mathbf{x}}_t)\| \cdot \|\hat{\mathbf{p}}_t\| \sqrt{B_t} + \frac{\lambda_{\mathbf{F}, \mathbf{x}, \vartheta}}{\pi_{\min}} B_t + \|\nabla \ell(\mathbf{x}_t) - \nabla \ell(\hat{\mathbf{x}}_t)\| \sqrt{B_t} \\ &\leq \frac{\lambda_{\nabla_{\mathbf{x}} \mathbf{F}, \mathbf{x}, \vartheta}}{\pi_{\min}} \|\mathbf{x}_t - \hat{\mathbf{x}}_t\| C_p \sqrt{B_t} + \frac{\lambda_{\mathbf{F}, \mathbf{x}, \vartheta}}{\pi_{\min}} B_t + \beta \lambda_{\nabla \ell, B_R} \|\mathbf{x}_t - \hat{\mathbf{x}}_t\| \sqrt{B_t}. \end{aligned}$$

Taking expectation and setting $u(t) := \sqrt{\mathbb{E}_\omega[B_t]}$, we obtain

$$\dot{u}(t) \leq \frac{\lambda_{\mathbf{F}, \mathbf{x}, \vartheta}}{2\pi_{\min}} \max\{C_p, 1\} u(t) + C \left(\mathbb{E}_\omega \|\mathbf{x}_t - \hat{\mathbf{x}}_t\|^2 \right)^{1/2}.$$

By [Theorem 3.1](#) and Grönwall's inequality, we get

$$\mathbb{E}_\omega [B_t] \leq C e^{CT} S(\mathbf{x}_0, \vartheta) h. \quad (8.33)$$

Combining [\(8.32\)](#)–[\(8.33\)](#) in [\(8.31\)](#) and taking $\max_{t \in [0, T]}$, we conclude

$$\max_{t \in [0, T]} \mathbb{E}_\omega \|\mathbf{p}_t - \hat{\mathbf{p}}_t\|^2 \leq C \left(\sqrt{\|\Gamma(\mathbf{x}_0, \vartheta)\|_{L^1(0, T)}} + S(\mathbf{x}_0, \vartheta) \right) h. \quad (8.34)$$

Different controls. We proceed as in the proof of [Corollary 3.2](#). Apply the triangle inequality with an intermediate term:

$$\|\mathbf{p}_{\vartheta_1, t} - \hat{\mathbf{p}}_{\vartheta_2, t}\|^2 \leq 2\|\mathbf{p}_{\vartheta_1, t} - \mathbf{p}_{\vartheta_2, t}\|^2 + 2\|\mathbf{p}_{\vartheta_2, t} - \hat{\mathbf{p}}_{\vartheta_2, t}\|^2. \quad (8.35)$$

The second term is controlled by [\(8.34\)](#) with $\vartheta = \vartheta_2$. For the first, denote $\Delta \mathbf{p} = \mathbf{p}_{\vartheta_1} - \mathbf{p}_{\vartheta_2}$, $\Delta \mathbf{x} = \mathbf{x}_{\vartheta_1} - \mathbf{x}_{\vartheta_2}$, $\Delta \vartheta = \vartheta_1 - \vartheta_2$ and expand (for a.e. t):

$$\begin{aligned} \frac{1}{2} \frac{d}{dt} \|\Delta \mathbf{p}_t\|^2 &= - \left\langle \nabla_{\mathbf{x}} \mathbf{F}(\mathbf{x}_{\vartheta_2, t}, \vartheta_2, t)^\top \Delta \mathbf{p}_t, \Delta \mathbf{p}_t \right\rangle \\ &\quad - \left\langle (\nabla_{\mathbf{x}} \mathbf{F}(\mathbf{x}_{\vartheta_1, t}, \vartheta_1, t) - \nabla_{\mathbf{x}} \mathbf{F}(\mathbf{x}_{\vartheta_2, t}, \vartheta_2, t))^\top \mathbf{p}_{\vartheta_1, t}, \Delta \mathbf{p}_t \right\rangle - \beta \left\langle \nabla \ell(\mathbf{x}_{\vartheta_1, t}) - \nabla \ell(\mathbf{x}_{\vartheta_2, t}), \Delta \mathbf{p}_t \right\rangle. \end{aligned}$$

For [\(A2\)](#), [\(A3\)](#) (uniformly on B_R) and [\(2.2\)](#),

$$\begin{aligned} \frac{1}{2} \frac{d}{dt} \|\Delta \mathbf{p}_t\|^2 &\leq \lambda_{\mathbf{F}, \mathbf{x}, \vartheta} \|\Delta \mathbf{p}_t\|^2 + \|\mathbf{p}_{\vartheta_1, t}\| (\lambda_{\nabla_{\mathbf{x}} \mathbf{F}, \mathbf{x}, \vartheta} \|\Delta \mathbf{x}_t\| + \lambda_{\nabla_{\mathbf{x}} \mathbf{F}, \vartheta, B_R} \|\Delta \vartheta_t\|) \|\Delta \mathbf{p}_t\| \\ &\quad + \beta \lambda_{\nabla \ell, B_R} \|\Delta \mathbf{x}_t\| \|\Delta \mathbf{p}_t\|. \end{aligned}$$

We bound $\|\Delta \mathbf{x}_t\|$ using [\(8.8\)](#) as

$$\max_{t \in [0, T]} \|\Delta \mathbf{x}_t\| \leq \lambda_{\mathbf{F}, \vartheta, B_R} e^{(\lambda_{\mathbf{F}, \mathbf{x}, \vartheta_1} \vee \lambda_{\mathbf{F}, \mathbf{x}, \vartheta_2}) T} \|\vartheta_1 - \vartheta_2\|_{L^1(0, T; \Theta)},$$

and close with [Lemma 8.3](#) and [\(8.9\)](#):

$$\max_{t \in [0, T]} \|\Delta \mathbf{p}_t\|^2 \leq e^{2\lambda_{\mathbf{F}, \mathbf{x}, \vartheta} T} \left[\lambda_{\nabla_{\mathbf{x}} \mathbf{F}, \vartheta, B_R} C_p + \left(\lambda_{\nabla_{\mathbf{x}} \mathbf{F}, \mathbf{x}, \vartheta} C_p + \beta \lambda_{\nabla \ell, B_R} \right) \lambda_{\mathbf{F}, \vartheta, B_R} e^{(\lambda_{\mathbf{F}, \mathbf{x}, \vartheta_1} \vee \lambda_{\mathbf{F}, \mathbf{x}, \vartheta_2}) T} \right]^2 \|\vartheta_1 - \vartheta_2\|_{L^1}^2.$$

Take expectations and maximum over time in [\(8.35\)](#). Then, collecting the pieces yields

$$\max_{t \in [0, T]} \mathbb{E}_\omega [\|\mathbf{p}_{\vartheta_1, t} - \hat{\mathbf{p}}_{\vartheta_2, t}\|^2] \leq C \left(\sqrt{\|\Gamma(\mathbf{x}_0, \vartheta_1)\|_{L^1(0, T)}} + S(\mathbf{x}_0, \vartheta_1) \right) h + C \|\vartheta_1 - \vartheta_2\|_{L^1(0, T; \Theta)}^2.$$

By symmetry (swap ϑ_1, ϑ_2 in the triangle step) we obtain the same bound with ϑ_2 in place of ϑ_1 . Taking the minimum between both completes the proof. \square

The following lemma quantifies the deviation in the functional derivatives of J evaluated at any pair of controls:

Lemma 8.7. Assume (A1)–(A5), for any $\vartheta_1, \vartheta_2 \in L^\infty(0, T; \Theta)$ there exists $C > 0$ independent of h such that

$$\mathbb{E}_\omega[\|\nabla J(\vartheta_1) - \nabla \hat{J}(\vartheta_2)\|_{L^2(0, T; \Theta)}^2] \leq C \left(\mathbb{E}_\omega\|\vartheta_1 - \vartheta_2\|_{L^2(0, T; \Theta)}^2 + C_1(\vartheta_1, \vartheta_2) + hC_2(\vartheta_1, \vartheta_2) \right). \quad (8.36)$$

where $C_1(\vartheta_1, \vartheta_2)$ and $C_2(\vartheta_1, \vartheta_2)$ are two positive constants dependent on the controls and the dataset, and uniformly bounded with respect to $h > 0$.

Proof of Lemma 8.7. Fix one datum and omit the index m throughout. Then, for ϑ_1, ϑ_2 ,

$$\nabla J(\vartheta_1) - \nabla \hat{J}(\vartheta_2) = \alpha(\vartheta_1 - \vartheta_2) + (A_t + B_t),$$

with

$$A_t := \left(\nabla_\theta \mathbf{F}(\mathbf{x}_{\vartheta_1, t}, \vartheta_{1, t}) - \nabla_\theta \hat{\mathbf{F}}(\hat{\mathbf{x}}_{\vartheta_2, t}, \vartheta_{2, t}) \right)^\top \mathbf{p}_{\vartheta_1, t}, \quad B_t := \nabla_\theta \hat{\mathbf{F}}(\hat{\mathbf{x}}_{\vartheta_2, t}, \vartheta_{2, t})^\top (\mathbf{p}_{\vartheta_1, t} - \hat{\mathbf{p}}_{\vartheta_2, t}).$$

(i) *Term A_t .* By the triangle inequality and (A4), (A5), we can bound

$$\begin{aligned} \|\nabla_\theta \mathbf{F}(\mathbf{x}_{\vartheta_1, t}, \vartheta_{1, t}) - \nabla_\theta \hat{\mathbf{F}}(\hat{\mathbf{x}}_{\vartheta_2, t}, \vartheta_{2, t})\| &\leq \|\nabla_\theta \mathbf{F}(\mathbf{x}_{\vartheta_1, t}, \vartheta_{1, t}) - \nabla_\theta \mathbf{F}(\mathbf{x}_{\vartheta_1, t}, \vartheta_{2, t})\| \\ &\quad + \|\nabla_\theta \mathbf{F}(\mathbf{x}_{\vartheta_1, t}, \vartheta_{2, t}) - \nabla_\theta \hat{\mathbf{F}}(\hat{\mathbf{x}}_{\vartheta_2, t}, \vartheta_{2, t})\| \\ &\quad + \|\nabla_\theta \mathbf{F}(\hat{\mathbf{x}}_{\vartheta_2, t}, \vartheta_{2, t}) - \nabla_\theta \hat{\mathbf{F}}(\hat{\mathbf{x}}_{\vartheta_2, t}, \vartheta_{2, t})\| \\ &\leq \lambda_{\nabla_\theta \mathbf{F}, \theta, B_R} \|\Delta \vartheta_t\| + \lambda_{\nabla_\theta \mathbf{F}, \mathbf{x}, \vartheta} \|\Delta \mathbf{x}_t\| \\ &\quad + \|\nabla_\theta \mathbf{F}(\hat{\mathbf{x}}_{\vartheta_2, t}, \vartheta_{2, t}) - \nabla_\theta \hat{\mathbf{F}}(\hat{\mathbf{x}}_{\vartheta_2, t}, \vartheta_{2, t})\|, \end{aligned}$$

where $\Delta \vartheta = \vartheta_1 - \vartheta_2$, $\Delta \mathbf{x} = \mathbf{x}_{\vartheta_1} - \hat{\mathbf{x}}_{\vartheta_2}$ and $B_R \subset \mathbb{R}^d$ contains all trajectories. Using $(a + b + c)^2 \leq 3(a^2 + b^2 + c^2)$ and Lemma 8.5,

$$\begin{aligned} \|A_t\|^2 &\leq 3 \|\mathbf{p}_{\vartheta_1, t}\|^2 \left(\lambda_{\nabla_\theta \mathbf{F}, \theta, B_R}^2 \|\Delta \vartheta_t\|^2 + \lambda_{\nabla_\theta \mathbf{F}, \mathbf{x}, \vartheta}^2 \|\Delta \mathbf{x}_t\|^2 + \|\nabla_\theta \mathbf{F}(\hat{\mathbf{x}}_{\vartheta_2, t}, \vartheta_{2, t}) - \nabla_\theta \hat{\mathbf{F}}(\hat{\mathbf{x}}_{\vartheta_2, t}, \vartheta_{2, t})\|^2 \right) \\ &\leq 3C_p^2 \left(\lambda_{\nabla_\theta \mathbf{F}, \theta, B_R}^2 \|\Delta \vartheta_t\|^2 + \lambda_{\nabla_\theta \mathbf{F}, \mathbf{x}, \vartheta}^2 \|\Delta \mathbf{x}_t\|^2 + \|\nabla_\theta \mathbf{F}(\hat{\mathbf{x}}_{\vartheta_2, t}, \vartheta_{2, t}) - \nabla_\theta \hat{\mathbf{F}}(\hat{\mathbf{x}}_{\vartheta_2, t}, \vartheta_{2, t})\|^2 \right) \end{aligned}$$

with $C_p > 0$ independent of h . Taking expectations and integrating over $[0, T]$ gives, by Corollary 3.2,

$$\begin{aligned} \int_0^T \mathbb{E}_\omega \|A_t\|^2 dt &\leq 3C_p^2 \left(\lambda_{\nabla_\theta \mathbf{F}, \theta, B_R}^2 \|\vartheta_1 - \vartheta_2\|_{L^2}^2 + \lambda_{\nabla_\theta \mathbf{F}, \mathbf{x}, \vartheta}^2 \mathbb{S}(\mathbf{x}_0, \vartheta_1) \wedge \mathbb{S}(\mathbf{x}_0, \vartheta_2) T h \right. \\ &\quad \left. + \lambda_{\nabla_\theta \mathbf{F}, \mathbf{x}, \vartheta}^2 C(\vartheta_1, \vartheta_2) T \|\vartheta_1 - \vartheta_2\|_{L^1}^2 + \int_0^T \mathbb{E}_\omega \left[\|\nabla_\theta \mathbf{F}(\hat{\mathbf{x}}_{\vartheta_2, t}, \vartheta_{2, t}) - \nabla_\theta \hat{\mathbf{F}}(\hat{\mathbf{x}}_{\vartheta_2, t}, \vartheta_{2, t})\|^2 \right] dt \right). \end{aligned}$$

To see that the last integral is finite, note that by Lemma 8.4 the trajectory $\hat{\mathbf{x}}_{\vartheta_2, t}$ stays in a ball $B_R \subset \mathbb{R}^d$ for all $t \in [0, T]$. Let $\mathcal{S}_{\vartheta_2} := \{\vartheta_{2, t} : t \in [0, T]\} \subset \Theta$. By (A4), (A5), the maps $(\mathbf{x}, \theta) \mapsto \nabla_\theta \mathbf{F}(\mathbf{x}, \theta)$ and $(\mathbf{x}, \theta) \mapsto \nabla_\theta \hat{\mathbf{F}}(\mathbf{x}, \theta)$ are locally Lipschitz, hence bounded on the compact set $B_R \times \mathcal{S}_{\vartheta_2}$. Therefore there exists $M_1 < \infty$ such that

$$\sup_{(\mathbf{x}, \theta) \in B_R \times \mathcal{S}_{\vartheta_2}} \|\nabla_\theta \mathbf{F}(\mathbf{x}, \theta)\| \leq M_1, \quad \sup_{(\mathbf{x}, \theta) \in B_R \times \mathcal{S}_{\vartheta_2}} \|\nabla_\theta \hat{\mathbf{F}}(\mathbf{x}, \theta)\| \leq (1 + \pi_{\min}^{-1}) M_2,$$

and the integrand is uniformly bounded by $(1 + \pi_{\min}^{-1})^2 M_1^2$. Hence

$$\int_0^T \mathbb{E}_\omega \left[\|\nabla_\theta \mathbf{F}(\hat{\mathbf{x}}_{\vartheta_2, t}, \vartheta_{2, t}) - \nabla_\theta \hat{\mathbf{F}}(\hat{\mathbf{x}}_{\vartheta_2, t}, \vartheta_{2, t})\|^2 \right] dt \leq T (1 + \pi_{\min}^{-1})^2 M_1^2 < \infty.$$

(ii) *Term B_t .* By Rademacher's theorem applied to (A5), it holds

$$\|B_t\|^2 \leq \frac{\lambda_{\nabla_\theta \mathbf{F}, \theta, K}^2}{\pi_{\min}^2} \|\mathbf{p}_{\vartheta_1, t} - \hat{\mathbf{p}}_{\vartheta_2, t}\|^2.$$

By Proposition 3.8,

$$\int_0^T \mathbb{E}_\omega \|B_t\|^2 dt \leq C \left(\sqrt{\|\Gamma(\mathbf{x}_0, \vartheta_\bullet)\|_{L^1(0, T)}} h + \mathbb{S}(\mathbf{x}_0, \vartheta_\bullet) h + \|\vartheta_1 - \vartheta_2\|_{L^1(0, T; \Theta)}^2 \right),$$

where $\vartheta_\bullet \in \{\vartheta_1, \vartheta_2\}$ minimizes the right-hand side.

Combining (i)–(ii), using $(a+b)^2 \leq 2a^2 + 2b^2$, and reinstating the sum over m yields (8.36). Finally, we can choose the explicit constants

$$C_1(\vartheta_1, \vartheta_2) := 3C_p^2 \sum_{m \in [n_d]} \int_0^T \mathbb{E}_\omega \left[\|\nabla_\theta \mathbf{F}(\hat{\mathbf{x}}_{m,\vartheta_2,t}, \vartheta_{2,t}) - \nabla_\theta \hat{\mathbf{F}}(\hat{\mathbf{x}}_{m,\vartheta_2,t}, \vartheta_{2,t})\|^2 \right] dt + \frac{\lambda_{\nabla_\theta \mathbf{F}, \theta, \mathbf{K}}^2}{\pi_{\min}^2} C_T \|\vartheta_1 - \vartheta_2\|_{L^2}^2,$$

$$C_2(\vartheta_1, \vartheta_2) := 3C_p^2 \lambda_{\nabla_\theta \mathbf{F}, \mathbf{x}, \vartheta}^2 T \sum_{m \in [n_d]} \left(\mathbf{S}(\mathbf{x}_{m,0}, \vartheta_1) \wedge \mathbf{S}(\mathbf{x}_{m,0}, \vartheta_2) \right) + \frac{\lambda_{\nabla_\theta \mathbf{F}, \theta, \mathbf{K}}^2}{\pi_{\min}^2} \sum_{m \in [n_d]} \left(\sqrt{\|\Gamma(\mathbf{x}_{m,0}, \vartheta_{m,\bullet})\|_{L^1}} + \mathbf{S}(\mathbf{x}_{m,0}, \vartheta_{m,\bullet}) \right),$$

where for each m we pick $\vartheta_{m,\bullet} \in \{\vartheta_1, \vartheta_2\}$ minimizing the corresponding bracket. Both C_1, C_2 are finite under the standing assumptions and uniformly in h . \square

Proof of Theorem 3.11. Let $\mathbf{x}_{m,\vartheta}$ and $\mathbf{p}_{m,\vartheta}$ solve (3.11)–(3.18) with control $\vartheta \in L^\infty(0, T; \Theta)$. For $t \in [0, T]$ define

$$A_t(\theta) := \nabla_\theta H\left((\mathbf{x}_{m,\vartheta^*,t}, \mathbf{p}_{m,\vartheta^*,t})_{m \in [n_d]}, \theta\right) = \alpha \theta + \sum_{m \in [n_d]} \nabla_\theta \mathbf{F}(\mathbf{x}_{m,\vartheta^*,t}, \theta)^\top \mathbf{p}_{m,\vartheta^*,t},$$

$$\hat{A}_t(\theta) := \nabla_\theta \hat{H}\left((\hat{\mathbf{x}}_{m,\hat{\vartheta}^*,t}, \hat{\mathbf{p}}_{m,\hat{\vartheta}^*,t})_{m \in [n_d]}, \theta\right) = \alpha \theta + \sum_{m \in [n_d]} \nabla_\theta \hat{\mathbf{F}}(\hat{\mathbf{x}}_{m,\hat{\vartheta}^*,t}, \theta)^\top \hat{\mathbf{p}}_{m,\hat{\vartheta}^*,t}.$$

By the first-order optimality conditions (3.22), for a.e. $t \in [0, T]$,

$$A_t(\vartheta_t^*) = \hat{A}_t(\hat{\vartheta}_t^*) = 0. \quad (8.37) \quad \text{eq:AtthatAt0}$$

Under (3.25), the Hamiltonian H is α -strongly convex in θ (see Remark 3.10 with $M = 0$). Hence A_t is α -strongly monotone, i.e.,

$$\langle A_t(\theta_1) - A_t(\theta_2), \theta_1 - \theta_2 \rangle \geq \alpha \|\theta_1 - \theta_2\|^2, \quad \text{for all } \theta_1, \theta_2 \in \Theta.$$

Taking $\theta_1 = \vartheta_t^*$, $\theta_2 = \hat{\vartheta}_t^*$ and using (8.37) and Cauchy–Schwarz,

$$\alpha \|\vartheta_t^* - \hat{\vartheta}_t^*\|^2 \leq \langle A_t(\vartheta_t^*) - A_t(\hat{\vartheta}_t^*), \vartheta_t^* - \hat{\vartheta}_t^* \rangle = \langle \hat{A}_t(\hat{\vartheta}_t^*) - A_t(\hat{\vartheta}_t^*), \vartheta_t^* - \hat{\vartheta}_t^* \rangle \leq \|\hat{A}_t(\hat{\vartheta}_t^*) - A_t(\hat{\vartheta}_t^*)\| \|\vartheta_t^* - \hat{\vartheta}_t^*\|.$$

Integrating over $[0, T]$,

$$\alpha \|\vartheta^* - \hat{\vartheta}^*\|_{L^2(0,T;\Theta)} \leq \|\hat{A}(\hat{\vartheta}^*) - A(\hat{\vartheta}^*)\|_{L^2(0,T;\Theta)} = \|\nabla \hat{H}(\hat{\vartheta}^*) - \nabla H(\hat{\vartheta}^*)\|_{L^2(0,T;\Theta)}.$$

Squaring and taking expectations yields

$$\alpha^2 \mathbb{E}_\omega \left[\|\vartheta^* - \hat{\vartheta}^*\|_{L^2(0,T;\Theta)}^2 \right] \leq \mathbb{E}_\omega \left[\|\nabla \hat{H}(\hat{\vartheta}^*) - \nabla H(\hat{\vartheta}^*)\|_{L^2(0,T;\Theta)}^2 \right]. \quad (8.38) \quad \text{eq:key_alpha}$$

By our regularity assumptions, for a.e. t ,

$$\nabla J_t(\vartheta) = \nabla_\theta H((\mathbf{x}_t, \mathbf{p}_t), \vartheta), \quad \nabla \hat{J}_t(\vartheta) = \nabla_\theta \hat{H}((\hat{\mathbf{x}}_t, \hat{\mathbf{p}}_t), \vartheta).$$

Evaluating at $\theta = \hat{\vartheta}^*$ and using $\nabla \hat{J}(\hat{\vartheta}^*) = 0$,

$$\|\nabla \hat{H}(\hat{\vartheta}^*) - \nabla H(\hat{\vartheta}^*)\|_{L^2(0,T;\Theta)} = \|\nabla \hat{J}(\hat{\vartheta}^*) - \nabla J(\hat{\vartheta}^*)\|_{L^2(0,T;\Theta)}.$$

Plugging this identity into (8.38) and applying Lemma 8.7 with $\vartheta_1 = \vartheta_2 = \hat{\vartheta}^*$, we obtain

$$\alpha^2 \mathbb{E}_\omega \left[\|\vartheta^* - \hat{\vartheta}^*\|_{L^2(0,T;\Theta)}^2 \right] \leq C_1(\hat{\vartheta}^*) + C_2(\hat{\vartheta}^*)$$

with

$$C_1(\vartheta) := 3C_p^2 C \sum_{m \in [n_d]} \int_0^T \mathbb{E}_\omega \left[\|\nabla_\theta \mathbf{F}(\hat{\mathbf{x}}_{m,\vartheta,t}, \vartheta_t) - \nabla_\theta \hat{\mathbf{F}}(\hat{\mathbf{x}}_{m,\vartheta,t}, \vartheta_t)\|^2 \right] dt,$$

$$C_2(\vartheta) := 3C_p^2 C \lambda_{\nabla_\theta \mathbf{F}, \mathbf{x}, \vartheta}^2 T \sum_{m \in [n_d]} \mathbf{S}(\mathbf{x}_{m,0}, \vartheta) + \frac{\lambda_{\nabla_\theta \mathbf{F}, \theta, \mathbf{K}}^2}{\pi_{\min}^2} \sum_{m \in [n_d]} \left(\sqrt{\|\Gamma(\mathbf{x}_{m,0}, \vartheta)\|_{L^1(0,T)}} + \mathbf{S}(\mathbf{x}_{m,0}, \vartheta) \right).$$

Repeating the same argument with the roles of J and \hat{J} interchanged yields the analogous bound with admissible constants evaluated at ϑ^* . All these constants are uniform in h . \square

8.6. Proofs of Section 4.1.

Proof of Proposition 4.1. Let $S^{(k)} := \{i \in [p] : b_i^{(k)} = 1\}$. Since $b_i^{(k)}$ are independent Bernoulli(q_B), for any $S \subseteq [p]$ and k ,

$$\mathbb{P}(S^{(k)} = S) = \prod_{i \notin S} \mathbb{P}(b_i^{(k)} = 0) = q_B^{|S|} (1 - q_B)^{p-|S|} = q_S.$$

Therefore

$$\begin{aligned} \pi_i &= \sum_{S \ni i} q_S = \sum_{S \ni i} q_B^{|S|} (1 - q_B)^{p-|S|} = \sum_{T \subseteq [p] \setminus \{i\}} q_B^{1+|T|} (1 - q_B)^{(p-1)-|T|} \\ &= q_B \sum_{T \subseteq [p] \setminus \{i\}} q_B^{|T|} (1 - q_B)^{(p-1)-|T|}. \end{aligned}$$

For the last sum, group by cardinality and apply the binomial theorem:

$$\sum_{T \subseteq [p] \setminus \{i\}} q_B^{|T|} (1 - q_B)^{(p-1)-|T|} = \sum_{k=0}^{p-1} \binom{p-1}{k} q_B^k (1 - q_B)^{(p-1)-k} = (q_B + (1 - q_B))^{p-1} = 1,$$

hence $\pi_i = q_B$ for every i . Since $\mathcal{B}_{\omega_k} = S^{(k)}$ by construction, then on $[t_{k-1}, t_k]$ we have

$$\hat{\mathbf{F}}_t = \sum_{i \in \mathcal{B}_{\omega_k}} \frac{1}{\pi_i} \mathbf{f}_{i,t} = \frac{1}{q_B} \sum_{i \in S^{(k)}} \mathbf{f}_{i,t} = \frac{1}{q_B} \sum_{i \in [p]} b_i^{(k_t)} \mathbf{f}_{i,t} = \hat{\mathbf{F}}_t^{sd},$$

which proves the identification. \square

Derivation of Table 1. Below we show the computations for each canonical scheme. We use the bound $\|\Lambda\|_{L^1} \leq T \sup_t \Lambda_t$ and bound $\sup_t \Lambda_t$ with respect to σ_* and μ_* , defined in (4.3).

For concision, we will omit function arguments.

(1) **Single-batch** ($n_b = 1$, $\mathcal{B}_1 = [p]$, $q_1 = 1$). The two trajectories \mathbf{x}_t and $\hat{\mathbf{x}}_t$ coincide because

$$\hat{\mathbf{F}} = \mathbf{F}, \quad \Lambda = 0.$$

(2) **Drop-one** ($n_b = p$, $\mathcal{B}_j = [p] \setminus \{j\}$). Neuron i is inactive if and only if $\omega = i$:

$$\pi_i = 1 - q_i, \quad \mathbf{F}^{(j)} = \sum_{i \in [p] \setminus \{j\}} \frac{\mathbf{f}_i}{1 - q_i}, \quad \Lambda = \sum_{j \in [p]} \left\| \mathbf{f}_j - \sum_{i \in [p] \setminus \{j\}} \frac{q_i}{1 - q_i} \mathbf{f}_i \right\|^2 q_j.$$

For uniform probabilities ($q_j = p^{-1}$), we get

$$\sum_{j \in [p]} q_j^{-1} = p^2, \quad \pi_{\min} = 1 - \frac{1}{p}, \quad \Lambda = \frac{1}{p} \sum_{j \in [p]} \left\| \mathbf{f}_j - \frac{1}{p-1} \sum_{i \in [p] \setminus \{j\}} \mathbf{f}_i \right\|^2 = \frac{p^2}{(p-1)^2} \sigma^2.$$

Plugging into (4.1) (case $\lambda_{\mathbf{F}, \mathbf{x}, \vartheta} > 0$) gives, for $\sigma_*^2 = \sigma_*^2(\mathbf{x}_0, \vartheta)$ as in (4.3),

$$\mathbf{S}(\mathbf{x}_0, \vartheta) \leq \frac{2\lambda_{\mathbf{F}, \mathbf{x}, \vartheta} p^2 T}{(p-1)^2} e^{\frac{2\lambda_{\mathbf{F}, \mathbf{x}, \vartheta} p T}{p-1}} \left[\frac{T p^2 \sigma_*^2}{p-1} + \left(\|\mathbf{x}_0\| + \frac{\lambda_{\mathbf{F}, 0, \vartheta}}{\lambda_{\mathbf{F}, \mathbf{x}, \vartheta}} \right) \sigma_* \right].$$

(3) **Pick-one** ($n_b = p$, $\mathcal{B}_j = \{j\}$). Neuron i is active if and only if $\omega = i$:

$$\pi_i = q_i, \quad \mathbf{F}^{(j)} = \frac{\mathbf{f}_j}{q_j}, \quad \Lambda = \sum_{j \in [p]} \left\| \sum_{i \in [p]} \mathbf{f}_i - \frac{\mathbf{f}_j}{q_j} \right\|^2 q_j.$$

For uniform probabilities ($q_j = p^{-1}$),

$$\sum_{j \in [p]} q_j^{-1} = p^2, \quad \pi_{\min} = \frac{1}{p}, \quad \Lambda = \frac{1}{p} \sum_{j \in [p]} \left\| \sum_{i \in [p]} \mathbf{f}_i - p \mathbf{f}_j \right\|^2 = p^2 \sigma^2.$$

For $\sigma_*^2 = \sigma_*^2(\mathbf{x}_0, \vartheta)$ as in (4.3), we deduce:

$$\mathbf{S}(\mathbf{x}_0, \vartheta) \leq 2\lambda_{\mathbf{F}, \mathbf{x}, \vartheta} p^2 T e^{2\lambda_{\mathbf{F}, \mathbf{x}, \vartheta} p T} \left[p^2 T \sigma_*^2 + \left(\|\mathbf{x}_0\| + \frac{\lambda_{\mathbf{F}, 0, \vartheta}}{\lambda_{\mathbf{F}, \mathbf{x}, \vartheta}} \right) \sigma_* \right].$$

(4) **Balanced batches of fixed size.** More generally, fix $r \in [p-1]$ and sample \mathcal{B}_j uniformly among all subsets of size r (so $n_b = \binom{p}{r}$ and $q_j = \binom{p}{r}^{-1}$). Each neuron appears in exactly $\binom{p-1}{r-1}$ batches, hence

$$\sum_{j \in [n_b]} q_j^{-1} = \binom{p}{r}^2, \quad \pi_i = \frac{r}{p}, \quad \Lambda = \binom{p}{r}^{-1} \sum_{j \in [\binom{p}{r}]} \left\| \sum_{i \in [p]} \mathbf{f}_i - \frac{p}{r} \sum_{i \in \mathcal{B}_j} \mathbf{f}_i \right\|^2 = \frac{p^2(p-r)}{(p-1)r} \sigma^2.$$

Given p , we have that Λ decreases with r from $\Lambda = p^2 \sigma^2$ at $r = 1$ (pick-one) to $\Lambda = 0$ at $r = p$ (single-batch). For $\sigma_\star^2 = \sigma_\star^2(\mathbf{x}_0, \vartheta)$ as in (4.3), we deduce:

$$\mathbf{S}(\mathbf{x}_0, \vartheta) \leq \frac{2\lambda_{\mathbf{F}, \mathbf{x}, \vartheta} p^2 T}{r} e^{\frac{2\lambda_{\mathbf{F}, \mathbf{x}, \vartheta} p T}{r}} \left[\binom{p}{r} \frac{p(p-r)T}{(p-1)r} \sigma_\star^2 + \sqrt{\frac{(p-r)}{(p-1)r}} \left(\|\mathbf{x}_0\| + \frac{\lambda_{\mathbf{F}, 0, \vartheta}}{\lambda_{\mathbf{F}, \mathbf{x}, \vartheta}} \right) \sigma_\star \right]. \quad (8.39)$$

eq: S_balan

(5) **Balanced disjoint batches of fixed size.** Partition $[p]$ into $n_b = p/r$ disjoint batches of size r (assume r divides p) and sample one batch uniformly at each subinterval:

$$q_j = \frac{1}{n_b} = \frac{r}{p}, \quad \sum_{j \in [n_b]} q_j^{-1} = \left(\frac{p}{r} \right)^2, \quad \pi_i = \frac{r}{p}, \quad \mathbf{F}^{(j)} = \frac{p}{r} \sum_{i \in \mathcal{B}_j} \mathbf{f}_i.$$

Λ is the same as in (4), and \mathbf{S} is equal to (8.39) with the single replacement $\binom{p}{r} \mapsto \frac{p}{r}$.

(6) **All subsets uniformly** ($n_b = 2^p$, $\mathcal{B}_j \subseteq [p]$). Let \mathcal{B}_j range over all (possibly empty) subsets of $[p]$ with equal probability $q_j = 2^{-p}$. Then

$$\sum_{j \in [n_b]} q_j^{-1} = 2^{2p}, \quad \pi_i = \frac{2^{p-1}}{2^p} = \frac{1}{2}, \quad \mathbf{F}^{(j)} = 2 \sum_{i \in \mathcal{B}_j} \mathbf{f}_i$$

and

$$\Lambda = \frac{1}{2^p} \sum_{j \in [2^p]} \left\| \sum_{i \in [p]} (1 - 2\mathbf{1}_{\{i \in \mathcal{B}_j\}}) \mathbf{f}_i \right\|^2 = \sum_{i \in [p]} \|\mathbf{f}_i\|^2 = p\sigma^2 + p\mu^2.$$

For $\sigma_\star^2 = \sigma_\star^2(\mathbf{x}_0, \vartheta)$ and $\mu_\star = \mu_\star(\mathbf{x}_0, \vartheta)$ as in (4.3), we deduce:

$$\mathbf{S}(\mathbf{x}_0, \vartheta) = 4\lambda_{\mathbf{F}, \mathbf{x}, \vartheta} T e^{4\lambda_{\mathbf{F}, \mathbf{x}, \vartheta} T} \left[2^p p T (\sigma_\star^2 + \mu_\star^2) + \sqrt{p(\sigma_\star^2 + \mu_\star^2)} \left(\|\mathbf{x}_0\| + \frac{\lambda_{\mathbf{F}, 0, \vartheta}}{\lambda_{\mathbf{F}, \mathbf{x}, \vartheta}} \right) \right].$$

(7) **Bernoulli dropout.** By Proposition 4.1, we can write the usual implementation of Bernoulli dropout as an instance of random batch methods with “all subsets” ($n_b = 2^p$, $\mathcal{B}_j \subseteq [p]$) and a specific sampling distribution:

$$q_j = q_B^{|\mathcal{B}_j|} (1 - q_B)^{p - |\mathcal{B}_j|}, \quad \pi_i = q_B$$

We can now compute:

$$\sum_{j \in [2^p]} q_j^{-1} = (q_B(1 - q_B))^{-p}, \quad \Lambda = \frac{1 - q_B}{q_B} \sum_{i \in [p]} \|\mathbf{f}_i\|^2 = \frac{1 - q_B}{q_B} p(\sigma^2 + \mu^2).$$

Consequently, for $\sigma_\star^2 = \sigma_\star^2(\mathbf{x}_0, \vartheta)$ and $\mu_\star = \mu_\star(\mathbf{x}_0, \vartheta)$ as in (4.3),

$$\mathbf{S}(\mathbf{x}_0, \vartheta) = \frac{2\lambda_{\mathbf{F}, \mathbf{x}, \vartheta} T}{q_B^2} e^{\frac{2\lambda_{\mathbf{F}, \mathbf{x}, \vartheta} T}{q_B}} \left[p T \frac{1 - q_B}{(q_B(1 - q_B))^{p/2}} (\sigma_\star^2 + \mu_\star^2) + \sqrt{p(1 - q_B)q_B} (\sigma_\star^2 + \mu_\star^2) \left(\|\mathbf{x}_0\| + \frac{\lambda_{\mathbf{F}, 0, \vartheta}}{\lambda_{\mathbf{F}, \mathbf{x}, \vartheta}} \right) \right].$$

□

8.7. Proofs of Section 4.2.

Proof of Proposition 4.2. By (4.6), \mathbf{C}_{RM} is minimized by the largest h that is admissible, i.e., such that $\mathcal{E}(h) \leq \varepsilon$. Since the function $\mathcal{E}(h)$ is strictly increasing, the minimizer is characterized by $\mathcal{E}(h^*) = \varepsilon$. Setting $z = \sqrt{h}$ yields the quadratic $c_{\text{int}} \gamma z^2 + \sqrt{5} z - \varepsilon = 0$. Solving for its positive root and squaring gives

$$h^*(\varepsilon) = \frac{\mathbf{S}}{4(c_{\text{int}} \gamma)^2} \left(\sqrt{1 + \frac{4c_{\text{int}} \gamma \varepsilon}{5}} - 1 \right)^2 = \frac{4\varepsilon^2}{5} \left(1 + \sqrt{1 + \frac{4c_{\text{int}} \gamma \varepsilon}{5}} \right)^{-2},$$

where in the last step we used $(\sqrt{1+a} - 1)^2 = a^2(1 + \sqrt{1+a})^{-2}$ with $a = \frac{4c_{\text{int}} \gamma \varepsilon}{5}$. This proves (4.9). □

Proof of Proposition 4.4. By the first-order global error of Euler we have $C_{\text{FM}}^*(\varepsilon) = Tp c_{\text{int,FM}}/\varepsilon$. For the random model, (4.10) yields

$$C_{\text{RM}}^*(\varepsilon) = \frac{TrS}{4\gamma\varepsilon^2} \left(1 + \sqrt{1 + \frac{4c_{\text{int,RM}}\gamma\varepsilon}{S}} \right)^2,$$

and dividing gives (4.13). For regime-wise bounds use the global estimates (valid for all ε)

$$C_{\text{RM}}^*(\varepsilon) \leq \frac{(1+\sqrt{5})^2}{4} \frac{rT c_{\text{int,RM}}}{\varepsilon} \quad (\varepsilon \geq \varepsilon_c), \quad C_{\text{RM}}^*(\varepsilon) \leq \frac{(1+\sqrt{5})^2}{4} \frac{rTS}{\gamma\varepsilon^2} \quad (\varepsilon \leq \varepsilon_c),$$

and divide $C_{\text{FM}}^*(\varepsilon)$ by these upper bounds. Finally, since $c_{\text{int,RM}} \leq \kappa c_{\text{int,FM}}$, we get $c_{\text{int,FM}}/c_{\text{int,RM}} \geq 1/\kappa$, giving the discretization-limited form. \square

ACKNOWLEDGMENTS

AÁ has been funded by PID2023-146872OB-I00 of MICIU (Spain), and by FPU21/05673 from the Spanish Ministry of Universities. MH has been funded by the Transregio 154 Project Mathematical Modelling, Simulation, and Optimization Using the Example of Gas Networks of the DFG, project C07; by the fellowship ANID-DAAD Bilateral Agreement; and by the DAAD/CAPES grant 57703041 Control and Numerical Analysis of Complex Systems.

The authors thank Borjan Geshkovski and Domènec Ruiz-Balet for valuable comments.

REFERENCES

- [1] A. Álvarez-López, B. Geshkovski, and D. Ruiz-Balet. Constructive approximate transport maps with normalizing flows. *Applied Mathematics & Optimization*, 92(2):33, 2025.
- [2] J. Ba and B. Frey. Adaptive dropout for training deep neural networks. In C. Burges, L. Bottou, M. Welling, Z. Ghahramani, and K. Weinberger, editors, *Advances in Neural Information Processing Systems*, volume 26. Curran Associates, Inc., 2013.
- [3] H. Bahouri, J.-Y. Chemin, and R. Danchin. *Fourier analysis and nonlinear partial differential equations*, volume 343 of *Grundlehren der mathematischen Wissenschaften [Fundamental Principles of Mathematical Sciences]*. Springer, Heidelberg, 2011.
- [4] T. B. Brown, B. Mann, N. Ryder, M. Subbiah, J. Kaplan, P. Dhariwal, A. Neelakantan, P. Shyam, G. Sastry, A. Askell, S. Agarwal, A. Herbert-Voss, G. Krueger, T. Henighan, R. Child, A. Ramesh, D. M. Ziegler, J. Wu, C. Winter, C. Hesse, M. Chen, E. Sigler, M. Litwin, S. Gray, B. Chess, J. Clark, C. Berner, S. McCandlish, A. Radford, I. Sutskever, and D. Amodei. Language models are few-shot learners, 2020.
- [5] J. A. Carrillo, S. Jin, and Y. Tang. Random batch particle methods for the homogeneous Landau equation. *Commun. Comput. Phys.*, 31(4):997–1019, 2022.
- [6] L. Cesari. *Optimization—theory and applications*, volume 17 of *Applications of Mathematics (New York)*. Springer-Verlag, New York, 1983. Problems with ordinary differential equations.
- [7] R. T. Q. Chen, Y. Rubanova, J. Bettencourt, and D. Duvenaud. Neural ordinary differential equations. In *Proceedings of the 32nd International Conference on Neural Information Processing Systems*, page 6572–6583. Curran Associates Inc., 2018.
- [8] H. Cheng, M. Zhang, and J. Q. Shi. A survey on deep neural network pruning: Taxonomy, comparison, analysis, and recommendations. *IEEE Transactions on Pattern Analysis and Machine Intelligence*, 46(12):10558–10578, 2024.
- [9] L. Chizat, P. Marion, and Y. Yesbay. Phase diagram of dropout for two-layer neural networks in the mean-field regime, 2025.
- [10] A. Chowdhery, S. Narang, J. Devlin, M. Bosma, G. Mishra, A. Roberts, P. Barham, H. W. Chung, C. Sutton, S. Gehrmann, et al. Palm: Scaling language modeling with pathways. *Journal of Machine Learning Research*, 24(240):1–113, 2023.
- [11] C. Cuchiero, M. Larsson, and J. Teichmann. Deep neural networks, generic universal interpolation, and controlled ODEs. *SIAM J. Math. Data Sci.*, 2(3):901–919, 2020.
- [12] J. Devlin, M.-W. Chang, K. Lee, and K. Toutanova. Bert: Pre-training of deep bidirectional transformers for language understanding. In *Proceedings of the 2019 conference of the North American chapter of the association for computational linguistics: human language technologies, volume 1 (long and short papers)*, pages 4171–4186, 2019.
- [13] T. DeVries and G. W. Taylor. Improved regularization of convolutional neural networks with cutout, 2017.
- [14] Domínguez Corella, Alberto and Hernández, Martín. Mini-batch descent in semiflows. *ESAIM: COCV*, 31:28, 2025.
- [15] W. E. A proposal on machine learning via dynamical systems. *Communications in Mathematics and Statistics*, 5:1–11, 02 2017.
- [16] W. E, J. Han, and Q. Li. A mean-field optimal control formulation of deep learning. *Research in the Mathematical Sciences*, 6(1):10, 2018.
- [17] M. Eisenmann and T. Stillfjord. A randomized operator splitting scheme inspired by stochastic optimization methods. *Numerische Mathematik*, Feb 2024.
- [18] C. Esteve, B. Geshkovski, D. Pighin, and E. Zuazua. Large-time asymptotics in deep learning, 2021.

- e2018lottery [19] J. Frankle and M. Carbin. The lottery ticket hypothesis: Finding sparse, trainable neural networks. In *International Conference on Learning Representations*, 2019.
- Bayesian2016 [20] Y. Gal and Z. Ghahramani. Dropout as a bayesian approximation: Representing model uncertainty in deep learning. In M. F. Balcan and K. Q. Weinberger, editors, *Proceedings of The 33rd International Conference on Machine Learning*, volume 48 of *Proceedings of Machine Learning Research*, pages 1050–1059, New York, New York, USA, 20–22 Jun 2016. PMLR.
- creteddropout [21] Y. Gal, J. Hron, and A. Kendall. Concrete dropout, 2017.
- TurnpikeActa [22] B. Geshkovski and E. Zuazua. Turnpike in optimal control of PDEs, ResNets, and beyond. *Acta Numer.*, 31:135–263, 2022.
- h_steer_2020 [23] A. Ghosh, H. Behl, E. Dupont, P. Torr, and V. Nambodiri. STEER : Simple Temporal Regularization For Neural ODE. In *Advances in Neural Information Processing Systems*, volume 33, pages 14831–14843. Curran Associates, Inc., 2020.
- o2016dynamic [24] Y. Guo, A. Yao, and Y. Chen. Dynamic network surgery for efficient dnns. *Advances in neural information processing systems*, 29, 2016.
- haber [25] E. Haber and L. Ruthotto. Stable architectures for deep neural networks. *Inverse Problems*, 34(1):014004, 2017.
- ale_book_ode [26] J. K. Hale. *Ordinary differential equations*, volume Vol. XXI of *Pure and Applied Mathematics*. Wiley-Interscience [John Wiley & Sons], New York-London-Sydney, 1969.
- Han2016 [27] S. Han, H. Mao, and W. J. Dally. Deep compression: Compressing deep neural networks with pruning, trained quantization and huffman coding, 2016.
- Han2015 [28] S. Han, J. Pool, J. Tran, and W. J. Dally. Learning both weights and connections for efficient neural networks. In *Proceedings of the 29th International Conference on Neural Information Processing Systems - Volume 1*, NIPS’15, page 1135–1143, Cambridge, MA, USA, 2015. MIT Press.
- Hassibi1993 [29] B. Hassibi, D. Stork, and G. Wolff. Optimal brain surgeon and general network pruning. In *IEEE International Conference on Neural Networks*, pages 293–299 vol.1, 1993.
- e2017channel [30] Y. He, X. Zhang, and J. Sun. Channel pruning for accelerating very deep neural networks. In *Proceedings of the IEEE international conference on computer vision*, pages 1389–1397, 2017.
- ontinuousRBM [31] M. Hernández. Random domain decomposition for parabolic pdes on graphs, 2025.
- cretizedRBM [32] M. Hernández and E. Zuazua. Random batch methods for discretized pdes on graphs, 2025.
- horvitz [33] D. G. Horvitz and D. J. Thompson. A generalization of sampling without replacement from a finite universe. *Journal of the American Statistical Association*, 47(260):663–685, 1952.
- ikStochastic [34] B. Igel'nik and Y.-H. Pao. Stochastic choice of basis functions in adaptive function approximation and the functional-link net. *IEEE Transactions on Neural Networks*, 6(6):1320–1329, 1995.
- _neural_2019 [35] J. Jia and A. R. Benson. Neural Jump Stochastic Differential Equations. In *Advances in Neural Information Processing Systems*, volume 32. Curran Associates, Inc., 2019.
- MR4361973 [36] S. Jin and L. Li. On the mean field limit of the random batch method for interacting particle systems. *Sci. China Math.*, 65(1):169–202, 2022.
- IN2020108877 [37] S. Jin, L. Li, and J.-G. Liu. Random batch methods (rbm) for interacting particle systems. *Journal of Computational Physics*, 400:108877, 2020.
- MR4230431 [38] S. Jin, L. Li, and J.-G. Liu. Convergence of the random batch method for interacting particles with disparate species and weights. *SIAM J. Numer. Anal.*, 59(2):746–768, 2021.
- 015_bc731692 [39] D. P. Kingma, T. Salimans, and M. Welling. Variational dropout and the local reparameterization trick. In C. Cortes, N. Lawrence, D. Lee, M. Sugiyama, and R. Garnett, editors, *Advances in Neural Information Processing Systems*, volume 28. Curran Associates, Inc., 2015.
- ANSER1999201 [40] D. Lanser and J. Verwer. Analysis of operator splitting for advection–diffusion–reaction problems from air pollution modelling. *Journal of Computational and Applied Mathematics*, 111(1):201–216, 1999.
- LeCun1990 [41] Y. LeCun, J. Denker, and S. Solla. Optimal brain damage. In D. Touretzky, editor, *Advances in Neural Information Processing Systems*, volume 2. Morgan-Kaufmann, 1989.
- ee2025neural [42] J. Lee, Y. Oh, S. Kim, and D. Lim. Neural regenerative stochastic differential equation: Dropout scheme for neural differential equations, 2025.
- i2017pruning [43] H. Li, A. Kadav, I. Durdanovic, H. Samet, and H. P. Graf. Pruning filters for efficient convnets. In *International Conference on Learning Representations*, 2017.
- maximum_2018 [44] Q. Li, L. Chen, C. Tai, and W. E. Maximum Principle Based Algorithms for Deep Learning. *Journal of Machine Learning Research*, 18(165):1–29, 2018.
- iberzon_book [45] D. Liberzon. *Calculus of variations and optimal control theory*. Princeton University Press, Princeton, NJ, 2012. A concise introduction.
- in2021sparse [46] L. Liebenwein, R. Hasani, A. Amini, and D. Rus. Sparse flows: Pruning continuous-depth models. In A. Beygelzimer, Y. Dauphin, P. Liang, and J. W. Vaughan, editors, *Advances in Neural Information Processing Systems*, 2021.
- 0_Neural_SDE [47] X. Liu, T. Xiao, S. Si, Q. Cao, S. Kumar, and C.-J. Hsieh. How does noise help robustness? explanation and exploration under the neural sde framework. In *2020 IEEE/CVF Conference on Computer Vision and Pattern Recognition (CVPR)*, pages 279–287, 2020.
- acNamara2016 [48] S. MacNamara and G. Strang. *Operator Splitting*, pages 95–114. Springer International Publishing, Cham, 2016.
- 0convergence [49] P. Mianjy and R. Arora. On convergence and generalization of dropout training. *Advances in Neural Information Processing Systems*, 33:21151–21161, 2020.
- r-v202-mo23c [50] Z. Mo, H. Shi, and S. J. Pan. Pruning via sparsity-indexed ODE: a continuous sparsity viewpoint. In A. Krause, E. Brunskill, K. Cho, B. Engelhardt, S. Sabato, and J. Scarlett, editors, *Proceedings of the 40th International Conference on Machine Learning*, volume 202 of *Proceedings of Machine Learning Research*, pages 25018–25036. PMLR, 23–29 Jul 2023.

- 2018scalable [51] D. C. Mocanu, E. Mocanu, P. Stone, P. H. Nguyen, M. Gibescu, and A. Liotta. Scalable training of artificial neural networks with adaptive sparse connectivity inspired by network science. *Nature communications*, 9(1):2383, 2018.
- lization2018 [52] W. Mou, Y. Zhou, J. Gao, and L. Wang. Dropout training, data-dependent regularization, and generalization bounds. In J. Dy and A. Krause, editors, *Proceedings of the 35th International Conference on Machine Learning*, volume 80 of *Proceedings of Machine Learning Research*, pages 3645–3653. PMLR, 10–15 Jul 2018.
- 17structured [53] K. Neklyudov, D. Molchanov, A. Ashukha, and D. P. Vetrov. Structured bayesian pruning via log-normal multiplicative noise. *Advances in Neural Information Processing Systems*, 30, 2017.
- omprehensive [54] Y. Oh, S. Kam, J. Lee, D.-Y. Lim, S. Kim, and A. Bui. Comprehensive review of neural differential equations for time series analysis. *arXiv preprint arXiv:2502.09885*, 2025.
- inormalizing [55] G. Papamakarios, E. Nalisnick, D. J. Rezende, S. Mohamed, and B. Lakshminarayanan. Normalizing flows for probabilistic modeling and inference. *Journal of Machine Learning Research*, 22(57):1–64, 2021.
- MR4744252 [56] L. Pareschi and M. Zanella. Reduced variance random batch methods for nonlocal PDEs. *Acta Appl. Math.*, 191:Paper No. 4, 23, 2024.
- 5variational [57] D. Rezende and S. Mohamed. Variational inference with normalizing flows. In *International conference on machine learning*, pages 1530–1538. PMLR, 2015.
- nyan2014very [58] K. Simonyan and A. Zisserman. Very deep convolutional networks for large-scale image recognition. pages 1–14. Computational and Biological Learning Society, 2015.
- a2014dropout [59] N. Srivastava, G. Hinton, A. Krizhevsky, I. Sutskever, and R. Salakhutdinov. Dropout: A simple way to prevent neural networks from overfitting. *Journal of Machine Learning Research*, 15(56):1929–1958, 2014.
- StochasticT0 [60] Q. Sun, Y. Tao, and Q. Du. Stochastic training of residual networks: a differential equation viewpoint. *ArXiv*, abs/1812.00174, 2018.
- fficient2015 [61] J. Tompson, R. Goroshin, A. Jain, Y. LeCun, and C. Bregler. Efficient object localization using convolutional networks. In *2015 IEEE Conference on Computer Vision and Pattern Recognition (CVPR)*, pages 648–656, 2015.
- note_control [62] E. Trélat. *Control in finite and infinite dimension*. SpringerBriefs on PDEs and Data Science. Springer, Singapore, [2024] ©2024.
- trotter59 [63] H. F. Trotter. On the product of semi-groups of operators. *Proceedings of the American Mathematical Society*, 10(4):545–551, 1959.
- 023stability [64] D. W. M. Veldman, A. Borkowski, and E. Zuazua. Stability and convergence of a randomized model predictive control strategy. *IEEE Transactions on Automatic Control*, pages 1–8, 2024.
- MR4433122 [65] D. W. M. Veldman and E. Zuazua. A framework for randomized time-splitting in linear-quadratic optimal control. *Numer. Math.*, 151(2):495–549, 2022.
- notesdropout [66] F. Verdoja and V. Kyrki. Notes on the behavior of mc dropout, 2021.
- pmlrwan13 [67] L. Wan, M. Zeiler, S. Zhang, Y. Le Cun, and R. Fergus. Regularization of neural networks using dropconnect. In S. Dasgupta and D. McAllester, editors, *Proceedings of the 30th International Conference on Machine Learning*, volume 28 of *Proceedings of Machine Learning Research*, pages 1058–1066, Atlanta, Georgia, USA, 17–19 Jun 2013. PMLR.
- 020_a1140a3d [68] M. Zhang and Y. He. Accelerating training of transformer-based language models with progressive layer dropping. In H. Larochelle, M. Ranzato, R. Hadsell, M. Balcan, and H. Lin, editors, *Advances in Neural Information Processing Systems*, volume 33, pages 14011–14023. Curran Associates, Inc., 2020.
- 2024implicit [69] Z. Zhang and Z.-Q. J. Xu. Implicit regularization of dropout. *IEEE Transactions on Pattern Analysis and Machine Intelligence*, 46(6):4206–4217, 2024.